FOLDING AND CONFORMATIONAL STABILITY OF PORCINE GROWTH HORMONE

A thesis submitted by

Stan Bastiras, B.Sc.(Hons)

to the University of Adelaide,
South Australia for the degree
of Doctor of Philosophy.

Department of Biochemistry,
University of Adelaide,
South Australia 5001.

August, 1992.

TABLE OF CONTENTS

SUMMARY

The large scale production and purification of recombinant-derived porcine growth hormone (pGH) and mutants thereof, bream growth hormone (brGH) and human growth hormone (hGH) was carried out. Each of the protein products were analysed by various physicochemical means, in order to verify their identity and homogeneity.

The equilibrium denaturation of pGH using the chemical denaturant guanidine hydrochloride (GuHCl), was monitored by a variety of spectroscopic and hydrodynamic probes. The denaturation of pGH resulted in absorbance- and fluorescence-detected transitions which were coincident, whereas far-UV circular dichroism- and hydrodynamic radius-detected transitions occured at higher concentrations of GuHCl, indicative of a greater stability to denaturation. Conformations intermediate to the folded and fully unfolded states were found to be stable at equilibrium under partially denaturing conditions. These intermediate forms have the characteristics of *molten-globule* or *compact denatured states;* a compact structure with considerable helix content, yet possessing a tertiary structure similar to that of the fully unfolded state. At concentrations above 10μM, the intermediate was shown to aggregate, forming a stable associated intermediate. These results suggest that pGH does not follow a simple two-state folding mechanism, but is consistent with the framework model of protein folding.

The conformational stabilities of pGH, ten site-directed mutants of pGH, and wild-type bream and human GH, were determined using GuHCl-induced equilibrium denaturation under a standard set of conditions. Single amino acid changes in the sequence of pGH were shown to have different effects on (*i*) the conformational stability, (*ii*) the cooperativity of the denaturation transition, i.e., m_{GuHCl} and (*iii*) the midpoint of the denaturation transition, i.e., $[GuHCl]_{½}$. Bream GH was shown to have a stability similar to that of wild-type pGH whereas human GH, in accordance with previously published values [Brems, D. N., Brown, P. L., and Becker, G. W.

(1990) *J. Biol. Chem.* *265*, 5504-5511], was found to be significantly more stable than pGH and brGH.

One mutant in which a methionine residue was replaced by a tryptophan [pGH(M8)], was found to be significantly more stable than wild-type pGH, due to an increase in both m_{GuHCl} and $[GuHCl]_{½}$. The coincidence of the UV-, fluorescence- and hydrodynamic radius-detected equilibrium denaturation curves and the absence of significant amounts of associated forms suggests that pGH(M8) folding/unfolding is more closely approximated by a two-state mechanism than wild-type pGH.

STATEMENT

This thesis contains no material which has been accepted for the award of any other degree or diploma in any university. To the best of my knowledge, it contains no material that has been previously published or written by another person except where due reference is made in the text.

Stan Bastiras

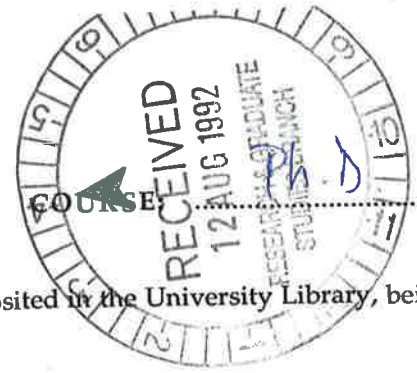

NAME: COURSE: Ph.D

I give consent to this copy of my thesis, when deposited in the University Library, being available for loan and photocopying.

SIGNATURE: ..... DATE: 11/8/92

ACKNOWLEDGEMENTS

I wish to thank Professor George E. Rogers for permission to undertake this project in the Department of Biochemistry, University of Adelaide and Dr. John R. Smeaton for allowing me to work on the premises of Bresatec Ltd.

I would like to thank my supervisors, Dr. John C. Wallace and Dr. Julian R. E. Wells for their advice and encouragement during the course of this study. I would also like to thank Dr. Tom Kuruscev for many valuable discussions during the writing of this thesis.

I would like to acknowledge the assistance of Carol Senn who conducted the fermentations and Dr. Allan Robins who provided the clones. I am also grateful to Ela Knapik for her assistance in the production and purification of the various growth hormones. I would like to thank Professor W. H. Sawyer for allowing me to perform the CD measurements in his laboratory. I am also indebted to Dr. Michael Waters and Scott Rowlinson for carrying out the radioreceptor assays, Dr. Margaret Sheil for performing the mass spectrometry, Denise Turner for performing protein sequence analysis and Mark Snoswell for assistance in various computing tasks.

I would also like to thank all of my colleagues at Bresatec Ltd. for Wednesday morning cake sessions; in particular those who went further than the German cake shop down the road. Finally, I would like to thank Rosie, Jamaica and Nicolas for their support and inspiration.

Publications and Conference Presentations Arising from Thesis Research.

Bastiras, S., & Wallace, J. C. (1992).
Equilibrium Denaturation of Recombinant Porcine Growth Hormone
Biochemistry 31, (in press).

Bastiras, S., Sawyer, W. H., Wallace, J. C., & Wells, J. R. E. (1992)
Equilibrium Denaturation of Recombinant Porcine Growth Hormone
Seventeenth Annual Lorne Conference on Protein Structure and Function, Feb. 1992.

Bastiras, S. (1992)
Mutational Effects on the Conformational Stability and Folding of Porcine Growth Hormone.
Workshop on "Understanding Protein Folding", NOVUM Research Park, Stockholm, August 1992.

ABBREVIATIONS

A_{xxx}	absorbance at xxx nm
AUFS	absorbance units of full scale
bGH	bovine growth hormone
brGH	bream growth hormone
C D	circular dichroism
DTT	dithiothreitol
F_{app}	the apparent fraction of unfolded protein
GH	growth hormone
GuHCl	guanidine hydrochloride
hGH	human growth hormone
HPLC	high performance liquid chromatography
K_a	association constant
λ_{max}	fluorescence emission maximum
pGH	porcine growth hormone
pGH_{wt}	wild type porcine growth hormone
PL	placental lactogen
pRL	prolactin
$\Delta\alpha_{app}$	apparent average difference in degree of exposure to solvent
ΔG_{app}	apparent free energy of unfolding
$\Delta G(H_2O)$	ΔG in the absence of denaturant (conformational stability)
m	measure of the dependence of ΔG on denaturant concentration

CHAPTER 1

INTRODUCTION

1.1 INTRODUCTION

Since the experiments of Anfinsen (1973), it has been largely accepted that the three-dimensional structure of a protein is determined by its sequence of amino acids. This view is incomplete however, if we ignore the fact that the environment in which a protein finds itself is just as significant in determining the structure. Thermodynamically, the sum of all of the interatomic interactions involving both protein and solvent molecules, under a prescribed set of conditions, is such that the Gibbs free energy of the whole system is at a minimum. If there is an input of energy into the system, e.g. heat, these interactions change accordingly. The interplay between solvent molecules and the polypeptide chain is crucial in determining the protein conformation. The protein structure we are most familiar with, referred to as the folded or biologically active structure, is usually attained under a physiological set of conditions; this conformation is also referred to as the *native state*. Because of its ability to carry out its assigned function in biological systems, it is this subset of protein structure that we are usually concerned with. The amino acid sequence is responsible for "programming" the conformation of the native state; recent evidence suggests that it is also a major determinant of the conformations of the *denatured state* (Dill & Shortle, 1991). The plural is used because the denatured or unfolded state should be viewed as a distribution of many microstates that change with the conditions of the solution and with the protein sequence. Indeed, this can also be said for the folded state (Honeycutt & Thirumalai, 1992), though the ensemble of folded conformations is small in comparison to the denatured state. The pathway by which a protein attains its biologically active conformation from the denatured state has come to be known as 'the protein folding problem'. Before we can discuss how protein structure is affected under different conditions, and the movement between various states, it is necessary to describe the various forces involved in stabilizing or destabilizing these states.

1.2 STABILIZATION ENERGIES OF PROTEIN CONFORMATION

Under a defined set of conditions, the native and denatured states exist in a dynamic equilibrium. The equilibrium constant K, for this reversible reaction is determined by the free energy difference ΔG, between the two states. In general, under physiological conditions, this free energy difference amounts to only about 5-15 kcal/mol protein (Pace, 1975). Even so the fraction of protein molecules in the denatured state under such conditions is extremely small, in the order of 10^{-3} to 10^{-11}. Altering the conditions by the addition of denaturants, heat, change of pH or pressure, alters the equilibrium distribution of the two-states. From equilibrium denaturation studies, the unfolding/refolding reaction of most small proteins can often be represented by the two-state model $N \Leftrightarrow D$, where N and D represents the native and denatured states, respectively. The two-state model suggests that only the native and denatured states are present in significant proportions throughout the denaturation transition. Due to the apparent cooperativity of the unfolding process, intermediates are not readily detectable in equilibrium studies of most small single-domain proteins. However, there are now many reported examples of proteins which deviate from a simple two-state equilibrium (Kim & Baldwin, 1990).

The stability of a protein is defined as the difference in free energy between the native and denatured states. The marginal stability of the native state over the array of denatured states, is due to the difference between two large energy values that are delicately balanced; the free energy of the non-covalent interactions in the folded state (mainly arising from interactions between the atoms of the protein), minus the free energy of the non-covalent interactions in the unfolded state, arising mainly from solvation energies. More specifically, this refers to the balance of forces primarily contributing to stabilization of the native state, namely hydrophobic interactions, hydrogen-bonding, van der Waals interactions and electrostatics (classical ion pairing), and those opposing stabilization, namely conformational entropy and classical charge repulsions (Dill, 1990). Early work examining the contributions of these forces toward protein stability, relied on the use of simple

chemical model systems. Amino acids sequestered from the solvent in the folded protein were emphasized, since these groups presumably undergo the largest changes in environment during folding (Tanford, 1968, 1970; Pace, 1975). Using the free energy values determined from thermodynamic studies of model systems the stabilizing contribution of each amino acid could be approximated. Some of the assumptions made in these early works on model systems may have led to slightly erroneous values of the energetics of protein folding (Sharp et al., 1991). More recently, site-directed mutagenesis of selected proteins has been used to determine if data from model systems accurately describe the contributions of specific interactions. There is still much controversy about the magnitude of the contributions of each interactive force in the stabilization of the folded state. The following section summarizes the current lines of work on the problem.

1.2.1 Electrostatic Interactions

There are two different ways in which electrostatic interactions can affect protein stability. (i) *Classical* electrostatic effects are the nonspecific repulsions which arise when a protein is highly charged, for example, at extremes of pH (Tanford, 1961). No electrostatic contribution to protein stability is expected near the isoelectric point. As the net charge on the native protein is increased by increasing the acidity or basicity of the solution, the increasing charge repulsion will destabilize the folded protein because the charge density on the folded molecule is greater than on the unfolded molecule. A recent examination of the pH dependence of the urea and GuHCl denaturation of ribonuclease A and ribonuclease T1 revealed that electrostatic interactions among the charged groups make a relatively small contribution to the conformational stability of these proteins (Pace et al., 1990). (ii) *Specific* charge interactions can also affect protein stability. When oppositely charged amino acids are in close spatial proximity (< 3.5Å), ion pairing (salt bridging) can occur. Charged residues in protein molecules are usually located on the surface (Rashin & Honig, 1984). The relative few which are buried are often found to be catalytically or

functionally important [e.g., Baldwin & Chothia (1979); Kossiakoff (1983)]. Recent studies have shown that few ion pairs are buried in the interiors of proteins; on average, only about one ion pair per 150-residue protein is buried (Barlow & Thornton, 1983). The strength of electrostatic interactions is variable, depending on the location in the protein structure. Internalized salt-bridges can contribute up to 3 kcal/mol to the stabilization of the native folded state (Fersht, 1972), whereas a single solvent-exposed salt-bridge only contributes 0.16 to 1 kcal/mol (Brown et al., 1978; Horovitz et al., 1990). Site-directed mutagenesis was used to neutralize three of the negatively charged surface residues located around the calcium binding site of bovine calbindin D_{9k} (Akke & Forsén, 1990). The calcium-free form of each mutant was more stable towards unfolding relative to the wild-type, with the increase in stability ranging from 0.1 to 1.2 kcal/mol. The absence of the local electrostatic repulsion present in the wild-type calbindin, increases the stability of the native structure of the mutant. The opposite effect was seen by introducing a calcium binding site into human lysozyme (Kuroki et al., 1989); the increased charge density of a mutant lysozyme in which two neutral residues were replaced by aspartic acids, destabilized the apo-form of the protein. The holo-form of the mutant, however, was more than 10°C more stable than the native lysozyme.

Twenty per cent of the buried charged groups do not form ion pairs and are solvated, instead, by hydrogen bonds (Rashin & Honig, 1984). The burial of an isolated charge in the nonpolar protein interior can be energetically costly. Various theoretical calculations (Gilson et al., 1985; Dao-pin et al., 1989; Sternberg et al., 1987) using a dielectric constant ranging from 2 to 8, have predicted that it would cost 10-40 kcal/mol to bury a charge in a protein interior (Gilson et al., 1985). To determine the energetic and structural consequences of placing a charged group within the core of a protein, two "buried charge" mutants, Met102→Lys (M102K) and Leu133→Asp (L133D) were constructed in phage T4 lysozyme (Dao-pin et al., 1991). The destabilization of the structure of the M102K mutant relative to that of wild-type increased from 2.2 kcal/mol at pH 10.4 to 8.9 kcal/mol at pH 3.0. Less

energy was required to bury the lysine in its uncharged form (i.e., at high pH) than at low pH where the lysine is protonated. The destabilization of the structure of the L133D mutant was not so pH-dependent, ranging from 3.7 to 6.9 kcal/mol over the same pH range. Insertion of polar residues into the hydrophobic core of the N-terminal domain of λ repressor caused significant destabilization of the native structure (Lim, et al., 1992). Thermal- and GuHCl-induced denaturation curves of these "polar mutants" were typical of a non-cooperative denaturation transition. In the absence of denaturants the protein had the characteristics of molten globule states: native-like secondary structure, yet having a tertiary structure similar to the unfolded state (Kuwajima, 1989). Disruption of the intricate "packing" arrangement of the hydrophobic core is likely to be the main reason for the loss of stability in these cases; placement of an unpaired charged residue exacerbates the disruption and stability loss.

Electrostatic interactions are also important in stabilizing α-helices. The peptide bond has a substantial dipole moment and in an α-helix the peptide dipole moments add end-to-end across the hydrogen bonds to generate a macrodipole with the positive pole at the N-terminus and the negative pole at the C-terminus (Wada, 1976; Hol, 1985). Many proteins fold with their α-helices aligned in an antiparallel fashion, resulting in favourable alignment of the dipoles (Ohlendorf et al., 1987). It has been suggested that the helix dipole is responsible for the more frequent appearance of Asp and Glu residues toward the N-termini, and Arg and Lys residues toward the C-termini, of α-helices (Blagdon & Goodman, 1975; Chou & Fasman, 1974). The favourable opposite-charge attraction of the helix dipole with terminal charged residues stabilizes the helical structure. Maxfield & Scheraga (1975) noted that pairs of oppositely charged residues at positions *i* and $i\pm 4$ along helices increase their stability. Using model peptides of repeated blocks of Glu_4Lys_4, the free energy of formation of a single Glu^-—Lys^+ salt-bridge was evaluated to be -0.5 kcal/mol at 4°C and neutral pH in 10mM salt (Lyu et al., 1992), in agreement with the value derived for a single salt-bridge in a helix on the surface of a globular protein.

In summary, electrostatic interactions provide a small but nevertheless important contribution to the stability of the folded state. Under acidic and basic conditions, electrostatic charge repulsions destabilize native proteins. Near neutral pH, ion pairing can stabilize the native state.

1.2.2 Hydrogen Bonding

A hydrogen bond occurs when a hydrogen atom is shared between two electronegative atoms. What is the value of the free energy change for formation of a hydrogen bond? The water-water hydrogen bond in the vapor phase is -6.4 kcal/mol (Weiner et al., 1984). Values of the strength of individual hydrogen bonds in proteins derived from protein engineering studies, range from 0.5 to 1.8 kcal/mol (Fersht et al., 1985). Recently, an average value of 1.3 ± 0.6 kcal/mol per hydrogen bond was obtained from urea and thermal unfolding studies of several mutants of ribonuclease T1 (Shirley et al., 1992). The critical argument is whether hydrogen bonds contribute differently to the folded and unfolded states of proteins, and therefore to stability.

Early discussions of protein structure deemed hydrogen bonding as the most important force contributing to the stability of the native state (Mirsky & Pauling, 1936). The importance of hydrogen bonding in the formation and stability of the α-helix and beta sheet is unquestionable. Baker & Hubbard (1984) found that almost all groups capable of hydrogen bonding are, in fact, hydrogen bonded, either to other protein groups, or to water. Hydrogen bond partners are exchanged during folding. Intramolecular bonds are formed at the expense of intermolecular hydrogen bonds with water. Water molecules are released to interact with each other, and specific water-binding sites are formed on the protein (Alber, 1989). Hydrogen bond strength is extremely sensitive to the geometric arrangement of the bond angles (Scheiner et al., 1986). However, the distribution of hydrogen bond angles in proteins is similar to that observed in small-molecule compounds (Baker & Hubbard, 1984). Creighton has suggested that the effective concentration of hydrogen-bonding groups in proteins is likely to be greater than that present in water (110M); intramolecular hydrogen bonds,

therefore, may be significantly more stable than those in water, resulting in a net contribution to the stability of the folded state (Creighton, 1983).

Model studies have not been able to yield a definitive estimate for the contribution of hydrogen bonds to protein stability. Some reports even suggested that hydrogen bonding with water would be preferential [see Dill (1990) for review]. Using a thermodynamic cycle, Dill (1990) has modelled the formation of a hydrogen bond and its concomitant transfer into the hydrophobic interior of a protein. The model compound, *N*-methylacetamide was used to examine the strength of hydrogen bonding in water and various nonpolar solvents. Even though it was shown that hydrogen bonding actually opposed folding, Dill suggests that if the transfer of the donor and acceptor species from water into a nonpolar medium is driven by some other force, such as hydrophobicity, then hydrogen bond formation would be favourable within the folded structure (Dill, 1990). Whereas hydrogen bonding may not assist in the collapse of the unfolded state, it must play a major role in directing the internal tertiary organization of proteins.

Site-directed mutagenesis studies have been hampered by the difficulty in attributing stability changes in mutants solely to hydrogen bonds. Side-chain alterations designed to examine individual hydrogen bond strengths inevitably introduce local changes in the packing (van der Waals interactions), hydrophobicity and electrostatic interactions of the folded state. Fersht's group has recently analysed several mutants of barnase, the small ribonuclease from *Bacillus amyloliquefaciens*, using urea-induced equilibrium denaturation (Serrano et al., 1992a). Mutations involving hydrogen bonding were classified into three groups: (i) isosteric changes involve side-chain substitutions of similar size but different chemical properties (i.e., Thr for Val, Asn for Asp or *vice versa*). (ii) mutations in which the hydrogen bonding group is deleted (i.e., Ser to Ala, Tyr to Phe). (iii) mutations in which multiple hydrogen bonding groups are deleted (Asn to Ala, Asp to Ala). For isosteric and multiple hydrogen bond changes, it was difficult to dissociate the effect due solely to hydrogen bonding from the experimentally determined change in stability. Deletion

of a double hydrogen bond between the buried Ser OH group and main-chain NH and CO groups in the Ser→Ala92 mutation, resulted in a net loss of 2.8 kcal/mol (i.e., 1.4 kcal/mol per hydrogen bond). In this example, the favourable hydrophobic contribution and minimal van der Waals interactions loss due to the mutation, may result in an underestimation of the contribution due to hydrogen bonding. Serrano et al. (1992a) concluded that the contribution of buried non-charged hydrogen bonds will depend on the nature of the residue mutated, the van der Waals contacts it makes and of the number and kind of hydrogen bonds. Shirley et al. (1992) have recently examined the contribution of hydrogen bonding to the stability of ribonuclease T1 (RNase T1). By compensating for hydrophobic (and in one case helix-forming) interactions, an average value of 1.3 ± 0.6 kcal/mol per hydrogen bond was obtained for the 17 representative intramolecular hydrogen bonds. Considering that RNase T1 has 86 intramolecular hydrogen bonds, it was suggested that the hydrogen bonding contribution toward the stability of the protein was comparable to the contribution of the hydrophobic effect.

Hydrogen bonding is crucial in determining the pattern of secondary and tertiary structures in proteins. Consequently, it may play an important role in determining the folding pathway of proteins. Individual hydrogen bonds make a small contribution toward stability with intramolecular bonds being more important. Because of the generally large number of hydrogen bonds in proteins, the total contribution toward stabilizing the folded state may be substantial. Pace and coworkers have also postulated that hydrogen bonding may be important in stabilizing compact denatured states (Shirley et al., 1992).

1.2.3 Dispersion Forces

Dispersion or van der Waals forces arise from interactions among fixed or induced dipoles. They are significant only at close atomic distances—but not too close. As atomic distances get too close, the electron charge clouds overlap appreciably and electron repulsion dominates. The interiors of proteins are found to

be very closely packed, with about 75% of adjacent atoms in van der Waals contact (Richards, 1974, 1977). This compares to 70-78% observed in crystals of small organic molecules and 58% in liquids such as water (Bello, 1978). The total number of van der Waals contacts in the denatured state, at any instant, would be expected to be lower than that in the folded state because of the transient nature of the peptide-water interactions. The additional stabilization of the folded state provided by hydrogen bonds and the hydrophobic effect would maintain the proximity of adjacent atoms, necessary for van der Waals contact.

Amino acid substitutions which affect packing of the interiors of proteins can reduce stability. Unfortunately, it is almost impossible to dissociate forces due to van der Waals interactions from those due to the hydrophobic effect and hydrogen bonding. Cavities in proteins are thought to be destabilizing because they reduce the relative contact surface of the folded state. When a bulky residue such as leucine is replaced with alanine, many favourable van der Waals contacts in the folded protein are often lost. The recent X-ray structure determination of several "cavity-creating" mutants of phage T4 lysozyme (Eriksson et al., 1992a) has verified previous predictions about the plasticity of proteins (Lim & Sauer, 1989). The removal of a wild-type side-chain in the core of a protein, e.g., Leu99→Ala, allowed some of the surrounding atoms to move toward the vacated space, but a cavity always remained (Eriksson et al., 1992a). The destabilization of the protein was found to be the sum of a constant energy term, equivalent to the difference in hydrophobicity of the wild-type and mutant amino acid replacement, and a second energy term that depended on the size of the cavity created by the substitution. Loss of van der Waals contacts was attributed to the cavity-dependent part of the destabilization. Destabilization due to the formation of the cavity was of the order of 24-33 cal/mol/Å^3 or in terms of cavity area, 20 cal/mol/Å^2. It was also shown that the cavity in the Leu99→Ala mutant was able to bind a benzene molecule (Eriksson et al., 1992b). The binding of benzene restored some of the stability to the mutant, increasing the melting temperature by

6°C. This could possibly be due to an increase in van der Waals contacts between the benzene molecule and residues on the periphery of the cavity site.

Dispersion or van der Waals forces individually contribute very little to the stabilization of the folded state. However, due to their ubiquitous nature and reliance on tight packing, they may play a crucial role in stabilization of the folded state. They may even be important in stabilization of the compact denatured state observed in the early stages of refolding (Kuwajima, 1989).

1.2.4 Disulphide Bonds

Disulphide bonds make large contributions to the stability of some globular proteins by decreasing the conformational entropy of the unfolded state (Anfinsen & Scheraga, 1975). The most substantial stabilization is expected by connecting residues that are distantly located in the amino acid sequence (Pace et al., 1988). This is substantiated by the fact that disulphide bonds linking N- and C-terminal regions have been shown to occur rather frequently in natural disulphide-containing proteins (Thornton, 1981). Disulphide bonds have been genetically engineered into many proteins, including T4 lysozyme (Perry & Wetzel, 1984; Wetzel et al., 1988; Jacobson et al., 1992), subtilisin (Mitchinson & Wells, 1989) and dihydrofolate reductase (Villafranca et al., 1987), to increase the stability of the native state. Not all of these have resulted in increased stabilization. The T4 lysozyme containing the engineered disulphide bridge between residues 21 and 142, is the most stable of the lysozyme variants, increasing the melting temperature of the oxidized form by 11°C at pH 2 (Matsumara & Matthews, 1989). The disulphide bond links flexible parts of the protein thus avoiding molecular strain on the folded state. A disulphide bond does not have to make the folded state more rigid in order to be effective in increasing stability (Jacobson et al., 1992).

Disulphide bonds may stabilize a folded conformation that is no longer thermodynamically stable. A classic example is that of insulin which is synthesized in the cell as an inactive precursor that folds and forms disulphide bonds. Proteolytic

cleavage converts the precursor to the mature insulin. Mature insulin loses its activity upon reduction of its disulphide bonds, due to the irreversible loss of its native fold.

Recently, using thermodynamic data previously determined on a set of six proteins (Privalov & Gill, 1988), Doig and Williams have suggested that at room temperature, disulphide bonds actually destabilize folded structures entropically, but stabilize them enthalpically to a greater extent (Doig & Williams, 1991). Disulphide bonds are known to decrease the hydrophobic effect by reducing the exposure of non-polar side-chains to water in the unfolded state (Greene & Pace, 1974). Because of this reduction in exposure of non-polar side-chains, Doig and Williams suggest that there is a decrease in the amount of water ordered by the unfolded state. Solvation of randomly coiled peptides requires the ordering of water molecules around the exposed hydrophobic sites (see below in section on hydrophobic effect). Disulphide bonds decrease the unfavourable "hydrophobic component" of the entropy of the unfolded state. It was calculated that the mean entropic stabilization of the unfolded state per disulphide bond is about five times larger due to the hydrophobic effect than the mean entropic stabilization due to the classical conformational entropy term (see 1.2.6 below). Their reasoning for an increase in the enthalpy term for folding is less convincing. They suggest that disulphide bonds restrict the hydrogen- and van der Waals-bonding network in the constrained unfolded state. Irrespective of this, the value they obtain for stabilization of the folded state is about 3 kcal/mol per 15-residue loop forming disulphide bond, in excellent agreement with the previously obtained mean experimental value (Pace et al., 1988).

Disulphide bonds do stabilize the folded state of proteins. However, at present, there is some disagreement in the literature as to how they exert this stabilizing effect.

1.2.5 The Hydrophobic Effect

One of the most obvious features of globular protein structures is that the non-polar side-chains are sequestered into a core, largely avoiding contact with water. In

addition, the polar side-chains tend to be located on or near the "surface". This bipartite distribution was predicted by Kauzman in 1959, before the first X-ray crystallographic structure of any protein was determined. Kauzmann referred to the interaction of the non-polar groups in the protein interior as "hydrophobic". There is now strong evidence to suggest that hydrophobicity is the dominant force that stabilizes the folded state of proteins.

Hydrophobicity can be defined phenomenologically in terms of the low solubility of non-polar molecules in water. Let us consider the solvation of a small non-polar model compound in water. At the molecular level, the transfer of a non-polar solute into water results in the ordering of water molecules around the non-polar groups. However, water molecules prefer to hydrogen bond with each other, rather than be arranged around the non-polar solute. This organization of water molecules around the solute has been referred to as an "iceberg" or clathrate (Nemethy & Scheraga, 1962; Muller, 1990). At room temperature, the ordered "water cages" surrounding the non-polar solute principally populate a low-energy, low-entropy state. To free the bound water molecules, and minimize the unfavourable interactions with water, the non-polar molecules aggregate. The entropy of the system increases due to the release of the bound water molecules. An increase in entropy results in the favourable decrease in the free energy of the system. Because of this, the hydrophobic effect is largely entropy driven at room temperature [at 140°C it is extrapolated to be enthalpically driven (Privalov & Gill, 1988)]. In considering proteins, the same principles apply. One minor difference is that the various non-polar groups are part of the same polypeptide (unless the protein concentration is high). In aqueous conditions, the unfolded state is energetically unfavourable and the protein folds.

The thermal unfolding of proteins involves a large increase in the heat capacity, characteristic of non-polar exposure (Privalov, 1979; Baldwin, 1986). The enthalpy and entropy of folding strongly decrease with temperature, resulting in a curved free-energy versus temperature profile: maximum protein stabilities are in the range of 0-30°C (Dill, 1990). Dill has suggested the most unambiguous definition of

hydrophobicity is in reference to non-polar transfers from non-aqueous media into aqueous media: (i) that are strongly disfavoured and (ii) whenever there is a large associated increase in heat capacity (Dill, 1990). The "ordering of water" (as described above) is appropriate for describing the situation at room temperature, but not over the broader range of temperatures.

The "oil-drop" concept of a protein molecule originated from early work on simple model compounds (Cohn & Edsall, 1943). The solubility of hydrocarbons and amino acids has been studied extensively both in water and in organic solvents including cyclohexane, ethanol, octanol and dioxane (Wolfenden et al., 1981; Nozaki & Tanford, 1971; Fauchère & Pliska, 1983; Kyte & Doolittle, 1982; Rose et al., 1985). By measuring the free energy that is gained by moving an amino acid from a solvent that models the protein interior, to water, it is possible to assign to each amino acid side-chain a value for its hydrophobicity i.e., its contribution to the hydrophobic effect. The difficulty is in deciding which solvent best characterizes the interior of a protein. A concensus derived from many measurements is that the transfer of an aliphatic hydrocarbon from a non-polar solvent to water, costs about 20-30 cal/mol/Å^2, where the area is defined as the solvent-accessible area (Lee & Richards, 1971). Similar measurements have been made to determine the free energy of transfer of amino acids and the peptide unit into aqueous solutions containing protein denaturants such as urea or guanidine hydrochloride [GuHCl] (Nozaki & Tanford, 1963, 1970; Pace, 1986). Tanford used these values to quantitatively describe the GuHCl and urea denaturation of proteins (Tanford, 1970). These denaturants decrease the hydrophobic effect, and this is likely to be the basis of their denaturing action (Creighton, 1983).

Site-directed mutagenesis experiments combined with thermal- and denaturant-induced denaturation measurements, have been used to dissect the contributions of individual amino acids to the hydrophobic effect. Substitutions of buried or partly buried non-polar residues in several proteins (Yutani et al., 1987; Kellis et al., 1988; Matsumara et al., 1988; Shortle et al., 1990; Sandberg &

Terwilliger, 1991; Serrano et al., 1992a) have shown that the change in conformational stability between the wild-type and mutant can be related to the free energies of transfer (Nozaki & Tanford, 1971; Fauchère & Pliska, 1983) and/or accessible surface areas of the individual substituted residues (Richards, 1977). However, some of these mutant studies have shown that solvent transfer experiments may underestimate the hydrophobic effect (Shortle et al., 1990; Serrano et al., 1992a; Eriksson et al., 1992a). Truncation of buried hydrophobic side-chains by a single methylene group (e.g., from the mutation of isoleucine to valine) can result in a loss of stability to the folded state of between 1 and 2.5 kcal/mol (Shortle et al., 1990; Serrano et al., 1992), with an average of about 1.5 kcal/mol (Serrano et al., 1992a). In terms of accessible surface area of the hydrophobic residues, this equates to a contribution of between 45 and 60 cal/mol/Å^2 toward protein stability i.e., 2-3 fold higher than that seen from solvent transfer experiments. Recently, a new estimate for the energy transfer of aliphatic compounds from hydrocarbon solvent to water, which takes into account changes in volume entropy (Sharp et al., 1991), has given a value of 46-47 cal/mol/Å^2. This value is closer to the experimental results obtained from mutagenesis studies. Shortle had previously questioned the validity of solvent transfer data by asking how good a model a dilute solution is for the transfer of a hydrophobic side-chain from its environment in the denatured state into the protein interior (Shortle et al., 1990). In contrast, Matthews and coworkers have provided a sound model for the effects of truncation of hydrophobic residues in the protein core, based on stability measurements and X-ray crystallography of each mutant examined (Eriksson et al., 1992a). They suggest that it is not necessary to revise the value of the hydrophobic effect from its accepted value of about 25-30 kcal/mol/Å^2. Rather, the previous discrepancy seen in studies involving mutations made at single sites in the hydrophobic core, can be explained by a constant energy term, approximately equal to the transfer free energy difference between the wild-type and mutant residue (i.e., the hydrophobic effect), and an energy term which increases with the size of the cavity formed upon mutation, equal to 20 cal/mol/Å^2. The previously observed

discrepancy is due to failure to take into account the loss of van der Waals interactions upon formation of a cavity.

Hydrophobic interactions play a major role in stabilizing the folded state of proteins. They are also important in stabilizing the unfolded state, especially in disulphide bonded proteins, where non-polar exposure to the solvent is decreased. They are instrumental in forcing the collapse of the unfolded state in the early stages of folding, resulting in the non-specific formation of local secondary structure elements (Montelione & Scheraga, 1989; Dill, 1985). Some of these structures may already be present in the unfolded state. There is still some dispute in the literature however, over the magnitude of the hydrophobic effect and about which solvent transfer data is best in modelling the transfer of a residue from the solvent-exposed denatured state to the folded state.

1.2.6 Conformational Entropy

Tanford (1962) and Brandts (1964a,b) calculated that the hydrophobic effect alone would result in protein stabilities in the order of 100-200 kcal/mol at 25°C, approximately 10-fold higher than measured values (Pace, 1975; Privalov, 1979). Therefore, there must be a force of magnitude nearly equal to the hydrophobic driving force which opposes folding. That force is the conformational entropy. If the number of conformations of the folded and unfolded states is F and U, respectively, then the entropy change upon unfolding, ΔS_c, is given by:

$$\Delta S_c = k \, ln \, [U/F]$$

where k is Boltzmann's constant (Baldwin & Eisenberg, 1987). Because the number of unfolded conformations is much larger than the number of folded conformations, ΔS_c is invariably positive. On the other hand, the hydrophobic effect will contribute a large negative entropy upon unfolding. As discussed above (1.2.5), the exposure of hydrophobic residues to water results in the ordering of water molecules around the

exposed sites, decreasing the entropy of the water. The ordering of the water molecules begins to diminish as the temperature is raised, decreasing the magnitude of the "hydrophobic entropy". Note that the two entropy terms are of opposite sign and are nearly equal in magnitude at room temperature. The conformational entropy is favourable and is therefore positive, while the hydrophobic entropy, due to the ordering of the water molecules, is unfavourable and is therefore negative. Also recall that $\Delta G^\circ = \Delta H^\circ - T\Delta S^\circ$, therefore a positive entropy makes $T\Delta S^\circ$ negative and if greater in magnitude than ΔH° , results in a favourable negative ΔG°. As the temperature is raised the magnitude of the total entropy increases, eventually overwhelming the stabilizing forces, resulting in the unfolding of the protein. Therefore, it is the conformational entropy which contributes to the destabilization of the native structure with increasing temperature.

Disulphide links stabilize proteins by reducing the conformational entropy of the unfolded state i.e., the number of possible conformations is decreased by the constraint imposed by the covalent link. As discussed above (1.2.4), the magnitude of the stabilization depends on the size of the loop that is crosslinked (Pace et al., 1988). We have already discussed the effects of disulphide links on the hydrophobic effect and the entropy associated with it (1.2.4). Site-directed mutagenesis has been used to examine the entropy associated with the freedom of the polypeptide backbone ("local entropy"). The introduction of an ala→pro mutation destabilized the unfolded state of T4 lysozyme by 1.4 kcal/mol (Matthews et al., 1987). Restricting the rotation around the polypeptide backbone lowers the entropy of the unfolded state.

Recently, Shortle et al. (1992) have suggested that single site mutations can exert their dominant effects on protein stability by changing the entropy of folding. Using a model for the protein-folding equilibrium ($N \leftrightarrow D_0$, where D_0 is the denatured state under folding conditions) based on short self-avoiding chains of hydrophobic/polar copolymers on a two-dimensional square lattice (Lau & Dill, 1989, 1990; Chan & Dill, 1991), they suggest that a single mutation can have a large effect on the stability of a protein by controlling how many highly compact denatured

conformations (D_0) are available. The entropy of the denatured state under strong folding conditions is therefore highly sequence dependent (Shortle et al., 1992).

It is difficult to determine an estimate of the conformational entropy of a protein. Using an empirical approach, Creighton (1983) has estimated the contribution to the free energy at room temperature in the range of 3.3 to 10 kcal/mol per amino acid residue. For a protein of 100 residues, this means 330 to 1000 kcal/mol must be overcome by favourable interactions in the folded state.

1.2.7 How Do These Forces Dictate The Fold?

How do these forces interact in dictating the unique fold of the native state? Is there a dominant force which influences the outcome? The evidence suggests that the hydrophobic effect is the dominant force of protein folding. Non-local forces encoded within the sequence, rather than local factors involving connected residues, determine the fold. Hydrophobic interaction is the major determinant in restricting the conformational space by bringing together these delocalized sites (Dill, 1990). Hydrophobicity may "select" a relatively small number of compact conformations, whereas hydrogen bonding, van der Waals and electrostatic interactions probably contribute to "fine-tuning" and reinforcing these conformations. The dominant opposing force to folding is the greater conformational entropy of the unfolded state. The folded state is stabilized if under the conditions the stabilizing forces (including hydrophobic interactions, hydrogen bonding, van der Waals interactions, electrostatic forces and disulphide bonding) outweigh the destabilizing effect of the conformational entropy. The marginal stability of proteins under physiological conditions, suggests that a single mutation may tip the balance in favour of the denatured state.

1.3 THE MECHANISM OF PROTEIN FOLDING

The majority of currently favoured protein folding theories suggest that some variant of *hierarchial condensation* is the dominant mechanism (Wetlaufer, 1973; Karplus & Weaver, 1976; Goldberg, 1985; Ptitsyn, 1987). However, there is still some disagreement about whether the final product, the native state, is the most stable possible form, or whether it is the most stable kinetically accessible product. These two types of mechanisms can be distinguished by comparing the distribution of products obtained under identical folding conditions but starting from different distributions of initial states. In the case of thermodynamic control, the final products of refolding are completely insensitive to the distribution of the initial states while, if kinetic barriers are present, the different distributions of unfolded states will be reflected as different distributions of products (Montelione & Scheraga, 1989). There is considerable evidence suggesting that the native structure of small single-domain proteins is the thermodynamically most stable one (Dill, 1987). Perhaps the most convincing evidence in favour of the native state being the most thermodynamically stable state encoded by the amino acid sequence, is the fact that the same protein structure can be achieved *in vivo* and *in vitro*, despite the obviously different folding pathways and conditions.

Refolding of proteins begins from a vast array of unfolded states with varying conformations but of nearly equal free energy. It follows that there must be a large number of folding pathways that converge onto the same native structure, representing the state of lowest free energy. How and when do the different classes of forces stabilize the different folding stages/substructures during protein folding? Let us begin by considering the denatured state.

1.3.1 The denatured state

One of the major obstacles in the elucidation of the protein folding problem is our general conception of the "starting point" in the folding process. What is the nature of the denatured state and how is this related, for example, to the situation in

the living cell? Is the denatured state a random coil, or is their some residual structure present? (Or more pertinent to folding, is there some embryonic structure present?) A random coil could only be stable under extreme conditions such as in high concentrations of protein denaturants (Tanford, 1968, 1970). In fact, there is now considerable evidence suggesting that the unfolded states of proteins are not true random coils under conditions such as extremes of pH, temperature, and even in high concentrations of denaturants (Dobson et al., 1984; Bierzynski & Baldwin, 1982; Haas et al., 1988). It is highly unlikely that under the physiological conditions of the cell, a polypeptide chain would ever approach the structure of a random coil. Even during its vectorial elongation from the protein synthesis machinery, a random coil would be energetically unstable. The partially folded nascent chain is stabilized by interaction with molecular chaperones (Fischer & Schmid, 1990; Ellis & van der Vies, 1991; Langer et al., 1992); Hsp70, a member of the chaperone family has been shown to have a high affinity for synthetic peptides containing a threshold level of hydrophobic residues (Flynn et al., 1991). Therefore, the important question to ask is: when is a polypeptide chain classified as denatured? Protein denaturation usually refers to the cooperative loss of the native structure (Tanford, 1968). Loss of biological activity usually accompanies this loss of structure. However, the cooperative loss of the native structure need not imply that there is no residual structure.

There is considerable experimental evidence that proteins have two classes of denatured conformations: unfolded and compact denatured. The "unfolded" state refers to highly open and solvent-exposed conformations with little or no residual structure; such states are usually obtained under harsh denaturing conditions. The "compact denatured" state is obtained under weaker denaturing conditions. Perhaps the most important of this subset of denatured states, referred to as D_0, is that which is in equilibrium with the native state under physiological conditions (Alonso et al., 1991; Dill & Shortle, 1991). Certain aspects of the amino acid sequence of a protein will determine the extent of unfolding following the cooperative breakdown of the

native state. Proteins of high non-polar content are predicted to form compact denatured states (Alonso et al., 1991). Some of these have been referred to as "molten globule" states (Ohgushi & Wada, 1983; Ptitsyn, 1987; Kuwajima, 1989), "collapsed forms" (Kim & Baldwin, 1990) or "compact intermediates" (Creighton, 1990). These compact forms will be discussed in detail later in this chapter. This implies that the denatured state encompasses a spectrum of conformations, ranging from compact forms to almost fully unfolded forms.

1.3.2 Initiation of folding

Historically, demonstration of the reversible denaturation of proteins required its complete denaturation prior to refolding. The idea was that if you had not completely denatured the protein, you could not fairly claim to have renatured it. Early studies examining the folding pathway used these highly denatured proteins to look at the initial stages of folding in aqueous solution. However, upon dilution, the majority of the folding reaction was completed within the mixing time of the experiment. More recently, peptide fragments have been used in combination with spectroscopic (Montelione & Scheraga, 1989) and two-dimensional NMR techniques (Wright et al., 1988), to examine early folding events. Structural characterization of these fragments is determined under conditions of solvent and temperature favouring folding of the intact protein. If short range interactions are involved in initiating folding, it follows that properly chosen peptide fragments should adopt some degree of ordered structure by themselves in solution. Scheraga and coworkers have suggested that short range interactions are involved in the formation of "chain folding initiation structures" (CFIS), at various sites along the polypeptide chain, in the initial stages of RNase A folding (Montelione & Scheraga, 1989). Several structural motifs, such as reverse turns, helices and hydrophobic clusters have been detected in these isolated peptides (Shoemaker et al., 1987; Wright et al., 1989; Sancho et al., 1992). From an energetics point of view, it makes sense to form local interactions in order to minimize entropic loss. In the fragments, these transient structures are in rapid

dynamic equilibrium with fully unfolded states. Whether these structures actually initiate folding in intact proteins remains to be seen. Stopped-flow experiments examining the refolding of denatured polypeptides detect the formation of a large portion of the secondary structure within the first 10 milliseconds [i.e., the dead-time of even rapid mixing techniques] (Kuwajima, 1989; Kiefhaber et al., 1990; Kuwajima et al., 1991; Chaffotte et al., 1992; Lu & Dahlquist, 1992). Therefore the formation of chain folding initiation sites would have to occur in the first 1-10 milliseconds. The separation of events on such short time scales is difficult to envisage. It is more likely that they form in concert with the hydrophobic collapse of the unfolded state, to form the compact molten-gobule state; energetically, the hydrophobic force could indirectly drive their formation. The fact that secondary structures are stable under folding conditions does not imply that they drive the folding process. Peptide studies have proven useful in investigating the earliest events in protein folding, by avoiding the highly cooperative stages observed when intact proteins are used. However, the results of such studies need to viewed with caution, because of the absence of the dominant force in folding, the hydrophobic effect.

1.3.3 Hydrophobic Collapse: Structure of the Molten Globule State

In the early eighties, Kim and Baldwin (1982) proposed that protein folding is a sequential process beginning with the rapid formation of secondary structure followed by collapse to a compact native-like state, before the tertiary structure is locked into place. This proposal was aptly named the *framework model* of protein folding. The model was based on previous experimental evidence from several small proteins which possessed stable equilibrium "intermediates". These intermediates were denatured states which possessed residual secondary structure. A recurring feature observed in the denaturation transitions of these proteins, including among others, carbonic anhydrase (Wong & Tanford, 1973), α-lactalbumin (Kuwajima et al., 1976) and bovine growth hormone (Burger et al., 1966; Holladay et al., 1974), was that the secondary structure was more stable to denaturation than the tertiary

structure. Ohgushi and Wada (1983) first labelled this intermediate, the "molten globule" state. [I shall also refer to this state as the "compact denatured state" (C). Historical aspects of the discussion require the use of the former term; however both terms refer to the same state.] The molten globule state was shown to possess the following characteristics: (i) a compact fold (a radius of gyration not far from the native state), (ii) pronounced secondary structure, (iii) a propensity to aggregate due to exposed hydrophobic residues, (iv) packing of side-chains more typical of the unfolded state, (v) no thermal transition upon heating [although there is some cooperativity upon chemical denaturation in some cases], (vi) slow but extensive intramolecular fluctuations. In addition to these equilibrium studies, a state identical in many respects to the molten globule state has recently been observed in the early stages of kinetic refolding starting from the fully unfolded state, for a number of proteins (Gilmanshin & Ptitsyn, 1987; Kuwajima et al., 1991; Miranker et al., 1991; Chaffotte et al., 1992; Lu & Dahlquist, 1992). Even though it is rarely observed in equilibrium studies, the molten globule state may be a common form present in the folding of most proteins (Baldwin, 1989).

In equilibrium denaturation experiments, the molten globule state is observed under conditions where the native structure is disrupted in a relatively mild way, by changing pH or temperature in the absence of strong denaturants, or by moderate concentrations of chemical denaturants (such as GuHCl). At present, the best characterized molten globule state is that seen at low pH in α-lactalbumin; this state was originally called the A state (Kuwajima et al., 1976). Acid-induced compact denatured states in other proteins have also been referred to as "A states" in the literature. Similar acid-induced states have been observed in β-lactamase from *Bacillus cereus* (Goto & Fink, 1989), bovine carbonic anhydrase B (Brazhnikov et al., 1985) and bovine growth hormone (Holzman et al., 1990). Unlike α-lactalbumin, β-lactamase requires a high concentration of salt to stabilize the A-state. The protonation of carboxyls at low pH results in intramolecular repulsion, leading to a relatively extended conformation. The addition of anions, either as salts or

surprisingly by the further addition of acid (which supplies the anions e.g., HCl), diminishes the electrostatic repulsion, resulting in the preferential formation of the A state (Goto et al., 1990). Dill and coworkers have predicted that proteins with fewer basic residues will favour the formation of the compact denatured state (C) upon acid denaturation (Alonso et al., 1991). Decreasing the number of basic residues will decrease the net charge on the molecule at low pH, thus stabilizing C.

As mentioned above, the molten globule state has been detected in kinetic refolding studies of a number of proteins. Fast CD measurements of the time-dependent changes in the peptide-absorption region during the kinetic refolding from the denatured state, generally detect the rapid formation of secondary structure within the dead time of the measurement (Kuwajima et al., 1991). The aromatic CD signal, a probe of the specific fixation of the aromatic residues within the tertiary structure, is maximal at later stages of refolding. Therefore, the folding reaction of these proteins can be divided into at least two stages:

$$D \rightarrow C \rightarrow N$$

where D, C and N correspond to the denatured, compact denatured (or molten globule or 'A' state), and native states, respectively. The first stage corresponds to the rapid formation of the molten globule state (D→C), and the second stage is the organization of the specific tertiary structure (C→N) [Kuwajima, 1989]. In general, the burst phase of the peptide-CD signal does not account for all of the secondary structure present in the native state, suggesting that some secondary structure is formed at a later stage of refolding. NMR studies have shown that some of the secondary structure present in the molten globule states of α-lactalbumin (Baum et al., 1989), cytochrome c (Roder et al., 1988) and hen egg-white lysozyme (Miranker et al., 1991) persist during later stages of folding. It appears that protection from hydrogen exchange, the basis of the NMR technique, in the early stages of refolding, occurs in regions of the protein that are well protected from solvent in the final folded

state. For example, in T4 lysozyme, helix E is mostly buried in the native state; this helix is mostly protected from exchange in early folding intermediates (Lu & Dahlquist, 1992). It is not certain how much of the native state secondary structure is already formed in the molten globule state. Decomposition of the CD spectrum into individual contributions from helix, strand, turn, and coil is not without ambiguity, posing difficulties in determining what form of secondary structure is most prevalent in these transient states.

Another feature of the molten globule state is its significant exposure of hydrophobic residues. Hydrophobic probes such as 8-anilinonapthalene sulphonate (ANS) are bound more strongly to the A-state of α-lactalbumin (Mulqueen & Kronman, 1982) and the burst-phase kinetic intermediate of DHFR (Jones & Matthews, 1992), than in the respective N states. The molten globule state of bovine growth hormone has been shown to aggregate at moderate protein concentrations due to the specific interaction between exposed hydrophobic helical regions (Brems et al., 1986). The molten globule state has clustering of non-polar residues but it lacks a hydrophobic core, i.e., the observed secondary structure is loosely packed in an inefficient manner. Human α-lactalbumin can adopt a molten globule conformation when one its four disulphide bonds is reduced. However, in this state the disulphide bonds rearrange spontaneously, but the isomers formed maintain a molten globule-like conformation (Ewbank & Creighton, 1991). This confirms the looseness of the packing of the secondary structure and the lack of tertiary interactions.

Recently, Dill and coworkers have augmented their statistical mechanical theory of protein stability, in order to predict the probability of a protein forming either the compact denatured state (C) or the denatured state (D) under certain conditions (Alonso et al., 1991). In summary they suggested that even though C is closer to the native state in its compactness, it is closer to the D in its heat capacity and in its number of non-polar contacts. Proteins with a higher non-polar content are expected to preferentially form C over the unfolded state. A critical non-polar content, Φ, is required to stabilize C. Below the critical value, the non-polar content is

insufficient to compete against the favourable entropy of the denatured state to cause clustering seen in C. This could explain why α-lactalbumin, which is more hydrophobic than lysozyme, has a compact denatured state whereas lysozyme does not. Increasing the chain length requires more interior core residues and therefore a higher Φ. Therefore shorter chain lengths favour C. This is consistent with the experiments of Shortle et al. (1989) that shortened forms of Staphylococcal nuclease tend to resemble compact denatured states.

What forces are responsible for stabilizing these compact, yet flexible structures? In some proteins, we have seen that they are stable enough to exist not only transiently but at equilibrium. The hydrophobic force must be instrumental in driving the collapse of the unfolded polypeptide into a more compact configuration, in order to prevent the exposure of hydrophobic side-chains to the aqueous solution. However, this collapse may at first be a random collapse, resulting in inefficient packing of the core of the molecule. Many core interactions involve side-chains of secondary structure elements, which may not have formed completely by this stage (<1 msec). The result is a loose core and incomplete secondary structure. Inefficient core packing can have large detrimental affects on protein stability (Lim et al., 1992; Dao-pin et al., 1991; Eriksson et al., 1992a; Sneddon & Tobias, 1992). During refolding the intimate packing of the core is probably organized at a later stage, say 0.1-1 sec. However, even in the few cases where they have been detected at equilibrium, compact denatured states still possess an inefficiently packed core. A compact state may not necessarily infer an increased number of non-polar contacts. Expansion of the native state radius by only 10% can lead to an increase in the number of internal water molecules from 10 or less to a number near 10,000 (Alonso et al., 1991). Recently, Colombo and Rau (1992) measured the changes in protein hydration in the molten globule to coil transition of apomyoglobin. They found that about 100-150 extra water molecules bind to the protein in the transition region, corresponding to an average of 2-3 bound waters per α-helical amino acid in the molten globule. This implies that the non-polar side-chains in the compact denatured

state are already largely solvated by water, and explains the nearly zero enthalpy change (ΔH) and heat capacity change (ΔC_p) for the C→D transition observed in α-lactalbumin and carbonic anhydrase (Ptitsyn, 1987). This is puzzling because on the one hand, the hydrophobic force drives the unfolded molecule to collapse, yet on the other, the number of non-polar contacts does not appear to increase appreciably. The small increase in non-polar contacts is probably due to local clustering. Therefore the compact denatured state screens some of the non-polar surface from water, but also retains considerable conformational entropy. What prevents the thermodynamically favourable hydrophobic collapse from going to completion? Why is water allowed to solvate the exposed hydrophobic sites? In the 'A' state at low pH, the electrostatic repulsion prevents the complete collapse, yet a small amount of hydrophobic interaction keeps the molecule in a compact format. The situation in GuHCl-induced compact states is more complex; the denaturing effects of GuHCl on proteins is poorly understood. It is possible that the preferential interaction of the protein with GuHCl may release some bound water molecules, increasing the entropy of the system. Nevertheless, the free energy difference between C and D is not large in comparison to that between C and N. This explains the rapid exchange between the C and D states at equilibrium.

Contrary to the above, the recent calorimetric evaluation of the energetics of the molten globule state of apo-α-lactalbumin has shown that there is a large $\Delta H°$ and $\Delta C_p°$ between the C and D states at 25°C (Xie et al., 1991; Haynie & Freire, 1992). Note that the parameters $\Delta H°$, and $\Delta C_p°$ are the intrinsic enthalpy and heat capacity differences, respectively. Using differential scanning calorimetry, these values can be dissociated from the respective apparent enthalpy and heat capacity changes (i.e. ΔH and ΔC_p), which contain additional contributions particularly those arising from GuHCl binding. About 82% of the $\Delta C_p°$, and 75% of both the $\Delta H°$ and the entropy difference ($\Delta S°$) of folding, i.e., between D and N, occurs between D and C. Furthermore, they suggest that only 15-19% of the non-polar surface area is exposed in C, and that only 16-20% of the hydrogen bonds present in the native state are

ruptured. This paints an almost entirely different picture of the compact denatured state. The small ΔC_p° between the N and C states suggests that water has not penetrated into the interior of C. The core may be well packed and there is an almost complete arrangement of hydrogen bonding; a very native-like arrangement. Pace and coworkers have recently suggested that hydrogen bonding may be important in stabilizing the compact denatured state (Shirley et al., 1992). These two reports may explain the stability of the prominent secondary structure observed in the compact denatured state, although the magnitude of the ΔH° and ΔC_p° in the denatured to compact denatured state transition is surprising.

1.3.4 The Final Stages of Folding

The final stages of folding involve consolidation of the core, completion of the secondary structure and rearrangement of side-chains to optimize packing. Native-like tertiary interactions begin to appear very soon after the hydrophobic collapse. For most small proteins, the folding reaction is complete within 1 sec, unless *cis-trans* isomerization of proline residues is involved (Brandts et al., 1985; Kim & Baldwin, 1982, 1990). Although the proline hypothesis appears to satisfactorily interpret the presence of slow refolding kinetics for some proteins, in many cases there is a lack of direct evidence for proline involvement in slow refolding processes (Schmid et al., 1986; Herning et al., 1991). Efficient packing of the core and correct alignment of the secondary structure via tertiary structure interactions follow the hydrophobic collapse. In dihyrofolate reductase (DHFR), formation of a native-like hydrophobic cluster around Trp74 immediately follows the formation of the secondary structure (Garvey et al., 1989). Of the five tryptophans in DHFR, Trp74 is the only one contained in one of the eight strands of the β-sheet that forms the structural core of the protein. The correct alignment via inter-strand hydrogen bonding would stabilize the supersecondary structure and consolidate the core. Fersht has suggested that at this stage in folding, tertiary interactions may stabilize and sometimes elongate secondary structures (Serrano et al., 1992b). The exact timing of the formation of the core is

variable between proteins: Goldberg and coworkers detected a rapid phase of ANS binding in the 4 msec burst phase, concomitant with the formation of the majority of the secondary structure, following refolding of the isolated F2-V8 peptide of the tryptophan synthase β chain (Chaffotte et al., 1992). The exclusion of water from the core would increase the hydrophobic interactions and make van der Waals interactions more favourable. This may also promote the formation of peptide hydrogen bonds, by removing an active competitor for the peptide NH and CO groups (Baldwin, 1989). So it appears that completion of the secondary structure is dependent on the synergistic effects of water exclusion and tertiary interactions. The correct placement of the side-chains within the layers surrounding the core of the molecule occur late in folding. This is evidenced as restoration of the aromatic CD signal. Formation of the native protein is accompanied by enzymatic or substrate binding activity. Methotrexate, a stoichiometric inhibitor of DHFR only binds in the late stages of folding (Garvey et al., 1989), while a-lactalbumin regains its ability to bind calcium very late in the folding pathway (Kuwajima et al., 1989).

The transition (or activated) state is the species with the highest free energy encountered in the folding pathway. As its occurence is hypothetical, its structure can only be inferred by measuring the effect on the rates of folding and unfolding of varying the conditions or by introducing mutations into the protein. Several studies have suggested that the transition state is a distorted, locally solvent-exposed form of the native conformation (Goldenberg & Creighton, 1985; Segawa & Sugihara, 1984a,b; Chen et al., 1989; Matouschek et al., 1989; Kuwajima et al., 1989). Using over 50 site-directed mutations strategically placed over the whole protein Fersht and colleagues have mapped out a detailed picture of the transition state of barnase (Serrano et al., 1992c). The results suggest that the structure of the transition state is very similar to that of the folded protein. They suggest that the final events in folding are (*i*) consolidation of the hydrophobic cores [barnase has one major and two minor hydrophobic cores], (*ii*) closing of the loops and (*iii*) capping of the N-termini of helices (Serrano et al., 1992c). Energetically, the transition state and native state have

similar heat capacities, suggesting the exclusion of water from the interior of the molecule (Chen et al., 1989; Segawa & Sugihara, 1984a). However, the high enthalpy difference between the native and transition states seen in T4 lysozyme (Chen et al.,1989) and hen lysozyme (Segawa & Sugihara, 1984a) is consistent with the breakup of some of the energetically favourable side-chain interactions which stabilize the native state.

1.3.5 Summary of Protein Folding

In summary, when a small, single domain protein refolds from a denatured state, there is a very rapid collapse to a compact state concomitant with the formation of a substantial amount of secondary structure. Rearrangement resulting in efficient packing of the hydrophobic core, completion of secondary structure, removal of water to the exterior and positioning of side-chains in the correct native-like configuration completes the process. This scheme is consistent with the hierarchial condensation process proposed as the *framework model* by Kim & Baldwin a decade ago. There are still many questions to be answered, in particular, the role of the compact denatured state and its relation to the unfolded and native states.

1.4 PORCINE GROWTH HORMONE: A SUITABLE MODEL PROTEIN FOR STUDYING PROTEIN FOLDING AND STABILITY.

Before discussing the folding, conformation and stability of porcine growth hormone, it is worthwhile reviewing some its structural features and its position within the growth hormone family of proteins. Previous work on the folding and stability of other members of the GH family will also be briefly introduced. A more complete review of this area of research is presented in Chapter 4.

1.4.1 Growth Hormone Structure

Growth hormone (GH), also known as somatotropin, is produced in the pituitary gland of all vertebrates and is an important endocrine factor for normal

growth and lactation in mammals (Li & Evans, 1944; Isaksson et al., 1985). Together with the prolactins (pRL), and placental lactogens (PL), GHs are part of a large family of hormonal proteins which share a number of common biological, immunological, and structural features (Nicoll et al., 1986). Most of the members of the vertebrate GH/pRL/PL family are globular proteins of about 190-200 amino acids in length. Some of the teleost GHs are smaller in length, e.g., flounder GH has only 171 amino acids (Watahiki et al., 1989). The most studied of the GHs, human growth hormone (hGH) is a polypeptide of 191 amino acids (Niall, 1971), while pGH contains 190 amino acids (Seeburg et al, 1983). All of the GHs and PLs have two disulphide-linked loops; a small loop near the carboxyl terminus, and a larger loop comprising as much as 70% of the amino acid residues. In addition to these, the mammalian pRLs contain a second small loop at the amino terminus. A striking feature of all of these proteins is their high α-helix content, which ranges from 45 ± 5% for human-PL to 55 ± 5% for hGH and ovine-pRL (Bewley et al., 1969). The recent X-ray crystallographic study of methionyl-pGH has confirmed the presence of four α-helices which comprise 54% of the amino acid sequence (Abdel-Meguid et al., 1987).

Figure 1 shows the alignment of the amino acid sequence of GHs from different species and the position of the four α-helices relative to these sequences (Abdel-Meguid et al., 1987), while Figure 2 shows the alignment of the GHs with the PLs and pRLs from several species, (Watahiki et al., 1989). Although there is extensive homology among all of the mammalian and avian GH sequences, with 98 invariant residues (Figure 1), it is clear that the α-helical regions show the greatest homology, with about two-thirds of these residues lying within the four α-helices. This suggests that these invariant residues are essential in maintaining the structural integrity of these hormones. It should be noted that the invariance is even greater amongst the mammalian GHs if we disregard the primate sequences e.g., ovine and bovine GH have only two non-identical residues. The primate sequences could almost be put in a subclass of their own. The number of invariant residues decreases to 37 if

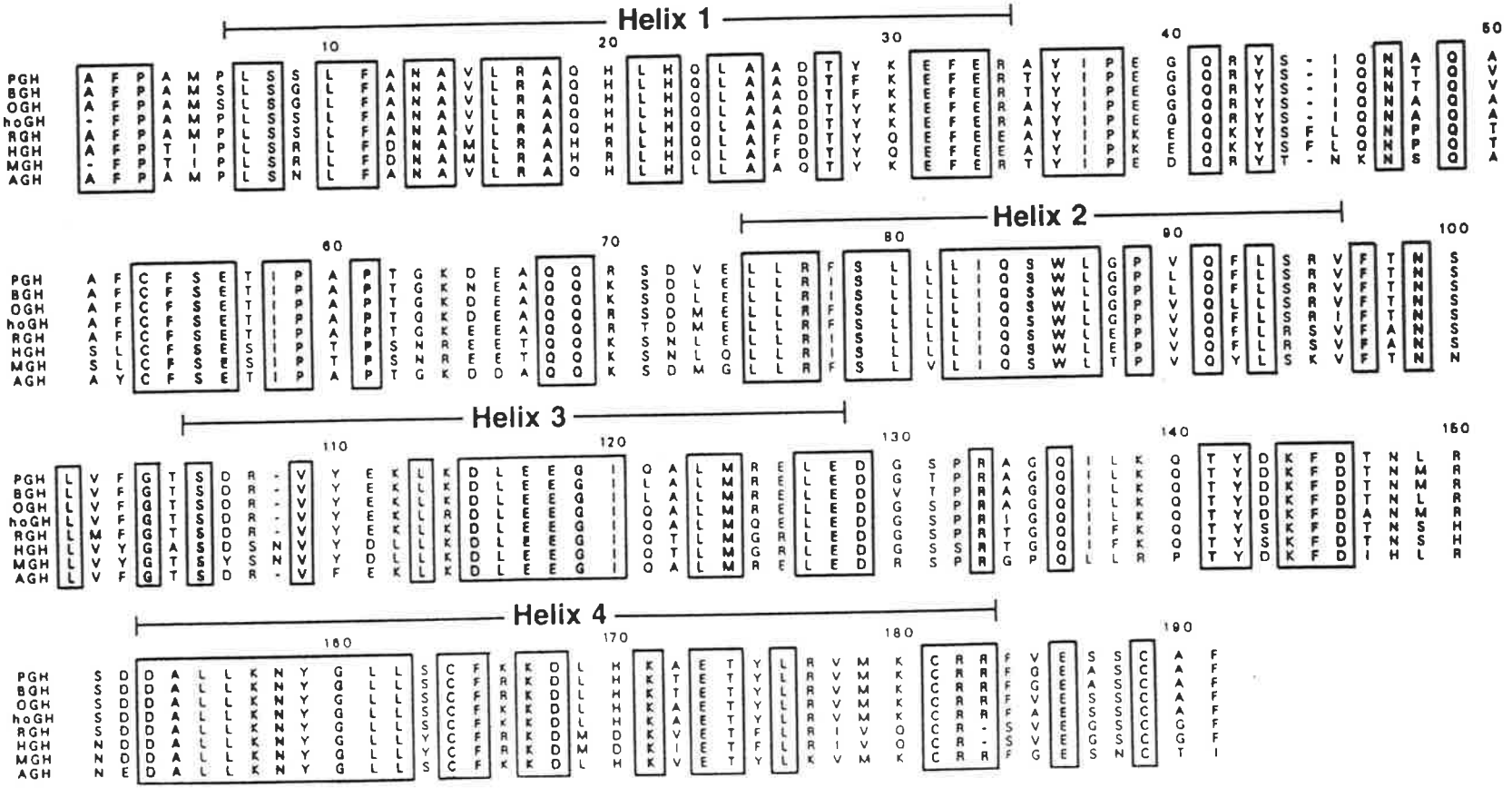

Figure 1. Amino acid sequences of porcine growth hormone (PGH; Deeburg et al., 1983), bovine growth hormone (BGH; Graf & Li, 1974), ovine growth hormone (OGH; Li et al., 1972), horse growth hormone (hoGH; Zakin et al., 1976), rat growth hormone (RGH; Page et al., 1981), human growth hormone (HGH; DeNoto et al., 1981), monkey growth hormone (MGH; Li et al., 1986), and avian growth hormone (AGH; Souza et al., 1984). Boxed amino acid residues are identical in all eight sequences. The positions of the pGH four helices are indicated above the amino acid sequences. Adapted from *Abdel-meguid et al., 1987.*

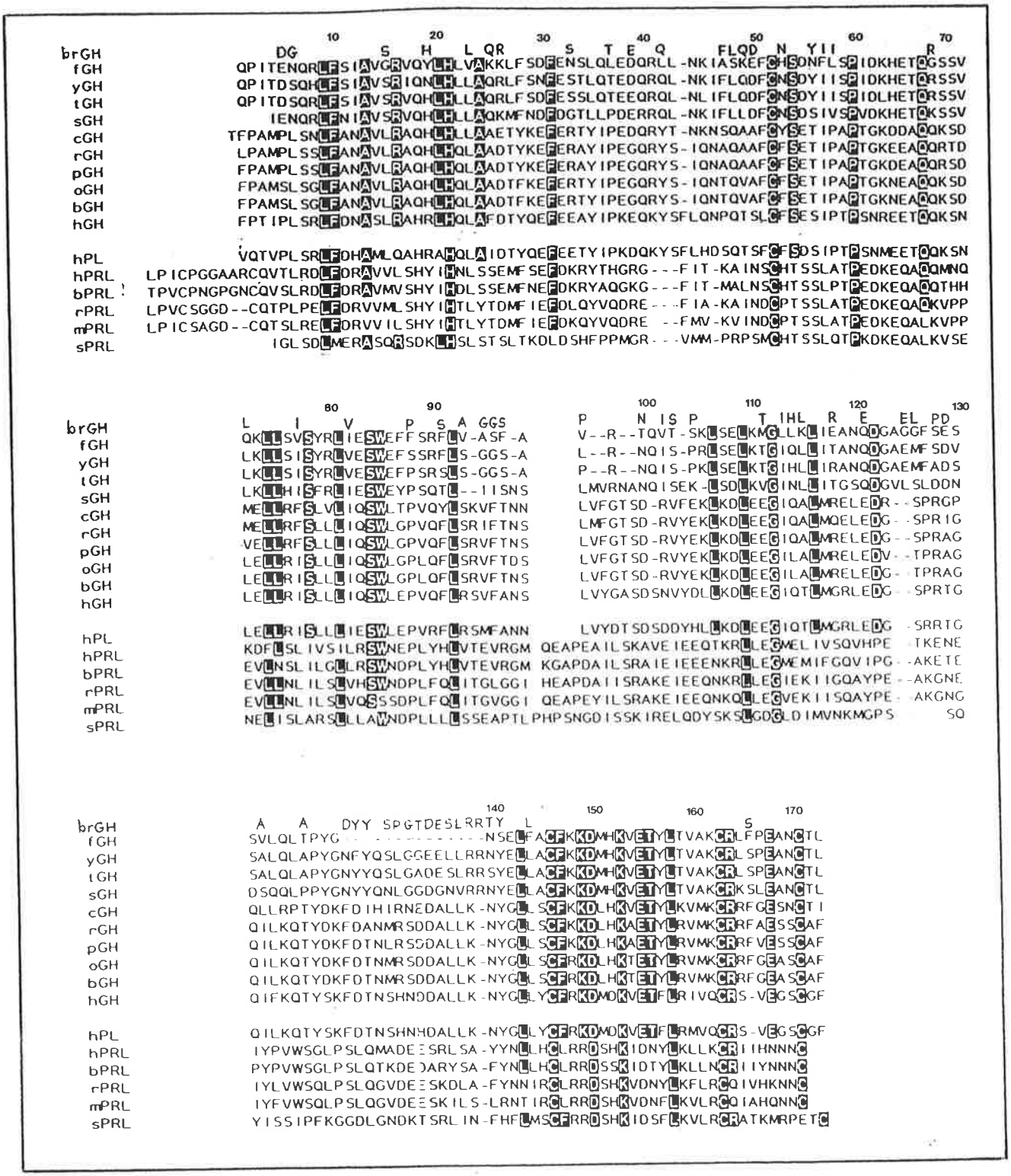

Figure 2. Conserved amino acids in GHs and other members of the gene family. The amino acid sequences of bream (brGH), flounder (fGH), yellowtail (yGH), tuna (tGH), salmon (sGH), chicken (cGH), rat (rGH), porcine (pGH), ovine (oGH), bovine (bGH), and human (hGH) growth hormones, human placental lactogen (hPL), and human (hPRL), bovine (bPRL), rat (rPRL), mouse (mPRL) and salmon (sPRL) prolactins. For the brGH sequence, only the residues which differ from the flounder sequence are shown. Residues conserved among the GHs are shown in black boxes. The numbering system is according to the flounder sequence. Adapted from *Watahili et al., 1989*.

the teleosts are included in the analysis (Figure 2). Once again these invariant residues lie within important structural and functional regions of the molecule. There is a high degree of homology within the teleost GHs, e.g., Australian black bream GH (brGH) shares 94% and 87% sequence identity with tuna GH and yellowtail GH, respectively (Knibb et al., 1991; Watahiki et al., 1989). Many of the residues that are not identical among the GHs, pRLs and PLs (Figure 2) involve replacements which are highly acceptable or conservative in terms of their physicochemical properties (Dayhoff, 1975).

The three-dimensional structure of a recombinant methionyl-pGH has been determined by X-ray crystallography (Abdel-Meguid et al., 1987). The structure comprises four antiparallel α-helices arranged in a tightly packed left-twisted helical bundle connected by largely unstructured loop regions (Chapter 4, Figure 1). Four α-helix bundles are a quite common arrangement of predominantly α-helical proteins (Weber & Salemme, 1980). What is unusual about pGH is the connectivity of the helices; 80-90% of four α-helix bundles have a simple up-down-up-down connectivity (Richardson & Richardson, 1989), whereas pGH has an up-up-down-down connectivity. The recent NMR determination of the structure of human interleukin-4 (hIL-4) has revealed a four-helix bundle structure with the same helix connectivity as pGH (Garrett et al., 1992). hIL-4 has three disulphide bonds which maintain the native structure in a very tight and stable configuration. Interestingly, along with pGH, they are the only naturally occuring helix bundle proteins which possess disulphide bonds [a *de novo* designed four-helix bundle protein, "Felix", has one inter-helix disulphide bond (Hecht et al., 1990]). The unusual helix connectivity of pGH does not affect the alignment of the helix macro-dipoles; helices 1 and 4 and helices 2 and 3 are arranged in pairs with their macro-dipoles aligned favourably. This contributes to the stability of the helix bundle. The X-ray structure of hGH has also recently been determined (de Vos et al., 1992); the structure, not surprisingly, is very similar to that of pGH. The only minor difference is an extra short helix in the segment between helices 2 and 3 which has an omega loop conformation in pGH.

Determination of the hGH structure confirmed previous suspicion that the GHs would all have a similar three dimensional structure. Although their structures have not been determined, the prolactins and placental lactogens are expected to have similar structures to the GHs. The stable and nearly ubiquitous α-helix content may be thought of as the architectural "core" or "foundation" of all these structurally related molecules. It is the tertiary structure which provides the different internal "plan" and external "facades". These finer details in turn determine the functionality and species specificity of this group of hormones.

The arrangement of the four α-helix bundle in pGH results in a tightly packed globular structure. [Unfortunately, the X-ray coordinates of the pGH structure (Abdel-Meguid et al., 1987) have not yet been released. Therefore, it is very difficult to define residue interactions within the molecule definitively.] The amphipathic helices have their hydrophobic faces facing inwards to form the hydrophobic core of the molecule. The central portion of helix-2, mostly buried in the core of the protein (Chapter 4, Figure 1), is almost completely made up of hydrophobic residues (Figure 1). A single conserved tryptophan residue, located halfway along this helix, forms part of the hydrophobic core of the molecule (Carlacci et al., 1991). The UV absorption and fluorescence properties of this residue make it useful as an intrinsic probe for monitoring the unfolding of the protein. In hGH, the core is mostly made up of hydrophobic residues with the exceptions of Ser79 and Asp169 (de Vos et al., 1992). These residues have their side-chain oxygens hydrogen bonded to nearby residues in the core. Other hydrophobic clusters in the hGH structure can be found between the four-helix bundle and the connecting loops.

The obvious feature of the GHs is their high α-helix content. The amphipathic nature of the helices suggests that the hydrophobic effect would be instrumental in stabilizing the tightly packed conformation. The connecting loops may also be important in stabilizing the bundle, via hydrogen bonding with the side-chains of the helices or as seen in hGH, via hydrophobic interactions. The greater sequence divergence in these connecting loop regions may explain the difference in stability

between the GH species (see Discussion in Chapter 4). The disulphide bonds, in particular the Cys53 to Cys164 link which connects helix-4 to the long unstructured loop between helices 1 and 2, stabilize the structure by decreasing the conformational entropy of the unfolded state. In addition, the Cys53-Cys164 bond promotes the favourable interaction between the long connecting loop and helix-4. The favourable electrostatic alignment of the helix macrodipoles also contributes, albeit minimally, to the stability of the folded state. The small species sequence variation in the helical regions, results in different intrinsic helix stabilities, i.e., α-helical potentials, which in turn may affect the stability of the whole molecule. It is the variation in the amino acid sequence which determines the overall stability and folding behaviour of the various GH species.

1.4.2 Folding and Stability of Bovine and Human Growth Hormones

Early studies on the pH-induced denaturation of pituitary bovine growth hormone (bGH) detected the presence of an intermediate containing considerable helical structure yet having no measurable tertiary structure. (Burger et al., 1966; Edelhoch & Burger, 1966). Holladay et al. (1974) demonstrated the presence of a similar intermediate in bGH as well as ovine- and rat-GH in the GuHCl-induced denaturation of these hormones. At the time it was thought that the non-coincident denaturation transitions observed in these experiments may be due to the inherent heterogeneity of the pituitary GH preparations. Brems et al. (1985) proved that this was not the case, when they showed that the pituitary- and a homogeneous recombinant-derived bGH had very similar denaturation profiles. It was conclusively shown that the secondary structure of bGH is more stable than the tertiary structure, consistent with the framework model of protein folding (Kim & Baldwin, 1982). Brems' group went on to show that the equilibrium denaturation of bGH is a multistate process in which at least four species are involved: native, a monomeric folding intermediate, an associated form of the monomeric intermediate, and the unfolded protein (Brems et al., 1986; Havel et al., 1986, 1988). Furthermore, the

monomeric folding intermediate was shown to have the characteristics of a molten globule: largely α-helical, with a compact hydrodynamic radius similar to the native state, yet possessing a tertiary structure similar to the unfolded state (Brems & Havel, 1989). This intermediate was also detected in kinetic refolding studies (Brems et al., 1987a); at dilute protein concentrations the refolding rate detected by far-UV CD is faster than the rate detected by UV absorbance, indicating the existence of a kinetic folding intermediate with appreciable amounts of α-helix. At high protein concentrations, the molten globule-like intermediate self-associates. The hydrophobic surface of helix-3 appears to be directly involved in the association process (Brems et al., 1986). A fragment of bGH containing the third helix, was shown to contain helical structure in aqueous solutions (Brems et al., 1987b). Following the partial denaturation of bGH, the hydrophobic face of helix-3 becomes exposed. The exposed face then interacts with similar exposed hydrophobic surfaces on adjacent molecules, to form the associated intermediate (Brems et al., 1986). A Lys112→Leu mutant which expanded the hydrophobic surface of the helix increased the intermolecular association process (Brems et al., 1988).

Unlike the non-human GHs, the denaturation of hGH follows a two-state mechanism with no detectable intermediates (Brems et al., 1990). The apparent absence of intermediates was attributed to their relative instability compared to the native structure. hGH is at least 5 kcal/mol more stable than GHs from other species (Brems et al., 1990). Lehrman et al. (1991) have recently shown that substitution of helix-3 in bGH with the helix-3 sequence of hGH (a protein which does not self-associate) does not completely abolish self-association. This suggested that helix-3 is not the only cause for the association process seen in wild-type bGH. Instead it implied that some more "global feature" of the non-human GHs is responsible for their lower stability and propensity to form stable equilibrium intermediates.

1.5 OBJECTIVES OF THIS STUDY

Equilibrium denaturation of bovine growth hormone deviates from a simple two-state mechanism; stable form(s) intermediate to the native and fully unfolded states are detected in the transition region. Human growth hormone however, is consistent with a two-state denaturation mechanism, with no detectable intermediates. Porcine growth hormone is a protein which shares 91% and 68% primary sequence identity with bGH and hGH, respectively. The specific aims of this study were:

(*i*) produce recombinant pGH and mutants thereof, and recombinant bream and human GH, in sufficient quantity and of a satisfactory homogeneity to carry out the following studies:

(*ii*) examine the guanidine hydrochloride-induced equilibrium denaturation of pGH using a variety of spectroscopic and hydrodynamic probes in order to determine the folding mechanism of pGH.

(*iii*) determine the conformational stability of wild-type pGH, brGH, hGH and various mutants of pGH under a standard set of conditions. The major emphasis was on the effect of site-directed mutations on the stability of pGH.

In the course of this work it was noted that one mutant had markedly enhanced stability. It was then decided to:

(*iv*) examine the effect of the mutation on the equilibrium denaturation and folding mechanism of this mutant.

CHAPTER 2

MATERIALS AND METHODS

2.1 MATERIALS

Water was purified by a Milli-Q apparatus (Millipore, Sydney, Australia). FPLC apparatus, Mono-Q HR 5/5 and Superose-12 HR10/30 columns, Q-Sepharose Fast Flow, Sephadex G-25, and Bioprocess columns were from Pharmacia Biotechnology, Uppsala, Sweden. Cartridge prefilters were from Pall Process Filtration Ltd., Portsmouth, England. The molecular modelling kit was from Labquip, Reading, England. "Ultrapure" GuHCl for circular dichroism experiments was from Schwarz/Mann Biotech, Orangeburg, NY, U.S.A. All other experiments used pure grade GuHCl from Sigma Chemical Company, St. Louis, MO, U.S.A. "Ultrapure" urea was from Merck, Darmstadt, F.R.G. Ampicillin, chloramphenicol, IPTG, acrylamide, bisacrylamide and protein molecular weight standards for size exclusion chromatography were all from Sigma Chemical Company. Protein molecular weight standards for SDS polyacrylamide gel electrophoresis were from Gibco BRL, Garthersburg, MD, U.S.A. All other chemicals were of analytical reagent grade.

2.2 METHODS

2.2.1 Large Scale Bacterial Fermentations

Large scale fermentation of *E.coli* strain JM101 carrying plasmids with a pGH gene or a mutant derivative thereof under the control of the *trc* promoter (Vize & Wells, 1987) was performed at Bresatec by Carol Senn. The following fermentation protocol is essentially the same one used for all GHs used in this thesis.

A single colony was picked off a minimal + 100ug/ml ampicillin plate and inoculated into 20ml of C1 (as below) + 100ug/ml ampicillin and grown at 37°C overnight with vigorous shaking. This was then used to inoculate a 15 litre fermenter for large scale fermentation. The 15 litre fermenter contained a basic solution referred to as C1 media: 1.61 g/L NH_4Cl, 1.22 g/L K_2SO_4, 2.65 g/L KH_2PO_4, 4.33 g/L Na_2HPO_4, 0.63 g/L $MgSO_4.7H_2O$, 20 g/L dextrose.H_2O, 0.004% (v/v) antifoam,

0.004% (w/v) thiamine solution, and trace metals: 20 mg/L $FeSO_4$, 5.1 mg/L $MnSO_4$, 8.6 mg/L $ZnSO_4$, 0.75 mg/L $CuSO_4$, 44 mg/L Na_3 citrate.

During the fermentation further nutrients were added to the fermenter as required: the nutrient feed consisted of 550 g/L dextrose.H_2O, 22.5 g/L K_2SO_4, 4.13 g/L $MgSO_4.7H_2O$, 3.54 g/L KH_2PO_4, 25 g/L Na_2HPO_4. With a starting A_{600} of 0.001, the culture was incubated at 37°C overnight in a pH range 6.9-7.2, and pO_2 46-69%, with 1.0 bar pressure. Doubling times were between 50 and 60 minutes. The cultures were induced with IPTG (0.25mM final) at an A_{600} of 50. The fermentation was terminated 5 hours after induction and stored overnight at 4°C.

2.2.2 Harvesting of Inclusion Bodies

During the induction phase and upon completion of fermentation cells were examined by microscopy to determine the percentage of cells with inclusion bodies. Inclusion bodies were purified by homogenisation and centrifugation. To disrupt the cells, the culture was passed three times through an APV CD30 homogeniser (APV Gaulin Inc., MA, U.S.A.) at 15,000 psi. Purification of the inclusion bodies by continuous flow centrifugation required estimation of inclusion body size to determine the centrifugation flow rate. The Stokes diameter of the inclusion bodies, ranging from between 0.3µm to 0.5µm, was determined using a Joyce Loebl disc centrifuge (Middelberg et al., 1990). The homogenate was passed through a continuous flow Verenosi centrifuge at 9,000 rpm and a flow rate of (inclusion body size/0.4)^2 x 400 ml/min. The harvested inclusion bodies were diluted in 30mM NaCl, 10mM KH_2PO_4 and recentrifuged at a flow rate of (inclusion body size/0.4)^2 x 900ml/min. The resulting concentrated paste of inclusion bodies was collected and either stored in aliquots at -20°C, or used immediately for refolding and purification.

2.2.3 Dissolution, Refolding and Oxidation of Inclusion Body GH

During the early stages of this work, inclusion bodies were routinely stored at -20°C at the end of each fermentation run. Harsh denaturation conditions, (6M

GuHCl), were necessary to dissolve the inclusion bodies prior to renaturation in urea solutions. Subsequently it was found that by processing the inclusion bodies immediately after collection, much gentler conditions could be employed (3.75M urea, pH 11.5). I shall describe both methods used. The following procedures are representative of all GHs used in this thesis unless stated.

2.2.3.1 Dissolution and Refolding/Reoxidation Using 6M GuHCl

Frozen inclusion bodies (25g wet weight) were suspended in 250ml 6M GuHCl, 40mM sodium borate pH 9.1, 10mM DTT, 1mM glycine (assuming an inclusion body dry weight ratio of 50%, this amounts to a protein concentration of approx. 50mg/ml). The suspension was gently stirred at room temperature for up to 2 hours until the inclusion bodies were dissolved. Dissolved inclusion bodies were diluted out 100-fold into 3.75M urea, 25mM sodium borate pH 9.1, 1mM glycine (25L final volume) and allowed to refold and oxidise at room temperature. Refolding and oxidation were monitored by size-exclusion chromatography on a Superose-12 column (Chapter 3, Figures 1a-f). The time allowed for refolding and oxidation varied from 2 to 16 hours. After refolding and oxidation the solution was diluted 4-fold in water (100L final volume) and the pH checked at pH 9.1, prior to chromatography.

2.2.3.2 Dissolution, Refolding and Oxidation in 3.75M urea, pH11.5

Inclusion bodies collected from the continuous flow centrifuge were weighed and directly suspended in unbuffered 3.75M urea, pH 11.5 (with NaOH) with stirring (the final protein concentration was approx. 1.5 g/L). The pH was monitored and maintained at pH 11.5 with 1M NaOH. Refolding was followed by size-exclusion chromatography on a Superose-12 column (Chapter 3, Figures 1a-f). After a period of up to 5 hours, the solution was diluted with 3 volumes of 33mM sodium borate pH 9.1 (pH 8.2 for hGH) and the pH adjusted with 1M HCl to pH 9.1 (or pH 8.2 for hGH).

2.2.4. Large Scale Chromatography

Following refolding and oxidation, correctly folded GH was separated from aggregated and incorrectly folded GH using anion-exchange chromatography. The refolding solution was loaded overnight onto a 113mm i.d. x 45mm, 450ml bed volume column of Q-Sepharose Fast Flow (FFQ) at a flow rate of 80 ml/min. Two Pall cartridge prefilters (10μm and 0.5μm) arranged in tandem removed any slight precipitate present. The column was pre-equilibrated in Buffer A (25mM sodium borate pH 9.1). The column eluent was monitored periodically on a Superose-12 column to check binding of correctly folded GH. Upon completion of loading the column was washed with Buffer A prior to elution of GH with Buffer A + 150mM NaCl at 50 ml/min. Fractions were collected (100 ml) and analysed on the Superose-12 column. Fractions containing monomeric, correctly folded GH were pooled and desalted on a 113mm i.d. x 300mm, 3L bed volume column of Sephadex G-25 Medium pre-equilibrated with 20mM ammonium bicarbonate pH 9.1 (pH 8.2 for hGH), at a flow rate of 50 ml/min. Fractions were collected and analysed on the Superose-12 column and by UV spectroscopy. Pure fractions were pooled and freeze-dried. The lyophilized powder was stored at -20°C.

2.2.5 Monitoring Refolding and Oxidation by Size Exclusion Chromatography

Refolding of GH was monitored on a 10mm i.d. x 300mm Superose-12 column equilibrated in either 100mM Na_2HPO_4 pH 12.0 or 25mM sodium borate pH 9.1 (see 3.2.2). The high pH buffer was preferentially employed at the early stages of refolding to increase the solubility of poorly soluble proteins. Each sample was filtered through a 0.22μm filter prior to injecting 100μl onto the column. A flow rate of 0.5 ml/min was controlled by a Pharmacia P-500 pump. Elution was monitored by UV absorbance at 280nm using a flow-through detector. The elution position of GH was predetermined by loading a standard of purified GH under identical conditions (Chapter 3, Figures 1a-f).

2.2.6 Analysis of Purified Recombinant Growth Hormones

The GHs used in this thesis were analysed for homogeneity and authenticity using a number of methods and criteria. An initial test was a single peak on a size-exclusion column as outlined above (2.2.5). Other tests performed are outlined below.

2.2.6.1 Detection of Deamidated Forms of GH

The extent of deamidation of the purified GH was determined by high performance ion-exchange chromatography on a Mono-Q column (see 3.3.5). A small amount of lyophilized protein was dissolved in 25mM sodium borate pH 8.8 (Buffer A) to a final concentration of approx. 1 mg/ml. The solution was filtered through a 0.2μm filter prior to loading onto a Mono-Q HR5/5 column pre-equilibrated in Buffer A. The flow rate was 1 ml/min. The column was eluted with a 15ml gradient of NaCl from 0-150 mM. The eluent was monitored by UV absorbance at 280nm. The extent of deamidation was determined by calculating the area under the acidic eluting peak(s) as a percentage of the total peak area.

2.2.6.2 Zero and Second-Order Derivative Spectroscopy

Zero order UV absorbance spectra were recorded on a dual-beam Cary 3 spectrophotometer in the wavelength range of 250-310 nm. The spectral band width was 2 nm, signal average time 0.1 sec, wavelength interval 0.05nm and the scan rate 30 nm/min. The spectra were stored as an ASCII text file onto floppy disc. The second derivative of the zero order absorbance spectrum was performed using a computer program written by Dr. Mark Snoswell based on a method by Savitsky and Golay, (1964). Wild-type pGH concentrations were determined by measuring the absorbance at 278nm using an extinction coefficient of 15,714 $M^{-1}cm^{-1}$ determined using the method of Bewley (1982). For pGH(M8) an extinction coefficient of 21,375 $M^{-1}cm^{-1}$ was used. This figure was determined using the method of Gill and von Hippel (1989). For hGH, measurements were made at 277nm using an extinction

coefficient of 20,350 $M^{-1}cm^{-1}$ (Bewley & Li, 1984). For brGH and all other pGH mutants, the same extinction coefficient as for wild-type pGH was used.

2.2.6.3 N-terminal Sequence Analysis

The identity of pGH_{wt}, pGH(M12) and hGH were verified by N-terminal sequence analysis on an Applied Biosystems Model 470A Protein Sequencer by Denise Turner at the Department of Biochemistry, University of Adelaide.

2.2.6.4.Electrospray Mass Spectrometry

Electrospray mass spectrometry of purified GHs was carried out by Dr. Margaret Sheil at the Department of Chemistry, University of Wollongong.

Growth hormones were analysed on a VG BioTech Quattro mass spectrometer (VG Biotech Ltd., Altringham, U.K.). The instrument has an electrospray ion source which operates at atmospheric pressure followed by a triple quadrupole analyser with a 4000 Da mass range. Protein solutions (10µl in 1% acetic acid, 20 pmol/µl) were introduced into the source at 3 µl/min. The electrospray solvent was 1:1 water:methanol. The instrument was scanned from m/z 800 to m/z 2000 in 10 sec and data from several such scans was summed in the final spectra. The molecular weight for each protein was characterized from an envelope of multiply-charged ions using the data system routines. Results are the mean molecular mass and standard deviation derived from a number of multiply-charged ion peaks. The mass range was calibrated in a separate experiment using multiply-charged ions from horse heart myoglobin (16950.5 Da). The molecular weights are average values based on average atomic weights of the elements.

2.2.7 Circular Dichroism

Circular dichroism (CD) spectra were recorded on an AVIV 62DS model spectropolarimeter in the laboratory of Professor W. H. Sawyer at the Department of Biochemistry, University of Melbourne. Far-UV CD spectra were recorded in the

wavelength range 250-190 nm at 0.2nm resolution using a signal averaging time of 3 sec. The concentration of pGH used was 0.16 mg/ml in a 1mm path length cuvette. The spectrum of a buffer blank was subtracted from the sample spectrum. Deconvolution of the far-UV CD spectrum of pGH to obtain a value of the percentage of α-helix was done using the PROSEC software available on the AVIV spectropolarimeter (Yang et al., 1986).

Near-UV CD spectra of pGH_{wt} and pGH(M8) were recorded in the wavelength range 320-250 nm at 0.2nm resolution using a signal averaging time of 3 sec. The concentration of pGH_{wt} was 1 mg/ml whereas that for pGH(M8) was 0.69 mg/ml. A 5mm path length cuvette was used. The near-UV CD spectrum of a buffer blank was also recorded for each buffer used. Raw spectral data was smoothed using the spectral smoothing software available with the instrument. Spectra were smoothed using a 3rd order polynomial function over a 10 data point window. To minimize noise, smoothed buffer blank spectra were deducted from the smoothed sample spectra.

In the equilibrium denaturation experiments, the α-helix content of pGH at each concentration of GuHCl was determined by measuring the mean residue ellipticity at 222nm, $[\theta]_{222}$, in $deg.cm^2.dmol^{-1}$, using a mean residue weight of 115. The mean residue ellipticity was calculated using the following equation:

$$[\theta(\lambda)] = \frac{[100 \times \psi(\lambda)]}{lC}$$

where $[\theta(\lambda)]$ = mean residue ellipticity at wavelength λ,

$\psi(\lambda)$ = ellipticity at wavelength λ in degrees,

l = optical path length in cm

The symbol C denotes the concentration per residue, found by dividing the concentration of protein in grams per litre by the mean residue molecular weight of its constituent amino acids. For each concentration of GuHCl, $[\theta]_{222}$ was measured using a signal averaging time of 3 sec, every 3 sec over a period of 1 min. The twenty

data points were then averaged to obtain the final value. The concentration of pGH used was 0.16 mg/ml in a 1mm path length cuvette.

The mean residue ellipticity at 300nm, $[\theta]_{300}$ was determined in a similar manner using a 1 mg/ml solution of pGH in a 5mm path length cuvette, except that a signal averaging time of 5 sec was employed.

2.2.8 Fluorescence Spectroscopy

Intrinsic fluorescence measurements were performed on a Perkin-Elmer model LS-50 fluorescence spectrophotometer in the Department of Paediatrics, University of Adelaide. The single tryptophan of pGH was selectively excited using an excitation wavelength of 295nm. Emission spectra were scanned from 305 to 400nm using a scan rate of 60 nm/min with the emission and excitation slit widths set at 5nm. All measurements were made 25^{o}C. The emission spectra were corrected for the Raman peak by subtracting a buffer only spectrum from each sample spectrum. Raw spectra were stored as ASCII files and transferred to an Excel spreadsheet where the subtraction of the background buffer fluorescence was performed.

In the equilibrium denaturation experiments pGH was incubated at each concentration of GuHCl in 25mM sodium borate pH 9.1 at a final protein concentration of 0.08 mg/ml. The samples were centrifuged (15,000 $\times$ g, 5min) prior to fluorescence spectroscopy.

2.2.9 Size Exclusion Chromatography for Equilibrium Denaturation

The results of these experiments are described in 4.2.3. For the equilibrium denaturation experiments involving pGH_{wt} and pGH(M8), samples were prepared by incubating the protein at each GuHCl concentration in 25 mM sodium borate pH 9.1 (Buffer A). The protein concentration during incubation was 0.66 mg/ml and 0.48 mg/ml for pGHwt and pGH(M8), respectively. Following incubation for a minimum of 2h to ensure equilibrium had been reached, samples were briefly centrifuged, prior to injecting 100µl of the supernatant onto a 10mm i.d. x 300mm Superose-12 column

pre-equilibrated in the same concentration of GuHCl in Buffer A. The concentration of GuHCl was controlled by mixing the appropriate ratio of Buffer A and 25mM sodium borate pH 9.1, 6M GuHCl (Buffer B), using two P-500 pumps connected to an FPLC. A constant flow rate of 0.5 ml/min was maintained. Peak detection was at 280nm with a detector output of 0.1 AUFS. At the end of each sample run, the column was re-equilibrated with a minimum of 40ml of buffer (approx. 2 column volumes) of the next highest GuHCl concentration, before injection of the next sample. Protein molecular weight calibration curves for the Superose-12 column in 6M GuHCl were determined and utilized to calculate the Stokes radius of pGH at each concentration of GuHCl as described by Corbett & Roche (1984). The proteins used to calibrate the column were bovine serum albumin (BSA), ovalbumin, carbonic anhydrase, haemoglobin monomer, bovine ribonuclease, lysozyme and insulin. At the end of the pGH injections, all of the protein standards, dissolved in Buffer B, were injected individually onto the column pre-equilibrated in Buffer B. The equation to calculate Stokes radius (R_S) from elution volume was obtained by a least-squares fit of the three R_S values from Table II of Corbett & Roche (1984), namely those for BSA, ribonuclease and insulin, with the elution volumes of those three proteins from the above calibration experiment.

2.2.10 Radioreceptor Assays

Radioreceptor assays were performed by Scott Rowlinson in Dr. Michael Waters' laboratory, Department of Physiology and Pharmacology, University of Queensland. These were done to determine any changes in receptor binding as a result of mutations made in the pGH mutants. The receptor affinity constant (K_a) of each pGH mutant was compared to that for wild type pGH. The affinity constant of each pGH mutant for the rabbit liver GH receptor was determined by Scatchard analysis (Scatchard, 1949) of ^{125}I-labelled pGH mutant binding to the rabbit liver microsomes in the presence of increasing concentrations of unlabelled hormone competitor. The radioreceptor assay buffer was 25mM Tris-HCl pH 7.5, 20mM $MgCl_2$, 0.1% BSA.

Rabbit liver microsomal preparations were prepared from fresh female rabbit livers by the method of Tsushima & Friesen (1973). The bream growth hormone affinity constant was determined in a homologous assay using ^{125}I-bGH displacement from a fresh bream liver microsome preparation, by increasing amounts of unlabelled brGH. Hormones were iodinated by the Iodogen method of Salacinski et al. (1981).

2.2.11 Determination of Conformational Stability

2.3.11.1 Sample Preparation and UV Absorbance Measurements

The conformational stability, $\Delta G(H_2O)$, of each GH was determined using UV absorbance spectroscopy. All determinations were done at 25°C and pH 9.1.

For $\Delta G(H_2O)$ determinations using GuHCl as the denaturant all samples were prepared by mixing 100µl of a stock solution of GH dissolved in 25mM sodium borate pH 9.1 (Buffer A), with the appropriate volumes of Buffer A and Buffer A + 6.6M GuHCl as shown in Table I. Even though the protein concentration in each sample of a single $\Delta G(H_2O)$ determination was constant, the concentration between different determinations varied between 0.20 and 0.28 mg/ml. For all of the pGH mutants tested, the same concentrations of GuHCl were used. For hGH, the GuHCl concentrations were accordingly centred around the denaturation midpoint of 4.4M GuHCl (see 5.2.4). For each GuHCl concentration a reference containing 100µl of Buffer A instead of protein was also prepared. The samples and references were left to incubate for a minimum of 2 hours. The samples were centrifuged briefly (15,000 × g for 5 min) immediately prior to measuring the absorbance of 1ml of the supernatant in a dual-beam Cary 3 spectrophotometer equipped with a temperature controller set to 25°C. The spectrophotometer was zeroed at 400nm with the sample and reference in place prior to measuring the absorbance at 290nm (A_{290}) and 278nm (A_{278}). The samples were then discarded and the cuvettes inverted onto tissue paper before the next pair of sample and reference were directly pipetted into the same cuvettes. The procedure was repeated until all samples were completed.

[GuHCl]	µl Buffer A	µl Buffer B	[urea]	µl Buffer A	µl Buffer C
0	1000	0	0	950	0
0.25	958	42	1	850	100
0.5	917	83	2	750	200
0.75	875	125	3	650	300
1	833	167	4	550	400
1.25	792	208	4.25	525	425
1.5	750	250	4.5	500	450
1.75	708	292	4.75	475	475
2	667	333	5	450	500
2.2	633	367	5.25	425	525
2.4	600	400	5.5	400	550
2.6	567	433	5.75	375	575
2.8	533	467	6	350	600
3	500	500	6.2	330	620
3.25	458	542	6.4	310	640
3.5	417	583	6.6	290	660
3.75	375	625	6.8	270	680
4	333	667	7	250	700
4.5	250	750	7.2	230	720
5	167	833	7.4	210	740
5.5	83	917	7.6	190	760
6	0	1000	7.8	170	780
			8	150	800
			8.25	125	825
			8.5	100	850
			8.75	75	875
			9	50	900
			9.25	25	925
			9.5	0	950

Table I. Volumetric Proportions of Buffers Used in $\Delta G(H_2O)$ Measurements.

For the GuHCl denaturation curves, Buffer A (25mM sodium borate pH 9.1) and Buffer B (Buffer A + 6.6M GuHCl) were first aliquoted into tubes in the proportions listed above for each final GuHCl concentration. 100µl of a GH stock solution in Buffer A was then added to each tube and mixed gently. For the urea denaturation curves, Buffer A and Buffer C (Buffer A + 10M urea) were first aliquoted into tubes in the proportions listed above for each final urea concentration. 50µl of a GH stock solution in Buffer A was then added to each tube and mixed gently. For each concentration of GuHCl and urea, a reference tube was also prepared in the same way except that Buffer A was added instead of the GH solution. All pipetting was done manually with a calibrated set of pipettes.

For $\Delta G(H_2O)$ determinations using urea as the denaturant the above procedure was used except that all samples were prepared by mixing 50µl of a stock solution of pGH dissolved in Buffer A, with the appropriate volumes of Buffer A, and Buffer A + 10M urea, as shown in Table I.

2.2.11.2 $\Delta G(H_2O)$ Calculations

After measuring the A_{290} and A_{278} at each denaturant concentration, the data was entered onto an Excel spreadsheet. All mathematical manipulations were carried out using the Excel software.

To analyze the GuHCl and urea denaturation curves a two-state folding mechanism was assumed (Hartley, 1968). The analysis of denaturation curves in terms of a two-state approximation is useful even when denaturation has been shown to deviate from a two-state mechanism (see Chapter 4). This allows the calculation of the apparent free energy of unfolding ΔG_{app} as a function of denaturant concentration from the points in the transition region using

$$\Delta G_{app} = -RT \ln K_{app} = -RT \ln [(A_F - A) / (A - A_U)]$$

where K_{app} is the apparent equilibrium constant, R is the gas constant (1.987 cal/deg/mol), T is the absolute temperature (°Kelvin), A is the observed ratio of absorbance at 290nm over absorbance at 278nm, and A_F and A_U are the ratio values characteristic of the folded and unfolded conformations of the protein, respectively (Pace et al., 1989). A_F and A_U were obtained by extrapolation of the pre- and post-transition baselines into the transition region. A least-squares analysis ("line of best fit") was used to determine the equations given for A_F and A_U. In most cases the A_{290}/A_{278} values between 0 and 1.75M GuHCl and 3.5-6M GuHCl were used to determine the A_F and A_U equations, respectively. Using the above equation, ΔG_{app} was calculated for each point of the denaturation curve using the experimental A values, and the A_F and A_U values determined from the least-squares analysis of the pre- and post-transition regions. Using all of the ΔG_{app} values in the transition region within the range ± 1.5 kcal/mol, the $\Delta G(H_2O)$ was determined by a least-squares fit

of the data. ΔG_{app} was found to vary linearly with denaturant concentration, and the data were fitted to

$$\Delta G_{app} = \Delta G(H_2O) - m[\text{denaturant}]$$

where $\Delta G(H_2O)$ is the free energy of unfolding in the absence of denaturant and m is a measure of the dependence of ΔG_{app} on denaturant concentration. The denaturation midpoint, $[\text{denaturant}]_{½}$, was determined using the equation

$$[\text{denaturant}]_{½} = \Delta G(H_2O) / m$$

2.2.12 Detection of Intermediates Assay

Growth hormone was incubated at an initial protein concentration of 2 mg/ml in a series of buffers containing 25mM sodium borate pH 9.1 and increasing concentrations of GuHCl (1.5, 2, 2.25, 2.5, 2.75, 3, 3.25, 3.5, 4, 4.5, 5, and 6M). Following a 30min incubation at 25°C, each tube was rapidly diluted to a final protein concentration of 0.18 mg/ml and GuHCl concentration of 0.8M. After a further 30min incubation period, the samples were centrifuged briefly (15,000 × g for 5min). The absorbance of the supernatant was measured at 278nm against water as the reference.

2.2.13 SDS Polyacrylamide Gel Electrophoresis

Proteins were electrophoresed according to the method of Laemmli (1970) on vertical 14cm × 14cm × 0.5mm SDS polyacrylamide gels. A 4% stacking gel and 15% separating gel was employed. Proteins were visualized by staining with 0.1% (w/v) Coomassie brilliant blue in 50% methanol/10% acetic acid (v/v) at 65°C for 1 hour and destained in several changes of 50% methanol/10% acetic acid (v/v) at room temperature.

2.2.14 Construction of the pGH Model

Using the amino acid sequence, helix assignments and the two-dimensional representation of the three-dimensional X-ray structure from Abdel-Meguid et al.

(1987), a model of pGH was constructed using a molecular modelling kit (Chapter 4, Figure 2). The model was constructed with the assistance of Dr. Mark Snoswell and Mr. Tam Vu. The helices were made first, using the average bond lengths for a helix hydrogen bond as descibed by the supplier. They were stabilized by "superglued hydrogen bonds", i.e., the backbone carbonyl oxygen was glued to the backbone NH of the fourth residue along the chain (these hydrogen bonds never break!). The helices were then assembled on a wire stand in the "most favourable orientation" according to the Abdel-Meguid et al. cartoon (Chapter 4, Figure 1). Special attention was paid to minimizing helix hydrophobic side-chain "solvent-exposure", and tight packing of hydrophobic side-chains. The connecting loops were then assembled and added in the approximate orientation shown in the cartoon, again maximizing favourable interactions. The presence of disulphide bonds made this task slightly easier. The model proved to be useful in examining possible effects of mutations on structure. However, no attempt shall be made to suggest that this model is in fact the correct structure of pGH.

CHAPTER 3

PURIFICATION AND CHARACTERIZATION OF THE RECOMBINANT GROWTH HORMONES

3.1 INTRODUCTION

Before the advent of recombinant DNA technology, proteins of importance to medicine and research could only be obtained in limited amounts using long and laborious purification procedures. More often than not, this resulted in heterogeneous products as a result of the time involved in extracting the desired protein from its source. The source itself was a problem in that the possibility of copurification of potentially harmful proteins was always present. Only since the awareness of the dangers of human immunodeficiency virus has it become obvious that purification of protein products from animal sources, including human, for use in the pharmaceutical industry has many shortcomings. Research into the action of enzymes was hampered by the miniscule amounts of purified protein available. Indeed more time was spent in purifying the protein than determining its structure and function.

In the past decade, the use of recombinant DNA technology has allowed the production of large amounts of recombinant proteins in both eukaryotic and prokaryotic systems. Several of these proteins have already reached the human pharmaceutical market including human insulin (replacing porcine insulin), human growth hormone (replacing cadaver-derived material), human interferon and human tissue plasminogen activator. In the U.S. recombinant bovine growth hormone (bGH) is being administered to cows for the increased production of milk.

The ability to produce almost any variant of a protein of interest using site-directed mutagenesis has accelerated research in the area of protein structure, folding and stability. Early studies on growth hormone (GH) folding and stability involved the use of protein purified from animal sources (Burger et al., 1966; Holladay et al, 1974). Brems et al., (1985) were the first to use recombinant-derived bGH (r-bGH) in their equilibrium denaturation study. Even though the r-bGH was more homogeneous than that derived from pituitary sources, the denaturation profiles were very similar.

The overexpression of cloned genes in *Eschericia coli* often leads to the formation of insoluble cytoplasmic aggregates, often referred to as inclusion bodies

(Marston et al., 1984). These inclusion bodies consist of dense masses of partially folded, reduced and biologically inactive protein. How and why inclusion bodies form is still the subject of much discussion (Schein, 1989; Kane & Hartley, 1988). A recent report suggests proteins with a high charge average and turn forming residue fraction are more likely to form inclusion bodies (Wilkinson & Harrison, 1991). To obtain active protein, the inclusion bodies must be dissolved and the soluble protein refolded and oxidized into its native state. This process is usually performed as two separate operations: solubilization at high concentrations of denaturant such as urea or guanidine hydrochloride followed by dilution or gradual removal of the denaturant to allow refolding and oxidation to occur. Yields of correctly folded protein vary greatly depending on a number of factors such as refolding protein concentration, temperature and pH as well the intrinsic folding characteristics of the protein itself.

The large scale production of recombinant methionyl porcine growth hormone (met-pGH) in *E.coli* has been developed at Bresatec using two main refolding methods. Initially a method using GuHCl to solubilize the inclusion bodies, followed by their dilution into non-denaturing concentrations of urea was used. Later it was found that the process could be simplified by dissolving inclusion bodies in non-denaturing concentrations of urea at an elevated pH. This, essentially one-step dissolution/refolding process was based on a similar method used in the production of r-bGH (Bentle et al., 1987; Storrs & Przybycien, 1991). The chromatography procedures used are essentially the same for both the GuHCl and urea/high pH methods. Since the refolding of inclusion bodies inevitably results in a substantial amount of incorrectly folded and aggregated protein, it is imperative that these misfolded forms be separated from the correctly folded protein. The production of a homogeneous correctly folded GH is imperative to the studies outlined in the latter chapters of this thesis.

The aim of this chapter is twofold. Firstly I wish to describe the procedures used in the production of the various recombinant growth hormones used in this thesis. Secondly I shall present their characterization and verify the identity and

homogeneity of the purified products. Discussion on methods for improving refolding yields is outside the scope of this thesis.

3.2 PRODUCTION OF RECOMBINANT PORCINE GROWTH HORMONE, PORCINE GROWTH HORMONE MUTANTS, BREAM GROWTH HORMONE AND HUMAN GROWTH HORMONE

All of the growth hormones used in this thesis were produced in *E.coli* with a methionyl residue at the amino terminus. All of the pGH molecules contain an N-terminal methionine substituted for the natural sequence alanine (Seeburg et al., 1983). The hGH and brGH contain an N-terminal methionine added to the natural sequence (Nicoll et al., 1986; Knibb et al., 1991). All of the GHs will be referred to as pGH (this refers to the wild type only), hGH and brGH even though they do contain the extra methionine residue. Mutants of pGH will be referred to as pGH with the mutant number following it in brackets (i.e. pGH(M8)). The rationale behind the mutations made is described in detail in Chapter 5 (see 5.2.3.1).

3.2.1 Fermentation and Inclusion Body Harvesting

The following description is representative of all the GHs produced at Bresatec (unless specified otherwise). The fermentation, homogenization and centrifugation were carried out by Carol Senn.

To ensure the purity of expressing strains, single colonies were passaged 4 times on minimal plates. A 10ml overnight culture taken from a single colony was used to inoculate the 15L fermenter, as described (2.2.1). The culture was induced after overnight fermentation, at an A_{600} of 50. The fermentation was terminated 5 hours after induction. During the induction period the proportion of cells containing inclusion bodies and the inclusion body size, as monitored by light microscopy, steadily increased. The homogenization and centrifugation processes resulted in the

rapid and quantitative separation of GH containing inclusion bodies from cellular protein. The culture was passed 3 times through a homogeniser at 15,000 psi. The inclusion body size varied slightly in each GH preparation with an average diameter of 0.45μm. The homogenate was centrifuged twice at a flow-rate dependent on inclusion body size (2.2.1). For most 15L fermentations, a final yield of approx. 125g of inclusion bodies with a wet weight protein content of approx. 33% was achieved. SDS polyacrylamide gel electrophoresis of purified inclusion bodies revealed a GH purity of greater than 90%.

3.2.2 Dissolution, Refolding and Oxidation of Inclusion Body GH

During the early stages of the development of a process for the production of pGH, inclusion bodies were routinely stored in 25g wet weight aliquots, at -20°C at the end of each fermentation run. It was subsequently found that the longer they were stored, their solubility decreased, resulting in poor refolding yields and an impure final product. Because of the poor solubility of stored inclusion bodies it was necessary to use 6M GuHCl to dissolve them. The addition of dithiothreitol (DTT) improved their solubility suggesting that storage had resulted in partial oxidation, perhaps with the formation of intermolecular crosslinks. However, by processing the inclusion bodies immediately after harvesting them from the centrifuge, solubility increased dramatically. Furthermore it was found that the use of GuHCl could be avoided. The inclusion bodies were soluble in 3.75M urea at pH 11.5. The major advantage in using the urea based procedure was that it was essentially a single step process: dissolution, refolding and oxidation occuring simultaneously.

Both of the procedures used in the purification of the various GHs used in this thesis have been described (2.2.3.1 and 2.2.3.2). The main difference between the two methods is the increased yield of purified GH. The refolding and oxidation profiles were similar except for increased levels of correctly folded GH. For the purpose of the discussion, I shall describe the results from the urea/pH 11.5 method and refer to

any differences seen in the GuHCl/DTT method. All procedures were carried out at room temperature.

Immediately after collection from the continuous flow centrifuge, the inclusion bodies were weighed and suspended in unbuffered 3.75M urea pH 11.5, at a final protein concentration of approx. 1.5 mg/ml. A typical refolding run commenced with 125g of inclusion bodies (wet weight) dissolved in 25L of the urea/pH 11.5 buffer. Upon complete visual dissolution of all of the paste-like inclusion body material (usually about 10 min), a small aliquot was taken for analysis by size exclusion chromatography on a Superose-12 column equilibrated in 25mM sodium borate pH 9.1 (2.2.5). The Superose-12 elution profile of this sample, referred to as the 0-hour oxidation, is shown in Figure 1a. There are three main peaks in the chromatogram: the first peak which elutes in the void volume of the column at approx. 7.5ml, is aggregated material with a molecular weight greater than the Superose-12 exclusion weight of 250kD. A second broader peak eluting between 8 and 10 ml also consists of aggregates. The third peak eluting at approx. 11.5 ml is monomeric, correctly folded pGH. Aliquots were taken from the refolding solution at hourly intervals and analysed on the Superose-12 column. Figures 1a-f show the gradual increase in the amount of correctly folded pGH with time as depicted by the increase in the area under the peak eluting at 11.5 ml. The area under this peak as a percentage of the total area in the chromatogram is a reasonable measure of the yield of refolding. The percentage of correctly folded material varied between runs from 15-45% with a mean of approx. 25%. Closer examination of the Superose-12 elution profiles reveals that the increase in correctly folded pGH is at the expense of lower molecular weight aggregates eluting near 10ml. It is also apparent that the refolding process reaches equilibrium at 4-5 hours.

The time allowed for refolding and oxidation was optimised to minimise GH exposure to urea at the elevated pH. Prolonged exposure increases the level of deamidation at asparagines and glutamines, resulting in charge heterogeneity of the purified GH (Secchi et al., 1986). One advantage of the elevated pH is that disulphide

Figure 1. Time course of refolding and oxidation of GH.

Following dissolution of inclusion body GH in 3.75M urea pH 11.5, a small aliquot was taken for analysis by size-exclusion chromatography on a 10mm × 30cm Superose 12 column pre-equilibrated in 25mM sodium borate pH 9.1. The flow rate was 0.5 ml/min. A_{280} was monitored (—).v_0 is the void volume of the column. The elution volume (ml) is indicated at the bottom of each chromatogram. *Sample a:* "0-hour" oxidation i.e., immediately following complete dissolution. *Samples b-f:* 1-, 2-, 3-, 4- and 5-hours after complete dissolution. *Sample g:* Non-binding eluent of the Q-Sepharose Fast Flow column after 90L of the refolding solution had been loaded.

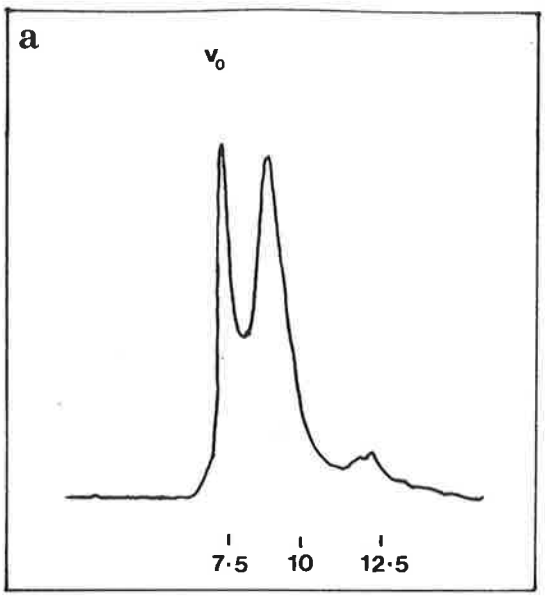
a
V_0
7·5
10
12·5

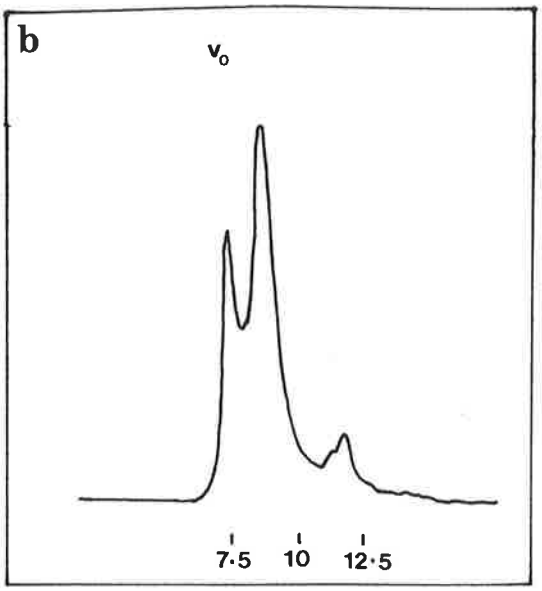
b
V_0
7·5
10
12·5

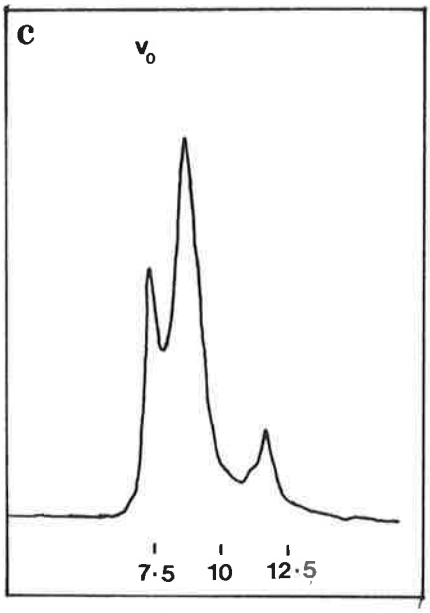
c
V_0
7·5
10
12·5

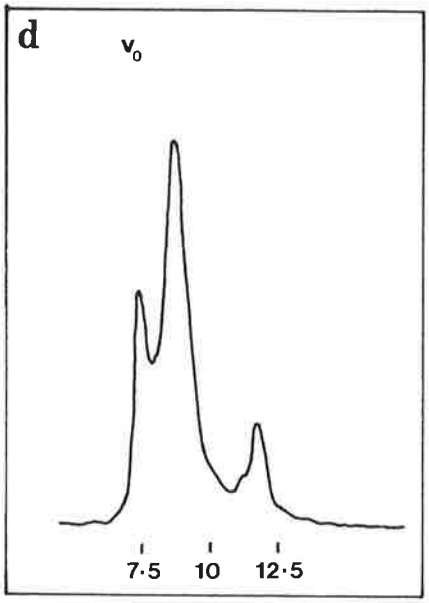
d
V_0
7·5
10
12·5

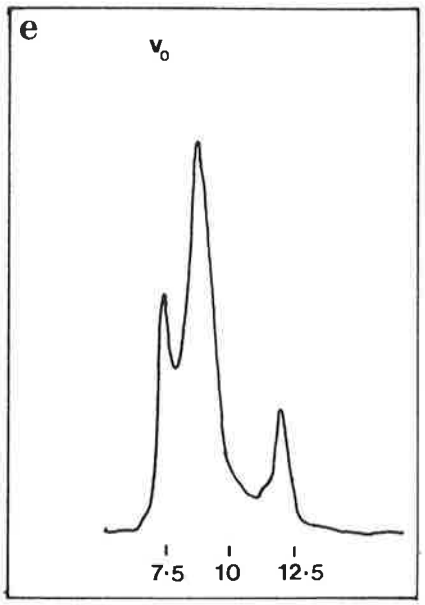
e
V_0
7·5
10
12·5

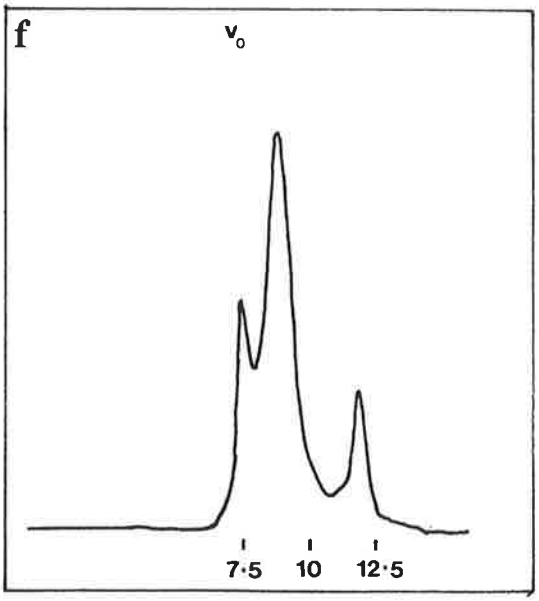
f
V_0
7·5
10
12·5

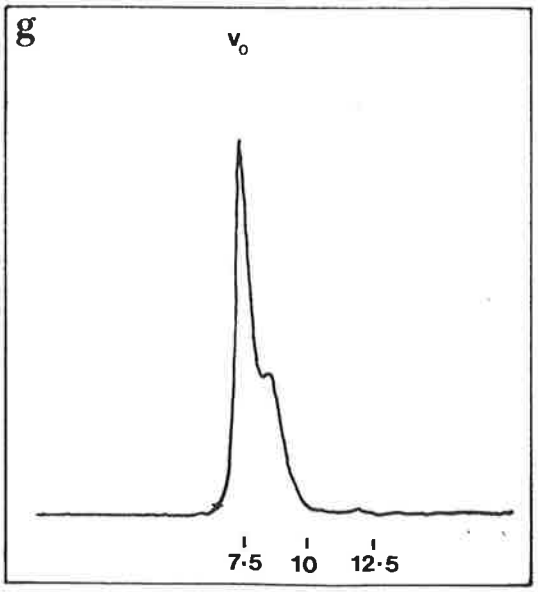
g
V_0
7·5
10
12·5

bond shuffling can occur, thus allowing the possibility for incorrectly formed disulphides present in the inclusion bodies, to break and reform the correct disulphides. This abolishes the need for a reducing agent such as DTT and explains why the dissolution, refolding and oxidation occurs under the same conditions. An incorrectly formed disulphide could break thus allowing the molecule momentary freedom to rearrange its fold toward the native configuration, whereupon formation of the correct disulphide bond would lock the molecule into a thermodynamically stable state.

Refolding and oxidation was terminated by diluting the urea concentration to approx. 1M and lowering the pH to 9.1. This had no effect on the proportion of correctly folded to aggregated forms of GH observed at the end of refolding. Dilution was necessary to allow the selective binding of only the correctly folded GH to the anion-exchange column. Following dilution, up to 100L of the refolding solution was loaded onto the Q-Sepharose Fast Flow column (FFQ) overnight (2.2.4). A sample of the non-binding eluent was analysed on the Superose-12 column (Figure 1g). This demonstrates that after loading of 90L of the refolding solution, the correctly folded GH is still being selectively retained by the column. It is also apparent that the aggregate distribution has altered during the loading time. A small amount of aggregated GH is also retained by the column. Fortunately, these aggregated forms are eluted off the column at higher salt concentrations than the correctly folded GH.

Upon completion of loading the column was eluted with Buffer A containing 150mM NaCl (Figure 2a). Fractions were collected and analysed on the Superose-12 column. Fractions eluting at the front of the peak usually contained a small fraction of aggregated GH, whereas fractions in the middle and trailing edge of the peak were pure monomeric correctly folded GH (Figure2b). The pure fractions were pooled together and desalted on a Sephadex G-25 column pre-equilibrated in 20mM ammonium bicarbonate pH 9.1 (Figure 3a). The Superose-12 profile of the desalted GH is shown in Figure 3b. Finally, the GH was freeze dried and stored as the lyophilized powder at -20°C.

Figure 2. Anion-exchange chromatography of GH refolding solution.

At the completion of refolding and oxidation, the refolding solution was diluted to approximately 1M urea at pH 9.1, prior to loading onto a 113mm i.d. × 45mm Q-Sepharose Fast Flow column at 80 ml/min. Upon completion of loading, the column was washed with 25mM sodium borate pH 9.1 (Buffer A) prior to elution of the bound GH with Buffer A + 150mM NaCl at a flow-rate of 50 ml/min. A_{280} was monitored (—). (*a*) elution of GH-containing peak from Q-Sepharose Fast Flow column. The elution volume (in L) is indicated below the chromatogram. (*b*) Analysis of the Q-Sepharose Fast Flow column GH-containing peak on Superose 12. 100µl of the peak fraction from the Q-Sepharose Fast Flow column was loaded onto a Superose 12 column pre-equilibrated in 25mM sodium borate pH 9.1, at a flow-rate of 0.5 ml/min. A_{280} was monitored (—). The elution volume (ml) is shown below the chromatogram.

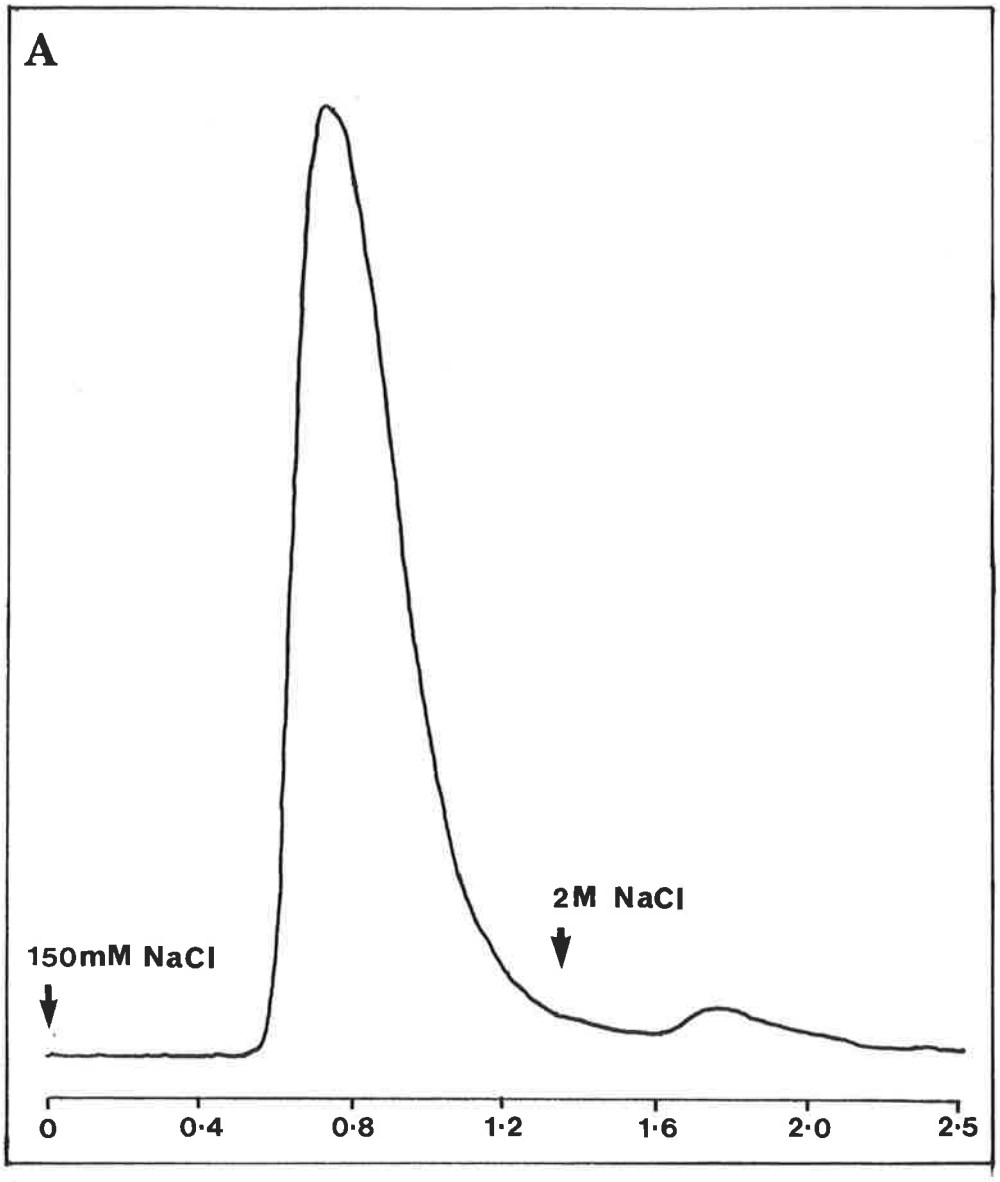
A
150mM NaCl
2M NaCl
0
0·4
0·8
1·2
1·6
2·0
2·5

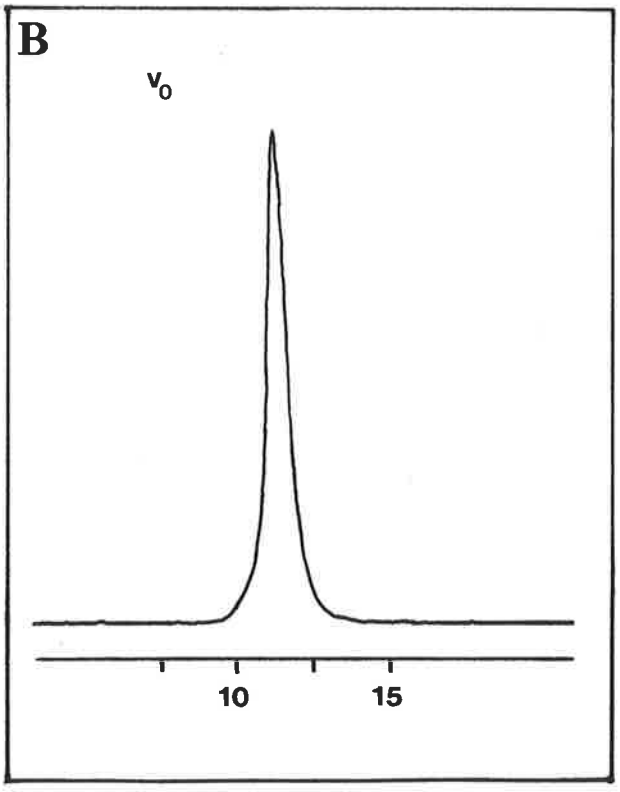
B
V_0
10
15

Figure 3. Desalting of purified GH fraction.

Q-Sepharose Fast Flow fractions containing monomeric, correctly folded GH were pooled and desalted on a 113mm i.d. × 300mm column of Sephadex G-25 Medium pre-equilibrated with 20 mM ammonium bicarbonate pH 9.1 (pH 8.2 for hGH), at a flow rate of 50 ml/min. A_{280} was monitored (—). (*a*) Sephadex G-25 elution profile of GH fraction. The elution volume (ml) is shown below the chromatogram. (*b*) Analysis of the Sephadex G-25 peak on Superose 12. 100µl of the Sephadex G-25 peak was loaded onto a Superose 12 column pre-equilibrated in 25 mM sodium borate pH 9.1 at a flow-rate of 0.5 ml/min. A_{280} was monitored (—). The elution volume (ml) is shown below the chromatogram.

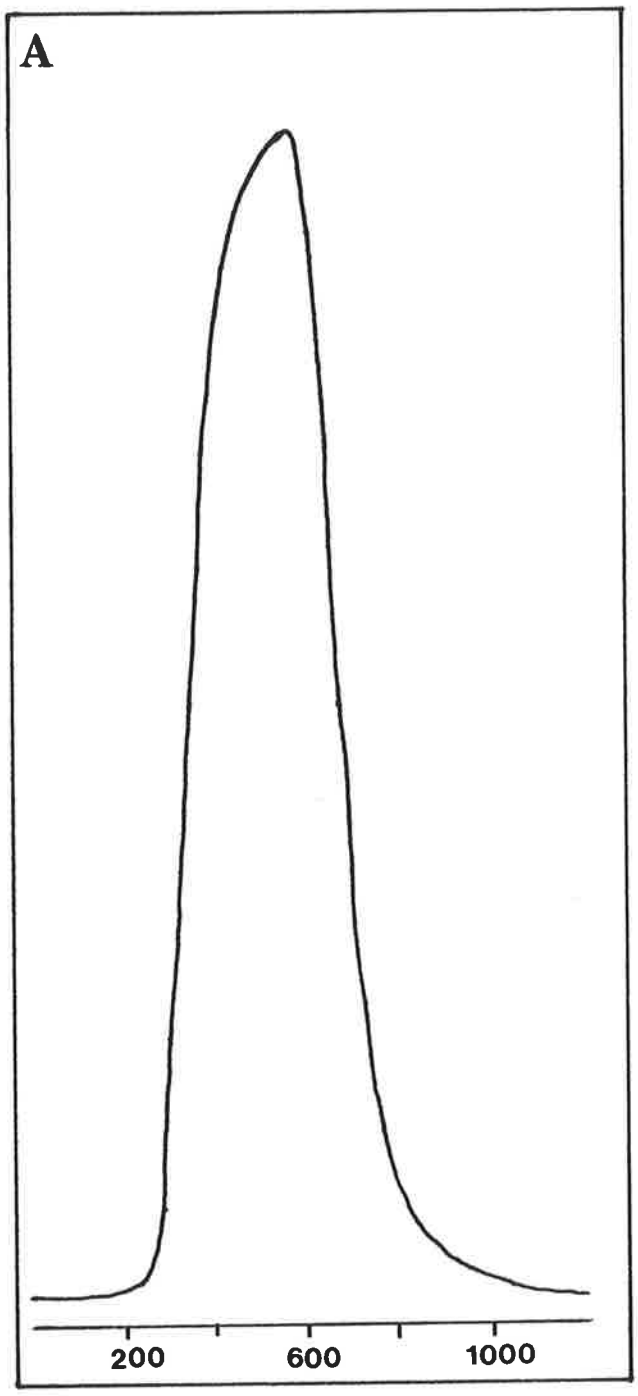
A
200
600
1000

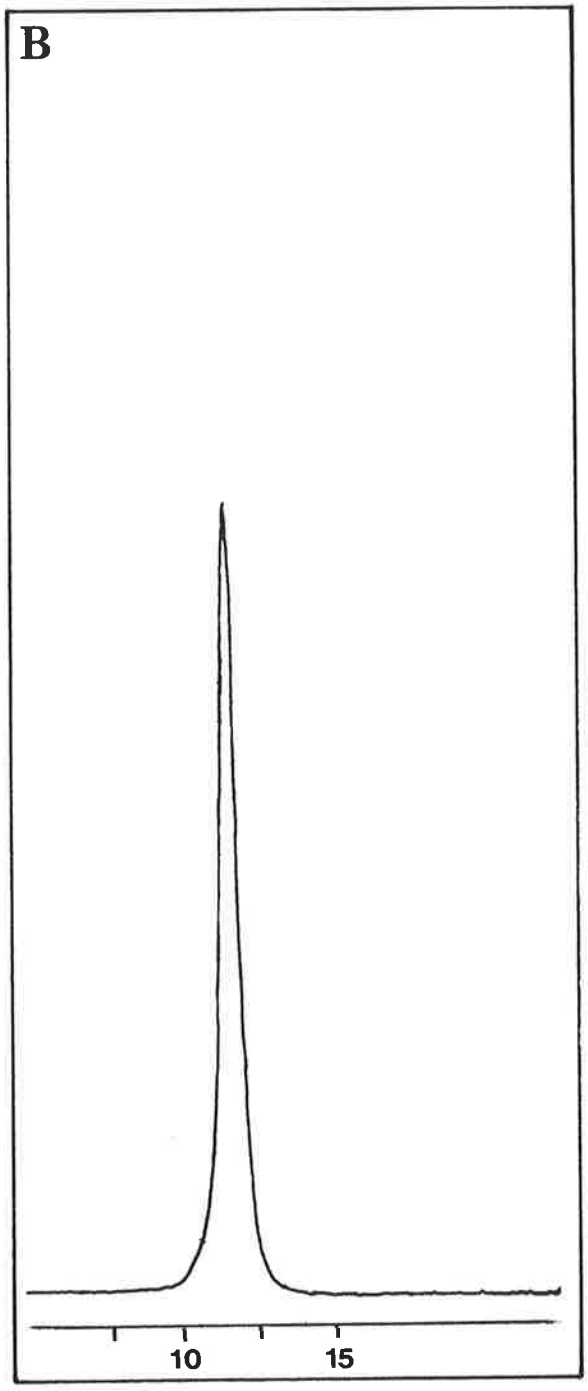
B
10
15

Some of the mutants used in this thesis were purified using the GuHCl/DTT method outlined in 2.2.3.1. Although the yields may have been lower the homogeneity of the purified GH was of the utmost importance. During the purification procedure, any fractions not containing a high percentage of monomeric species (e.g., >90% as monitored by the Superose-12 column) were discarded. To minimize aggregates binding to the FFQ column, some minor alterations to the pH of the chromatography were also made for the more acidic mutants: pGH(M16) which contained the double mutation K30Q;R34E (first letter being amino acid present in the wild-type pGH at the residue number specified and the second letter being the substitution made) and pGH(M17), also a double mutant with the changes K30E;R34E, were loaded and eluted off the FFQ column at pH 8.5. A rigorous column cleaning procedure was employed at the end of each GH run. This involved washing the column with 2M NaCl and 0.1M NaOH prior to storage in 20% ethanol. This ensured that no residual GH bound to the FFQ column could possibly contaminate following preparations.

3.3 CHARACTERIZATION OF THE PURIFIED GROWTH HORMONES

All of the purified GHs were routinely characterized using a number of methods. The criteria for homogeneity ranged from a simple UV absorbance spectrum to mass spectrometry to determine the exact molecular weight. As outlined above, the only method used to determine homogeneity during the purification, was a single peak on a size exclusion column. All of the site-directed mutant clones were fully sequenced prior to storage as glycerol stocks by Dr. Allan Robins. However there is always the possibility that contamination could arise in the production at the level of the fermentation or perhaps the chromatography. A determined effort was made to characterize the product at the protein level.

3.3.1 SDS Polyacrylamide Gel Electrophoresis

Figure 4 shows the various growth hormones on a 15% SDS polyacrylamide gel. Each lane was deliberately overloaded with approximately 20μg of protein in order to detect any contaminants present. Lanes 2 and 3 show the brGH and hGH, respectively. They are both very pure with no traces of contaminants present. Even though hGH has a higher molecular weight than brGH (and pGH), it has an apparently smaller molecular weight on SDS gels. This is probably due to the charge differences between these proteins. At the pH of the gel (pH 6.8), hGH has a net charge of -5, whereas brGH and pGH have no net charge. The charge difference may affect binding of SDS to the protein. The same effect occurs in the mutants of pGH, pGH(M17) and pGH(M16) [lanes 7 and 8, respectively]. These two proteins have a net charge of -4 and -3, respectively. All of the pGH mutants (see Chapter 5, Table IV for description of mutants), and wild-type pGH (lane 14) have a minor contaminant with an apparent molecular weight near 25kD. A densitometric scan of the gel has shown that the average level of this contaminant is about 5%. pGH(M8) [lane 13] also contains a minor contaminant near 30kD. Because of the deletion of 8 residues near the C-terminus, pGH(M10) [lane 12] is expected to run fractionally lower than wild-type pGH on SDS gels. However, both pGH(M10) and pGH(M17) have a smear present above the main band. Differences in molecular weight of this size, i.e., <1000D, would go undetected in high performance size-exclusion chromatography, the method used to check purity during the purification procedure. Mass spectrometry revealed that there was a minor contaminant present in the pGH(M10) preparation with a molecular weight slightly higher than the major protein present (3.3.7). The mass spectrum of pGH(M17), however showed one major peak, with only trace contaminants. The anomolous behaviour of pGH(M17) in SDS-polyacrylamide gel electrophoresis may be due to the presence of minor charge variants.

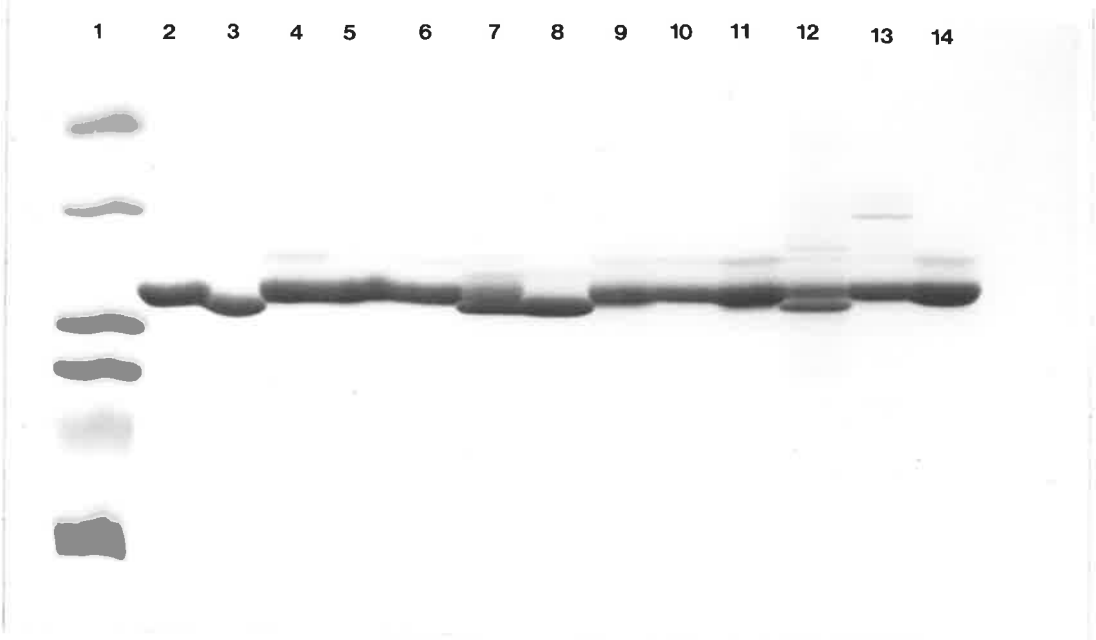

Figure 4. SDS Polyacrylamide Gel Electrophoresis of Purified GHs.

The purified GHs were subjected to SDS polyacrylamide gel electrophoresis as described in 2.2.13. *Lane 1:* protein standards (top to bottom): ovalbumin (43 kD), carbonic anhydrase (29 kD), β-lactoglobulin (18.4 kD), lysozyme (14.3 kD), bovine trypsin inhibitor (6.2 kD) and insulin (3 kD). *Lane 2:* brGH. *Lane 3:* hGH. *Lane 4:* pGH(M23). *Lane 5:* pGH(M21). *Lane 6:* pGH(M19). *Lane 7:* pGH(M17). *Lane 8:* pGH(M16). *Lane 9:* pGH(M14). *Lane 10:* pGH(M13). *Lane 11:* pGH(M12). *Lane 12:* pGH(M10). *Lane 13:* pGH(M8). *Lane 14:* pGH_{wt}.

3.3.2 UV Absorbance Spectroscopy

UV absorbance spectra were routinely performed on the purified GHs for quantitation as well as quality control. Analysis of the second derivative spectrum (2.2.6.2) can reveal many details about the microenvironment around the aromatic residues thus providing a "fingerprint" of the protein (Balestrieri et al. 1978). Figure 5 shows the UV absorbance spectrum of native pGH with the second derivative spectrum overlayed. The zero-order spectrum (*the* absorbance spectrum) displays an absorption maximum at 278.2 ± 0.1nm. The prominent shoulder centred near 290nm is due mainly to the absorption of the single tryptophan residue buried in the hydrophobic core of the GH (Bewley & Li, 1984). The three bumps in the 255-270nm region are due to phenylalanine absorption. The features of the zero-order spectrum become more prominent when observing the second-derivative spectrum. A peak or slight shoulder in the zero-order spectrum becomes an obvious minimum in the second-derivative spectrum.

The amino acid sequence in the GH family of proteins is highly conserved (Chapter 1, Tables I & II; Nicoll et al., 1986). All GHs contain a single conserved tryptophan, as well as several tyrosine and phenylalanine residues. However, the exact position of each of these residues in the molecular matrix may vary slightly between GHs. These slight differences can be observed using UV spectroscopy as well as CD and fluorescence spectroscopy. For example, by observing the red-shift of the trp ^1L_a band of hGH and comparing this shift to that seen in model indole derivatives (Strickland et al., 1972), Bewley and Li (1984) predicted the presence of a hydrogen bond between the tryptophan indole ring >NH and an internal carboxylate residue. Their prediction was later confirmed when the X-ray structure of hGH was reported (de Vos et al., 1992).

Figure 6a shows the zero-order absorption spectra of four of the purified proteins: pGH, pGH(M8), hGH and brGH. Each spectrum is an average of four recorded spectra. The higher absorbance in the 270-240nm region seen in the pGH spectrum is due to a greater light scattering component in the particular pGH sample

Figure 5. Zero- and second-order absorption spectrum of native pGH_{wt}.

Zero-order (red) UV-absorbance spectrum of pGH_{wt}. The spectrum was recorded on a Cary 3 spectrophotometer as described in 2.2.6.2. The protein concentration was 1mg/ml in a buffer of 25mM sodium borate pH 9.1. The second-order (second-derivative) spectrum of the zero-order spectrum is shown in green.

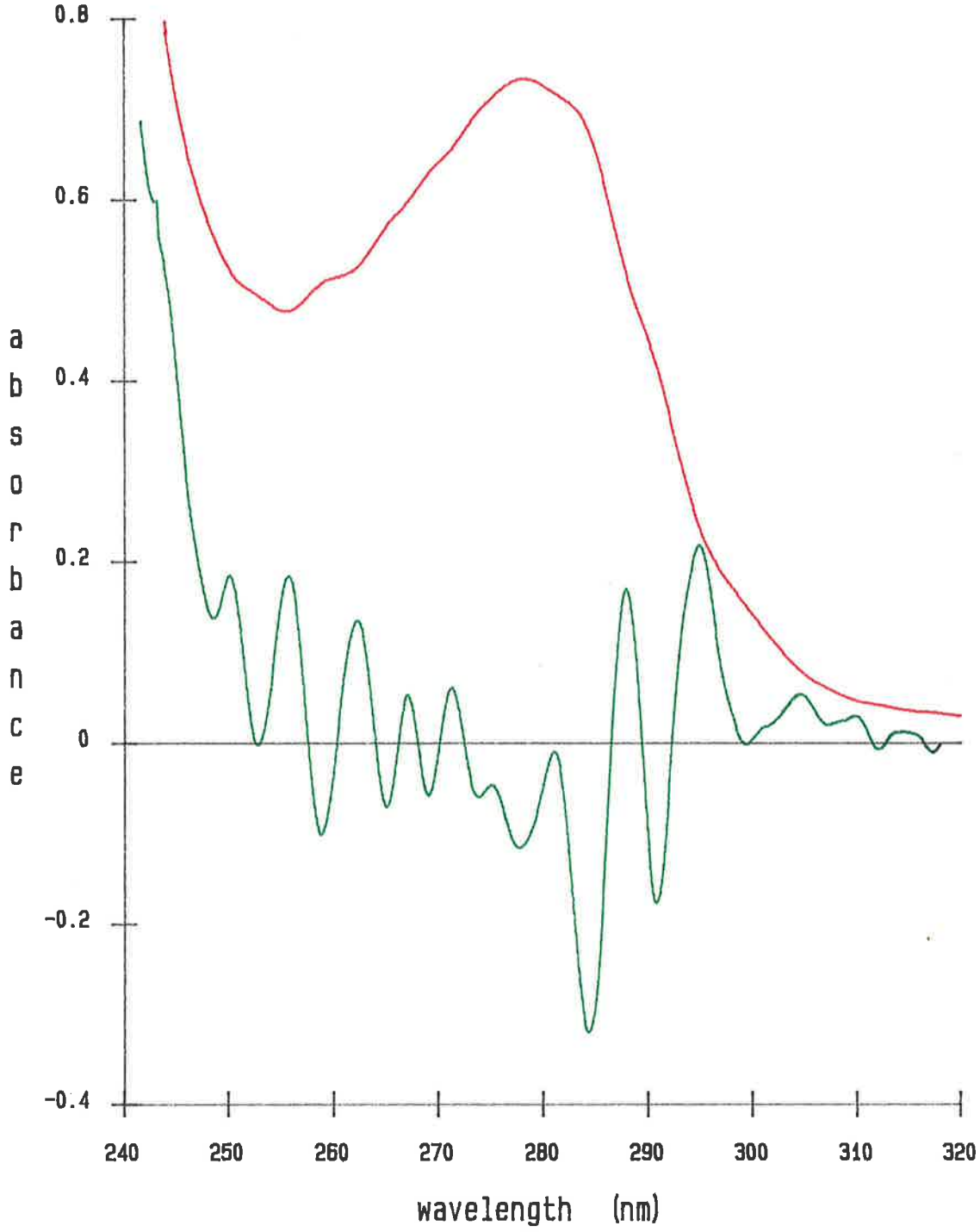
0.8
0.6
0.4
0.2
0
-0.2
-0.4
absorbance
240
250
260
270
280
290
300
310
320
wavelength (nm)

Figure 6. Zero- and second-order absorption spectra of pGH_{wt}, pGH(M8), brGH and hGH.

(*a*) Zero-order absorption spectra of the four GHs. pGH_{wt}, pGH(M8) and brGH were dissolved in 25mM sodium borate pH 9.1, while hGH was dissolved in 25mM Tris-HCl pH 8.2. The protein concentration was approximately 1 mg/ml for all proteins. All samples were filtered through a 0.2μm filter. Absorption spectra were recorded on a Cary 3 spectrophotometer between 320 and 240nm at a scan-rate of 6 nm/min. The spectral band width was 2nm, signal average time 0.5 sec and wavelength interval 0.05nm. (*b*) Second-order absorption spectra of the four GHs. The second derivative of the zero-order absorption spectra from (*a*) were calculated as described in 2.2.6.2. The spectra shown here are an average of several spectra recorded from several different purification runs. (*inset*) An expanded view of the region of tryptophan absorption. The trp ^1L_a triplet of hGH is shown: the [0-0] band is near 305nm, while the two higher vibronic bands are near 303nm and 300nm.

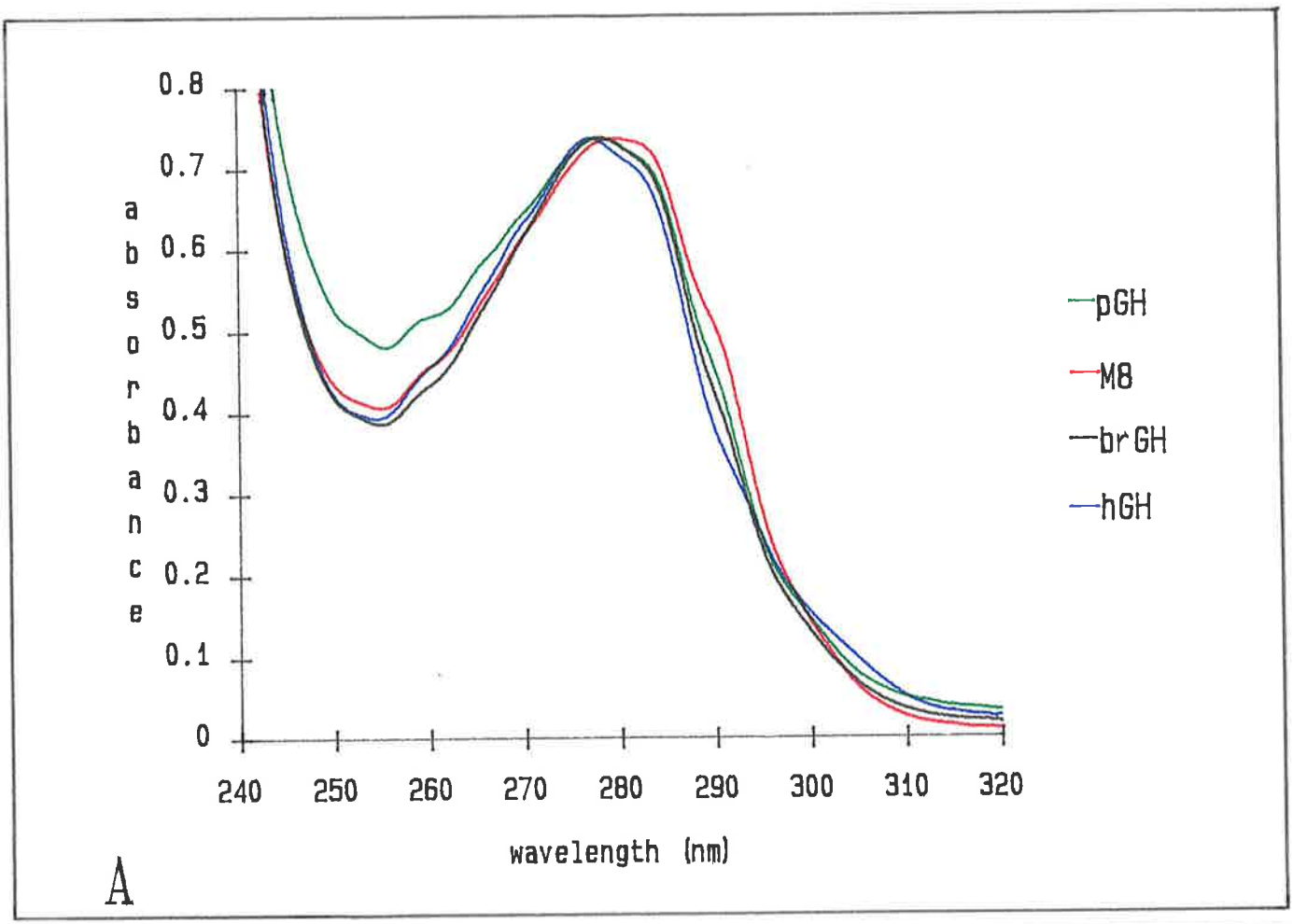
absorbance
0.8
0.7
0.6
0.5
0.4
0.3
0.2
0.1
0
240
250
260
270
280
290
300
310
320
wavelength (nm)
pGH
M8
brGH
hGH
A

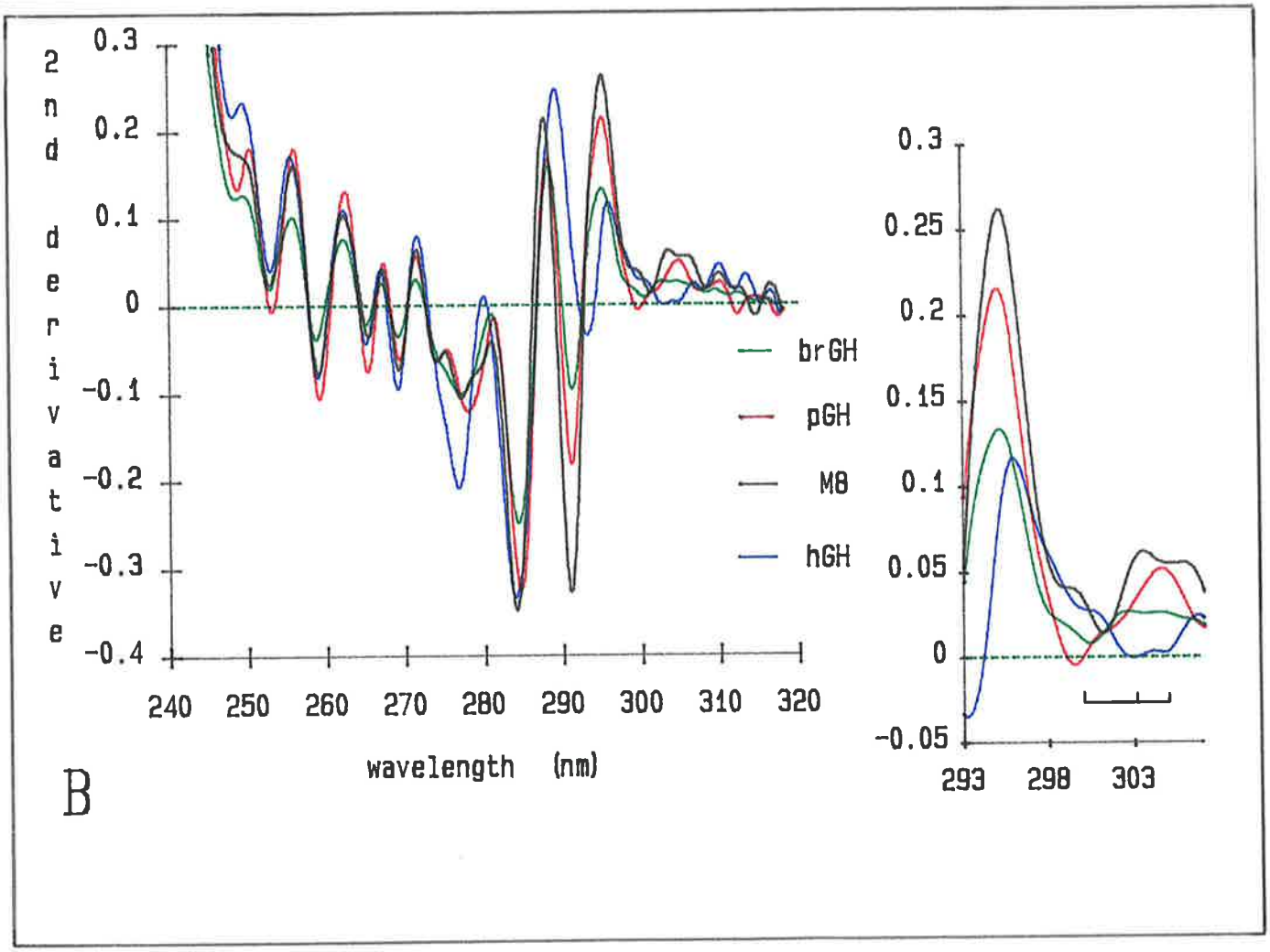
2nd derivative
0.3
0.2
0.1
0
-0.1
-0.2
-0.3
-0.4
240
250
260
270
280
290
300
310
320
wavelength (nm)
brGH
pGH
M8
hGH
0.3
0.25
0.2
0.15
0.1
0.05
0
-0.05
293
298
303
B

used in this analysis. This does not affect the wavelength positions of the second-derivative bands (see below). pGH(M8) is a mutant containing a methionine to tryptophan mutation at residue 124. The extra tryptophan results in the red-shifting of the 278-300nm region, and makes the shoulder at 290nm, characteristic of tryptophan, more prominent. The absorbance maximum is also red-shifted to 279.8nm compared to 278.2nm, 277.2nm, and 278.1nm for pGH, hGH and brGH, respectively. The second derivative spectra of these proteins is shown in Figure 6b. The shoulders in the zero-order spectra appear as sharp negative peaks. The wavelength positions of these peaks for each GH as well as the values for a pituitary preparation of hGH (Bewley & Li, 1984) are listed in Table I. By comparison with the second-order spectra of model compounds (Balestrieri et al., 1978; Wetlaufer, 1962; Jaffé and Orchin, 1962), Bewley and Li assigned each of these peaks to the absorption bands of the [0-0] transition and higher vibrational modes, of the respective phenylalanine, tyrosine and tryptophan residues. From Figure 6b and Table I, it can be seen that the phe^1L_b [0-0] transition at approx. 269nm, and its four higher vibrational modes are very reproducible in all GHs. This suggests that the average hydrophobicity of phenylalanine residues in all of the GHs is similar. The weaker phenylalanine vibrational mode near 261nm detected by Bewley and Li could not be detected in any of the spectra I recorded. Unlike the phenylalanine absorption bands, the wavelengths of tyrosine and tryptophan absorption bands vary between GHs. Most of the r-hGH second-order minima agree with the pituitary values except for the trp^1L_b[0-0] band (i.e., compare hGH_{Bres} with hGH_{Bew} in Table I). The reason for this discrepancy could be due to a difference between the pituitary- and recombinant-derived material. It could not be an error in the spectrophotometric reading as all the other minima agree reasonably well. This red-shift recorded for the r-hGH is probably real and correlates with the red-shift seen in the trp^1L_a band. The extra tryptophan in pGH(M8) has increased the intensity of the trp^1L_b band. The trp^1L_a region (297-305nm) is more difficult to interpret due to the low absorbance in this region. However, the trp^1L_a triplet (arising from the trp^1L_a[0-0] transition and two higher

	hGH_{Bew}	hGH_{Bres}	pGH_{Bres}	$M8_{Bres}$	$brGH_{Bres}$
$*Trp^1L_a$	304.2	304.7	301.4(s)	305.15	303.65
Trp^1L_a	301	302.9	299.45	301.1	300.35
Trp^1L_a	298.2	300.2(s)	297.5(vws)	299(s)	~298.25(s)
Trp^1L_a		297.8(vws)		-	-
$*Trp^1L_b$	290.9	293.15	290.9	290.9	291.2
$*Tyr^1L_b$	283.2	284	284.45	284	284.3
Tyr^1L_b	276.2	276.8	~279(vws) 277.7	278.9(s) 277.1	277.1
Trp^1L_b	~273(ws)	274.7(vws)	273.95	273.95	~274(ws)
$*Phe^1L_b$	268.3	269.15	269.15	269.15	269.15
Phe^1L_b	264.5	265.1	265.1	265.25	265.1
Phe^1L_b	261.5(w)	-	-	-	-
Phe^1L_b	258.6	258.95	258.8	258.95	258.65
Phe^1L_b	252.9	252.95	252.8	252.65	252.8
Phe^1L_b	247.8	248.3	248.6	248.9(s)	248.45

Table I. Second-derivative absorption bands of native GHs.

Wavelength positions of the second-derivative minima in the spectra illustrated in Figure 6b, are compared to those of a preparation of pituitary hGH [hGH_{Bew}](*Bewley & Li, 1984*). By comparison with the second-derivative spectra of model compounds, each minimum was assigned to the [0-0] transition and higher vibrational modes of the respective phenylalanine, tyrosine and tryptophan residues (see 3.3.2). The * denotes the [0-0] band of each chromophoric electron. w, weak peak; s, shoulder; ws, weak shoulder; vws, very weak shoulder. hGH_{Bres}, pGH_{Bres}, $M8_{Bres}$ and $brGH_{Bres}$, refer to the purified GHs.

vibrational modes) seen in the pituitary hGH can be clearly seen in the recombinant hGH (Figure 6b, inset). The wavelengths of the minima are not identical (Table I) but the general pattern of bands is similar. As previously mentioned this massive 12nm red-shift in the trp^1L_a band can occur when the indole ring >NH group is simultaneously surrounded by a non-polar environment, *and* is hydrogen bonded to a negatively charged carboxylate ion. The trp^1L_a triplet is more difficult to delineate in pGH and brGH possibly because they are not as red-shifted as the hGH bands, and are therefore overshadowed by the more intense ^1L_b bands. The trp^1L_a[0-0] transition assignments given to pGH(M8) and brGH in Table I are tentative at best because of the low absorbance signal in this region. However it appears as if this band is significantly red-shifted in all of the above GHs, suggesting that the tryptophan environment is similar in all of these species. This red-shift has been observed in other GHs such as sturgeon GH (Bewley & Papkoff, 1987) and elephant GH (Li et al., 1987), as well as human DNase, and the Kringle-2 of tPA (Mulkerrin et al., 1992). The red-shift varies from 6-10 nm depending on the proton acceptor, and the angle and length of the hydrogen bond (Mulkerrin et al., 1992).

The above description of the absorbance characteristics of four GHs has shown that the aromatic residues of the respective proteins are in similar environments. This suggests that their overall tertiary structures are similar and that the purification process has not disturbed their relative orientations in the molecular matrix. Furthermore, I have shown that the absorption bands coincide well with those published for other GH species. UV absorbance spectroscopy can be a powerful tool when used in conjunction with second-derivative analysis. I have not presented any UV absorbance data on any of the other mutant pGHs because aromatic residue substitutions are not involved (except for pGH(M23) which has a Y29K mutation). However, it may be possible to detect changes in their spectra caused by slight alterations in the vicinity of aromatic residues, as a result of a conformational change.

3.3.3 Fluorescence Spectroscopy

The fluorescence emission maximum (λ_{max}) of tryptophan residues is highly sensitive to the polarity of the environment surrounding the tryptophan (Teale, 1960). An increase in polarity may be a result of a direct interaction of the tryptophan with the aqueous solvent or with a charged internal residue. Using an excitation wavelength of 295nm, the corrected fluorescence emission spectrum of native pGH displays a broad single band with a maximum at 338.5 ± 0.5nm (Figure 7a). Native bGH has a λ_{max} of 335nm, and like pGH, this is indicative of a moderately non-polar tryptophan environment (Havel et al., 1988). The native state fluorescence spectra of 3 of the mutants is shown in Figure 7b. Except for pGH(M8) which contains an extra tryptophan residue, all of the mutants have a λ_{max} near 340nm. This suggests that none of the mutations has caused any great conformational change or altered the microenvironment of the tryptophan located in the hydrophobic core of the molecule.

3.3.4 Circular Dichroism of pGH

The recent X-ray crystallographic study of methionyl-pGH showing the protein to possess a four α-helix bundle motif (Abdel-Meguid et al., 1987), confirmed previous results predicting the protein to possess a high α-helix content. The far-UV CD spectrum of the pGH purified at Bresatec displays minima at 221nm and 209nm, which is characteristic of the presence of α-helix (Figure 8a). The $n \rightarrow \pi^*$ helix band at 221nm is fractionally less intense than the $\pi \rightarrow \pi^*$ band at 209nm. Using the PROSEC spectrum deconvolution software available on the AVIV spectropolarimeter (Yang et al., 1986), a value of 47% α-helix content was obtained. This value, close to previously published values of other members of the GH family (Holladay et al., 1974; Bewley & Yang, 1980) suggests that the purified pGH contains its full complement of α-helix. This is important as the secondary structure forms the basic framework of the protein.

The near-UV CD spectrum can often be partially resolved and is known to reflect the conformations and local environments of the aromatic and disulphide

Figure 7. Fluorescence spectra of pGH and pGH mutants.

Fluorescence spectra were recorded on a Perkin-Elmer model LS-50 fluorescence spectrophotometer using an excitation wavelength of 295nm. Emission spectra were scanned from 305 to 400nm using a scan rate of 60 nm/min with the emission and excitation slit widths set at 5nm. The emission spectra are corrected for the Raman peak as described in 2.2.8. The proteins were dissolved in 25mM sodium borate pH 9.1 at a concentration of 0.05-0.1 mg/ml. Samples were centrifuged at 15,000 × g for 5 min immediately prior to fluorescence spectroscopy. (*a*) corrected fluorescence emission spectrum of native pGH_{wt}. (*b*) corrected fluorescence emission spectra of pGH_{wt} and three mutant pGHs. In this case, the four samples differed in their protein concentration.

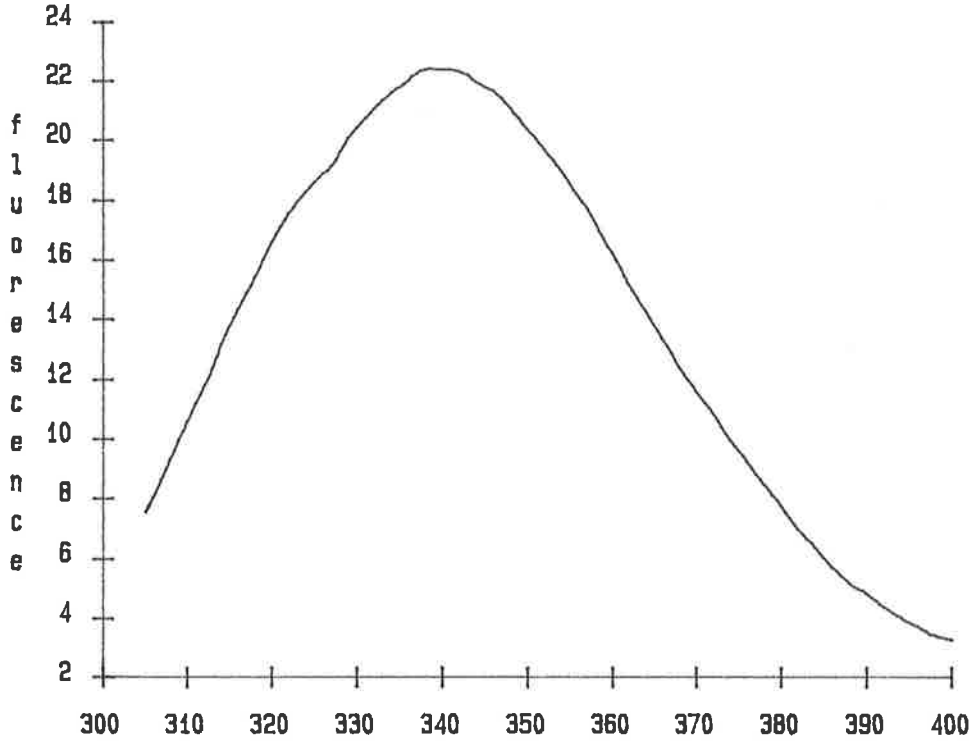
fluorescence
24
22
20
18
16
14
12
10
8
6
4
2
300
310
320
330
340
350
360
370
380
390
400
wavelength (nm)

A

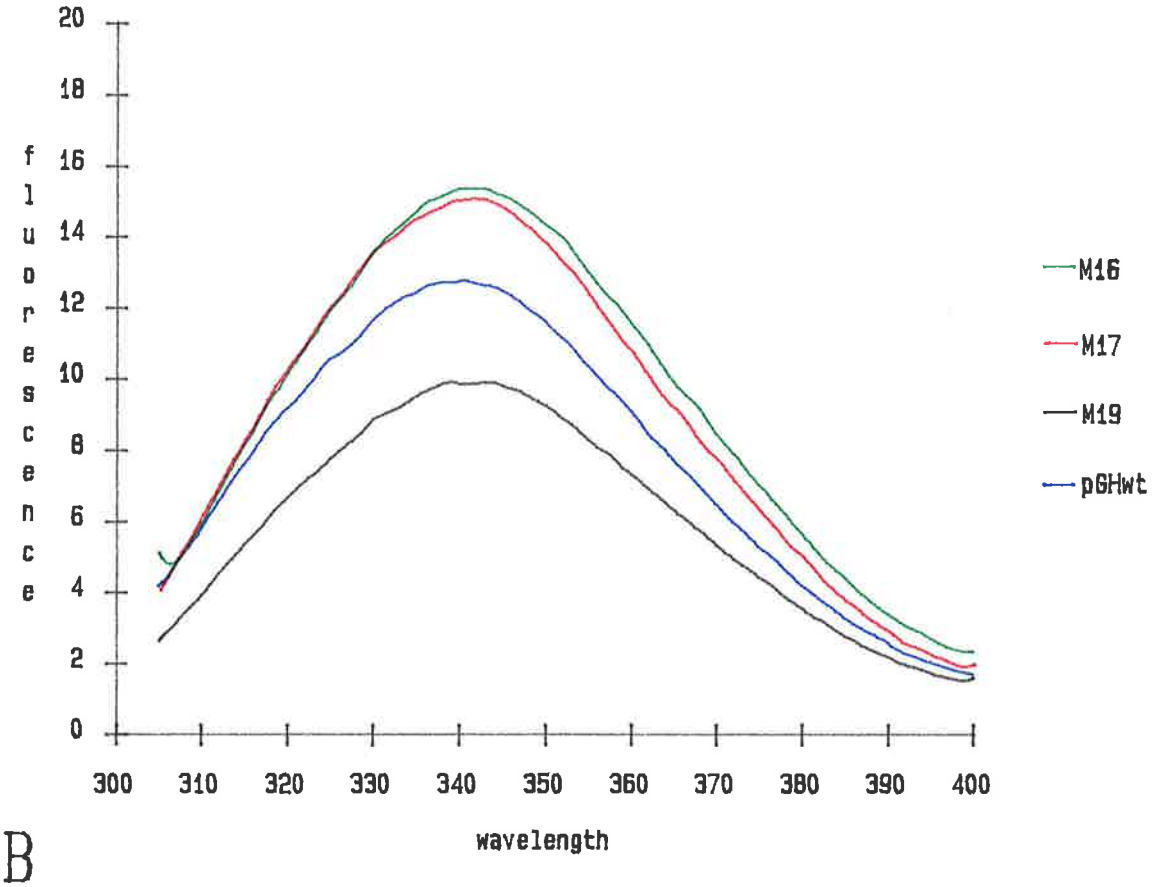
fluorescence
20
18
16
14
12
10
8
6
4
2
0
300
310
320
330
340
350
360
370
380
390
400
wavelength
M16
M17
M19
pGHwt

B

Figure 8. Circular Dichroism of Wild-Type pGH.

CD spectra were recorded on an AVIV 62DS model spectropolarimeter as described in 2.2.7. pGH was dissolved in 25mM sodium borate pH 9.1.(*a*) Far-UV CD spectrum of pGH showing minima at 221nm and 209nm characteristic of α-helix. The protein concentration was 0.16 mg/ml in a 1mm path length cuvette. (*b*) Near-UV CD spectrum of pGH. The protein concentration was 1 mg/ml in a 5mm path length cuvette. The mean residue ellipticity, [θ], has the units $deg.cm^2.dmol^{-1}$.

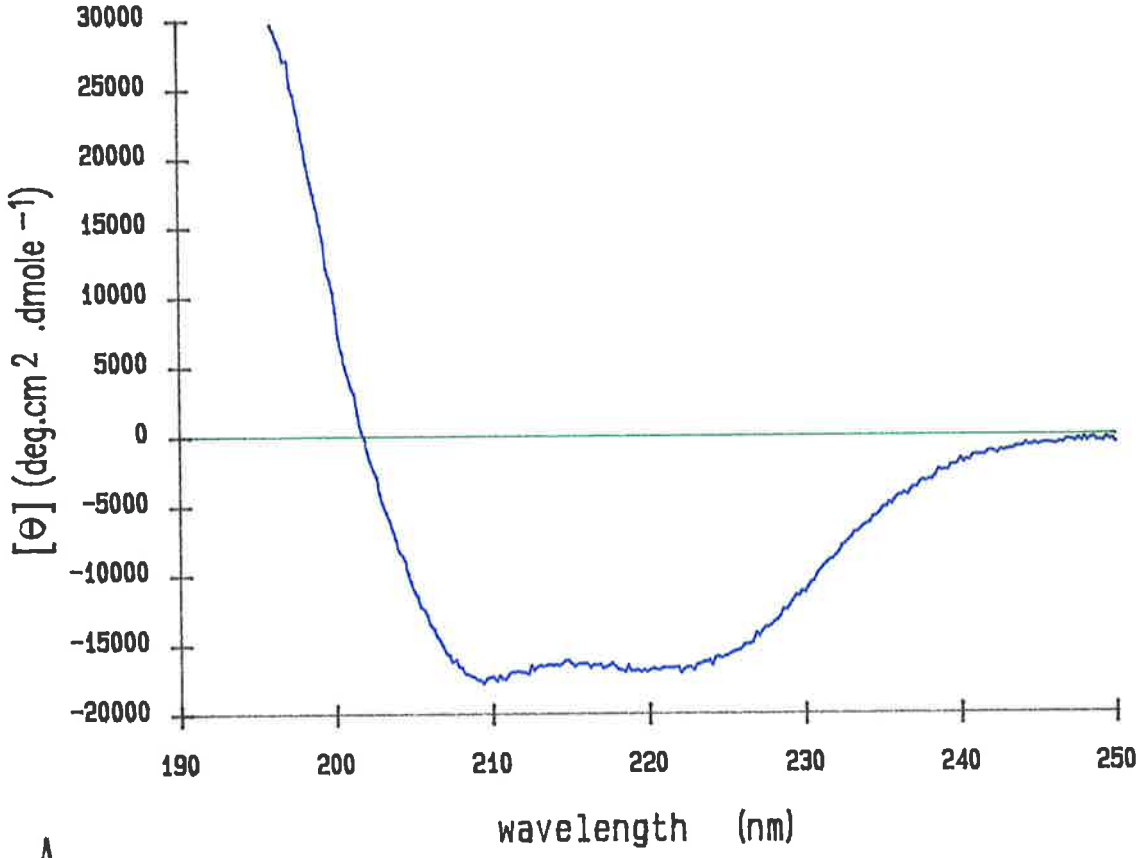
30000
25000
20000
15000
10000
5000
0
-5000
-10000
-15000
-20000
[θ] (deg.cm 2 .dmole -1)
190
200
210
220
230
240
250
wavelength (nm)

A

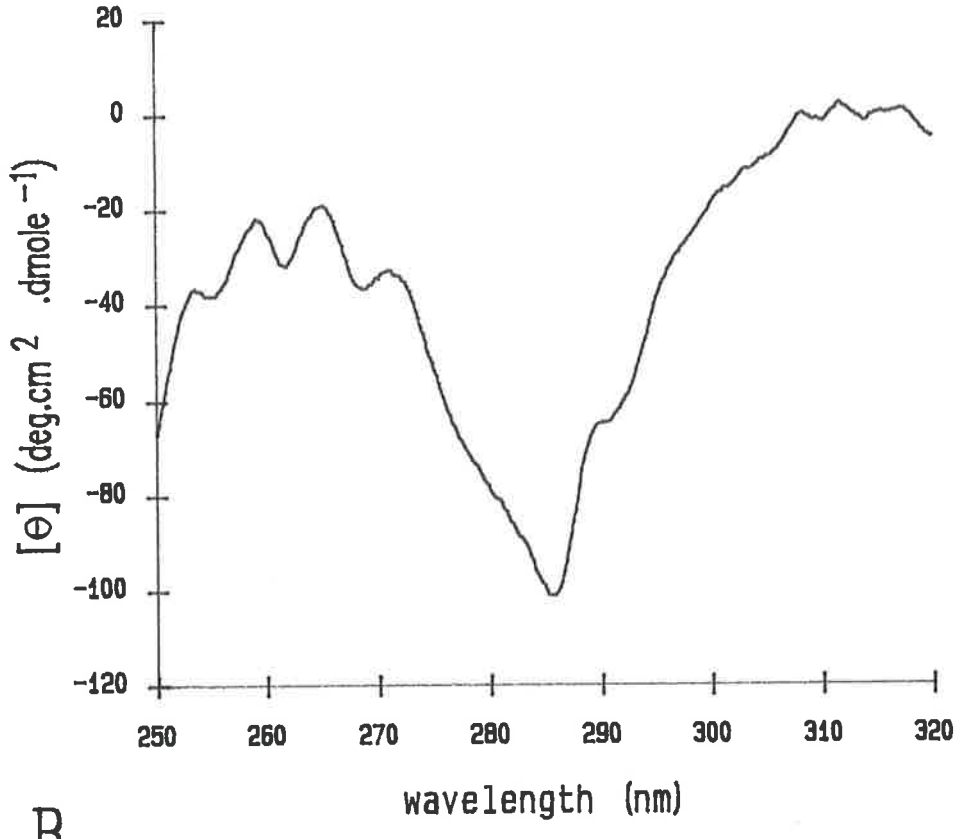
20
0
-20
-40
-60
-80
-100
-120
[θ] (deg.cm 2 .dmole -1)
250
260
270
280
290
300
310
320
wavelength (nm)

B

chromophores (Strickland, 1974). The near-UV CD spectrum of pGH, recorded in the wavelength range 320-250 nm is shown in Figure 8b. The three negative bands at approx. 268nm, 262nm and 256nm are due to the phe^1L_b[0-0] transition and two higher vibronic modes. Like the phenylalanine UV absorbance bands, the wavelengths of these bands are very similar to those reported for pituitary preparations of hGH, bGH, ovine growth hormone (oGH) and rat growth hormone (Holladay et al., 1974), as well as human placental lactogen (hPL) [Bewley & Yang, 1980]. Disulphide bonds also contribute to the negative dichroism in this region of the spectrum (Bewley & Li, 1970). The shoulder near 277nm can be assigned to a tyrosine vibronic mode, whereas the negative peak at 286nm is made up of overlapping the tyr[0-0] transition with the higher vibronic mode of the trp^1L_b transition. The shoulder near 292nm is probably due to the trp^1L_b[0-0] transition. These assignments are based on those found in rat GH due to the similarity in their near-UV CD spectra (Holladay et al., 1974). pGH also possesses two weak shoulders near 298nm and 303nm. These bands probably are due to red-shifting of the trp^1L_a CD band as was seen in the UV absorbance. The band at 298nm becomes very prominent as the protein is denatured in GuHCl. The discussion on this phenomenon will be suspended until Chapter 4 (see 4.2.4). The similarity between the rat GH and pGH spectra is not surprising considering that these two proteins share 95% sequence identity (Page et al., 1981). A recent examination of several members of the GH family of proteins has shown that elephant GH, fin whale GH and equine GH also have near-UV CD spectra similar to pGH (Bewley & Li., 1987). Both elephant (Hulmes et al., 1989) and equine (Bewley & Li., 1987) GHs have only three residues which differ from pGH (98% identity). What is more surprising is that human placental lactogen also has a very similar near-UV CD spectrum (Bewley & Yang, 1980) even though it does not share much sequence identity with non-primate GHs. This is further complicated by the fact that hPL shares 85% sequence identity with hGH.

3.3.5 High Performance Ion Exchange Chromatography

The extent of deamidation of the purified GH was determined by high performance ion exchange chromatography on a Mono-Q column (2.2.6.1). Figure 9a-d shows the Mono-Q gradient elution profile for pGH, pGH(M23), pGH(M16) and hGH, respectively. All of the profiles show a single major peak with only minute amounts of detectable charge variants (arrows). pGH(M23) contains the mutation Y29K whereas pGH(M16) is a double mutant with the changes K30Q;R34E. The net charge difference between these two mutants and pGH is +1 and -3, respectively. At pH 8.8, pGH(M23) elutes at the same NaCl concentration as pGH (50mM) whereas pGH(M16) being the more acidic protein elutes much later at 150mM NaCl. Negatively charged regions on the surface of a protein are responsible for its binding to an anion-exchange column. Apparently, the tyrosine to lysine mutation in pGH(M23) does not affect the surface negativity of the protein nor its affinity to the column. At pH 8.2, the major peak of the purified hGH elutes at 115mM NaCl.

All of the GHs purified contained less than 10% of ionic variants (such as deamidated forms) as detected by high performance ion exchange chromatography.

3.3.6 N-terminal Sequence Analysis

N-terminal sequence analysis (see 2.2.6.3) was used to verify the sequence of the first ten residues of pGH, hGH, brGH and a mutant of pGH, pGH(M12). This mutant was chosen to test the mutant production system because it contained a proline to serine substitution at position 6 in the sequence. The correct sequence was verified in all of the above proteins. Furthermore each cycle of the Edman degradation gave a clear single PTH-amino acid signal verifying the homogeneity of each preparation.

3.3.7 Electrospray Mass Spectrometry

Electrospray mass spectrometry of the purified GHs was carried out by Dr. Margaret Sheil at the Department of Chemistry, University of Wollongong. Conventional techniques used to measure molecular weights of proteins such as SDS

Figure 9. High performance ion exchange chromatography of purified GHs.

Purified GH preparations were subjected to high performance ion-exchange chromatography on a 5mm × 50mm Mono Q column as described in 2.2.6.1. A small amount of lyophilized protein was dissolved in 25mM sodium borate pH 8.8 [pH 8.2 for hGH] (Buffer A) to a final protein concentration of about 1 mg/ml. The protein was loaded onto a Mono Q column pre-equilibrated in Buffer A, at a flow-rate of 1 ml/min. The column was washed with Buffer A before the protein was eluted with a 15ml 0-150mM NaCl gradient. The A_{280} was monitored (—). The NaCl concentration is shown to the right of each chromatogram. *Sample a:* pGH_{wt}. *Sample b:* pGH(M23). *Sample c:* pGH(M16). *Sample d:* hGH. The arrows refer to minor charge variants present.

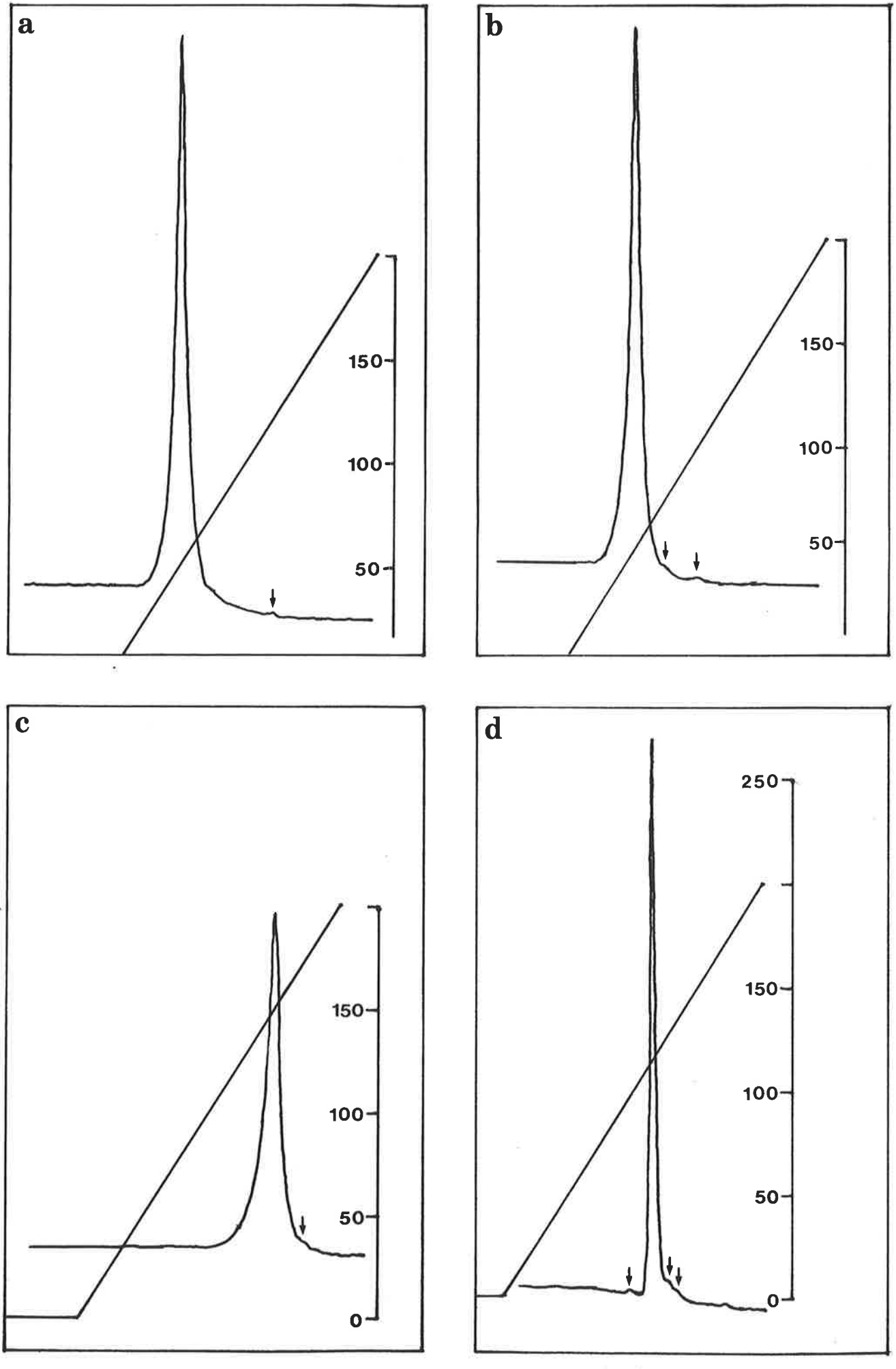
a
150
100
50
b
150
100
50
c
150
100
50
0
d
250
150
100
50
0

polyacrylamide gel electrophoresis and chromatography are typically accurate to 5 per cent. By comparison, electrospray mass spectrometry (ESMS) increases the accuracy of such measurements to around 0.01 per cent. Table II illustrates the accuracy possible when determining the molecular weight of proteins. The mass spectrometry derived molecular weights of four of the purified GHs are within 2 Da of the calculated molecular weight, based on the expected amino acid composition. Most of the GHs tested resulted in very clean spectra indicating the absence of contaminating modified forms of the proteins. The spectrum of pGH(M10) did show the presence of a minor contaminant with a higher molecular weight than the major peak. The 20,974.4 dalton mass of the major peak was equivalent to the calculated mass for the deletion mutant (Chapter 5, Table IV). Figure 10 illustrates the electrospray spectrum of pGH(M8). The peaks indicate the mass/charge ratio of a series of multiply-charged ions, with each ion in the series differing by plus and minus one proton from adjacent ions in the series. The results from the mass spectrometer verify that the purified GHs possess the correct molecular mass, and therefore are very likely to have the correct amino acid composition.

3.3.8 Radioreceptor Assays

In vitro receptor binding was used to verify the biological activity of the purified GHs. The assays were kindly performed by Scott Rowlinson at the University of Queensland (see 2.2.10). A radioreceptor assay using radiolabelled GH binding to rabbit liver microsomes was used to determine the affinity constants (K_a) of the various GHs. Because brGH binding to the rabbit liver receptor preparation was very low, a homologous receptor binding assay using freshly prepared bream liver microsomes was employed. Previous studies had confirmed that pituitary pGH and the Bresatec recombinant pGH were equipotent in inhibiting the binding of ^{125}I-pituitary pGH to rabbit liver microsomes (M.J. Waters, unpublished observations). This suggests that the conformation of the recombinant pGH is very similar to the pituitary pGH. Scatchard analysis gave K_a values of 5.0×10^9 M^{-1} and 2.75×10^9 M^{-1}

Table II. Comparison of the Calculated and Mass Spectrometry-Derived Molecular Weights of the GHs.

The molecular weight of each GH, based on the amino acid sequence, is compared to the experimentally-derived molecular weight from the mass spectrometer. The single letter code of each amino acid and their respective residue molecular weights are shown in Columns 1 and 2. Columns 3, 5, 7 and 9 show the amino acid composition of each methionyl-GH. Note that met-pGH and met-pGH(M8) differ only in the amount of methionine and tryptophan due to the single amino acid substitution. Columns 4, 6, 8 and 10 show the contribution of each amino acid (obtained by multiplying Column 2 with Column 3 for met-pGH, Column 2 with Column 5 for met-hGH, etc.) to the total mass of the protein. The sum of these is referred to as the Subtotal. A mass of 18 is added to each for the additional oxygen and two hydrogens at the N- and C-terminal ends, and a mass of 4 is subtracted due to loss of four hydrogens involved in forming the disulphide bonds. The "error" between the calculated and experimental mass is shown at the bottom of the latter columns.

1	2	3	4	5	6	7	8	9	10
Amino Acid	Mr	met-pGH		met-hGH		met-pGH(M8)		met-brGH	
A	71.09	17	1208.53	7	497.63	17	1208.53	11	781.99
R	156.2	13	2030.6	11	1718.2	13	2030.6	12	1874.4
N	114.12	5	570.6	9	1027.08	5	570.6	5	570.6
D	115.1	11	1266.1	11	1266.1	11	1266.1	10	1151
C	103.16	4	412.64	4	412.64	4	412.64	4	412.64
Q	128.15	12	1537.8	13	1665.95	12	1537.8	11	1409.65
E	129.13	13	1678.69	14	1807.82	13	1678.69	13	1678.69
G	57.07	8	456.56	8	456.56	8	456.56	7	399.49
H	137.16	3	411.48	3	411.48	3	411.48	6	822.96
I	113.18	6	679.08	8	905.44	6	679.08	10	1131.8
L	113.18	25	2829.5	26	2942.68	25	2829.5	26	2942.68
K	128.19	11	1410.09	9	1153.71	11	1410.09	9	1153.71
M	131.21	4	524.84	4	524.84	3	393.63	2	262.42
F	147.19	13	1913.47	13	1913.47	13	1913.47	8	1177.52
P	97.13	7	679.91	8	777.04	7	679.91	9	874.17
S	87.09	15	1306.35	18	1567.62	15	1306.35	22	1915.98
T	101.12	8	808.96	10	1011.2	8	808.96	9	910.08
W	186.23	1	186.23	1	186.23	2	372.46	1	186.23
Y	163.19	7	1142.33	8	1305.52	7	1142.33	7	1142.33
V	99.15	8	793.2	7	694.05	8	793.2	6	594.9
		Subtotal	21846.96		22245.26		21901.98		21393.24
		+H2O	18		18		18		18
		-disulphides	-4		-4		-4		-4
		CAL. TOTAL	21860.96		22259.26		21915.98		21407.24
		Mass-Spec.	21860.2		22257.5		21916.2		21407.2
		Error	-0.76		-1.76		0.22		-0.04

Figure 10. Electrospray Ionization Mass Spectrum of pGH(M8).

Electrospray mass spectrometry was performed as described in 2.2.6.4. The peaks indicate the mass/charge ratio of a series of multiply charged ions, with each ion in the series differing by plus and minus one proton from adjacent ions in the series. The series in this example includes from left to right, the 20^+ to 13^+ ions.

File: M8 LAB-BASE - The GC-MS Data System Date: 21/04/1992 Time: 17:12

Sample:

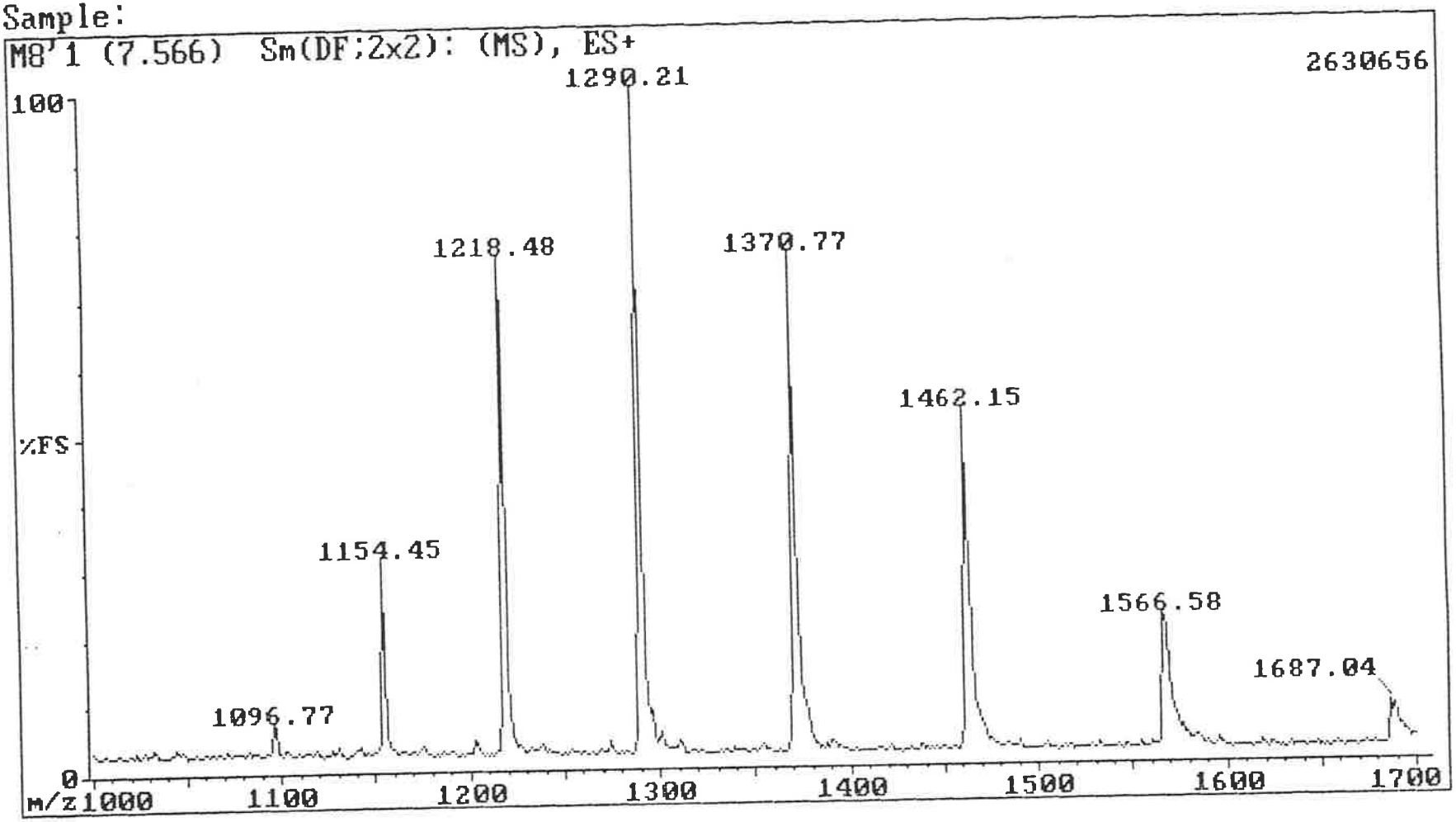

for pGH and brGH, respectively. These K_a values are comparable to the value obtained for recombinant hGH affinity to human liver receptors (9×10^9 M^{-1}). This indicates that the purified recombinant-pGH and brGH possess high affinity receptor binding activity.

The receptor binding affinity of each pGH mutant compared to wild-type pGH was determined using a homologous competition assay in which radiolabelled mutant was displaced from rabbit liver microsomes by increasing concentrations of unlabelled mutant (2.2.10). Table III shows the K_a(mutant)/K_a(wild-type) ratio for the 10 mutant pGHs purified. Two of the mutants have a more than 2-fold increase in binding affinity. These involve mutations in the putative receptor interactive Ca^{2+} chelation site at the carboxy terminal end of helix-1 (Barnard et al., 1989). In addition two of the mutants, pGH(M14) and pGH(M8) have a more than 2-fold decrease in binding affinity. Recent site specific mutagenesis studies (Cunningham et al., 1989, 1991) have delineated two separate regions of hGH important in binding to its receptor. One of these regions encompasses the exposed sides of helices 1 and 3. The substitution of methionine at residue 124, situated close to this region on helix-3, with a bulky tryptophan residue in the pGH(M8) mutant, may have interfered with the receptor interaction. The reason for the decrease in binding for pGH(M14) is not understood at present. The remaining mutants give K_a values close to the wild type pGH.

The difference in the affinity constants between mutant and wild-type pGH are only small and would represent local alterations in receptor interactive regions. Any gross conformational change would be detected as a large decrease in binding affinity in the order of one or two orders of magnitude. The receptor binding studies have further corroborated the conformational integrity of the GHs used in this thesis.

Mutant	n	$K_A$mut/$K_A$wt	S.E.M.
pGH(M8)	4	0.45	0.05
pGH(M10)	3	0.76	0.22
pGH(M12)	2	0.71	-
pGH(M13)	4	0.71	0.16
pGH(M14)	4	0.43	0.19
pGH(M16)	3	0.90	0.23
pGH(M17)	3	2.38	0.48
pGH(M19)	6	2.1	0.25
pGH(M21)	3	0.81	0.16
pGH(M23)	3	0.76	0.13

Table III. Relative binding affinity of pGH mutants.

Each mutant was tested in its ability to compete with homologous ^{125}I-labelled mutant binding to a rabbit liver microsome preparation, a source of GH receptors. The affinity constant was determined by Scatchard analysis (*Scatchard, 1949*) and compared to that for wild-type pGH. The assay buffer was 25mM Tris-HCl pH 7.5, 0.1% B.S.A., 20mM $MgCl_2$. S.E.M. is the standard error of the mean. n is the number of determinations for each mutant.

3.4 DISCUSSION

A method has been described for the production of up to 0.5 g of purified recombinant growth hormone per litre of *E.coli* fermentation broth. This method makes use of the relatively high purity and ease of purification of inclusion bodies, a highly concentrated source of the recombinant protein, from the induced cells. A single step combining inclusion body dissolution, GH refolding and oxidation followed by a single chromatographic extraction completes the overall procedure. This method has been applied to the production of pGH, and mutants thereof, as well as hGH and brGH.

The structural properties of the proteins have been examined using a combination of UV spectroscopy, near and far-UV circular dichroism and fluorescence spectroscopy. Far-UV CD of pGH detected the presence of 47% α-helix, a figure close to that obtained from the X-ray structure (Abdel-Meguid et al., 1987). The UV absorption bands in the aromatic region have been characterized by the use of second-derivative spectroscopy. The wavelengths of the second-derivative and near-UV CD absorption bands, indicative of the polarity of the environment surrounding the aromatic residues, have been described for pGH, brGH, hGH and a mutant of pGH, pGH(M8). The similarity between these results and those previously reported for pituitary preparations of other GHs (Bewley & Li., 1987) indicates a close structural relationship between these molecules. Fluorescence spectroscopy has also shown that the mutations made in the pGH mutants have not affected the overall conformation of the molecule.

The homogeneity of each purified hormone has been verified by the use of SDS polyacrylamide gel electrophoresis, ion-exchange chromatography (extent of deamidation), size-exclusion chromatography (extent of aggregation), N-terminal sequencing and electrospray mass spectrometry. The latter method has also proven the identity of each protein by measuring the mass to within one dalton of the calculated molecular weight. This has verified that the proteins are completely intact and have not been degraded by the purification process. Finally, the biological

activity of each GH has been verified by its receptor binding activity. In addition, the conformation of the mutant pGHs has not been drastically altered as no major disruption has occurred in their receptor binding capacity.

By the criteria met in this chapter, the homogeneity and identity of each of the recombinant GHs used in this thesis has been verified.

CHAPTER 4

EQUILIBRIUM DENATURATION OF RECOMBINANT PORCINE GROWTH HORMONE

4.1 INTRODUCTION

Protein folding/unfolding is generally a highly cooperative process in which only the completely folded and unfolded states are significantly populated. This is true for most small globular proteins of M_r <20,000, where the entire protein behaves as a single cooperative unit (Privalov, 1979). For larger multidomain proteins, the folding/unfolding transition is characterized by the presence of partially folded intermediates. However, these intermediates correspond to partially folded conformations in which some of the structural domains, which act in themselves as individual cooperative folding units, are folded and others unfolded (Jaenicke, 1987). At the beginning of the last decade, the existence of true intermediate states in protein folding transitions seemed highly improbable and the classical two-state theory seemed to be well established.

However, with the appearance of a few cases of proteins possessing populated equilibrium intermediates and the advent of technologies capable of observing short-lived kinetic intermediates, their existence was virtually confirmed. There are now several examples of small proteins which provide exceptions to the two-state rule: carbonic anhydrase (Wong & Tanford, 1973), α-lactalbumin (Kuwajima et al., 1976), penicillinase (Robson & Pain, 1973) and bovine growth hormone (Burger et al., 1966; Holladay et al., 1974). A recurring feature seen in the denaturation transitions of these proteins was that the secondary structure was more stable to denaturation than the tertiary structure. The intermediate state was almost as compact as the fully folded state, possessing native-like secondary structure but lacking a defined tertiary structure. The term "molten globule" was introduced to denote the intermediate state, but is often used to refer to the model of protein folding involving this intermediate state (Ptitsyn, 1987). This model is a subset of the framework model of protein folding which describes folding as a sequential process beginning with the rapid formation of secondary structure followed by collapse to a compact native-like state, before the tertiary structure is locked in place (Kim & Baldwin, 1982).

As mentioned above, early studies on the pH-induced denaturation of pituitary bovine growth hormone (bGH) detected the presence of an intermediate containing considerable helical structure yet having the UV absorbance of denatured protein (Burger et al., 1966). Holladay et al. (1974) demonstrated the presence of a similar intermediate in bGH as well as ovine- and rat-GH, induced by GuHCl as observed by the noncoincidence of the UV absorbance and CD detected transitions. More recently, the equilibrium denaturation of bGH has been shown to be a multistate process in which at least four species have been identified: native, a monomeric folding imtermediate, an associated folding intermediate, and unfolded protein (Brems et al., 1985,1986; Havel et al., 1986, 1988). The monomeric folding intermediate has the characteristics of a molten globule: largely a-helical, with a compact hydrodynamic radius similar to the native state, yet possessing a tertiary structure similar to the unfolded state (Brems & Havel, 1989). It is also less soluble than the native and unfolded states, tending to form insoluble aggregates in aqueous buffers (Brems, 1988). The presence of the associated folding intermediate, an aggregated form of the molten globule state, is protein concentration dependent, occurring at concentrations above 10μM. In addition, a bGH region that includes amino acid residues 109-133 appears to be directly involved in the association process (Brems et al., 1986).

Unlike the non-human species of GH examined thus far, the denaturation of human growth hormone (hGH) follows a two-state mechanism, with no detectable intermediates (Brems et al., 1990). The apparent absence of intermediates was attributed to the their relative instability compared with the native structure. The conformational stability of hGH is at least 5 kcal/mol more stable than GHs from other species (Brems et al., 1990). In the development of a procedure for the production of a recombinant porcine growth hormone (pGH) at Bresatec, it was necessary to study the properties of the purified protein in the presence of the denaturants GuHCl and urea. With the available information on the behaviour of bGH and hGH it was decided that studying the denaturation of pGH would prove to be an interesting comparative study.

pGH is a single chain polypeptide containing 191 amino acids arranged to form an antiparallel four α-helix bundle (Abdel-Meguid et al., 1987). A computer representation of the pGH polypeptide fold as seen in the 2.8Å electron density map is shown in Figure 1. Using this two-dimensional representation of a three-dimensional structure and the pGH helix assignments of Abdel-Meguid et al. (the X-ray coordinates have yet to be released), a rough model of the protein was made using a molecular modelling kit (Figure 2). In assembling this model it became obvious how tightly packed and globular the molecule is. This feature is not clearly obvious from the simplified representation of Figure 1. Several structural features of pGH are conserved amongst the growth hormones of other species; the primary structure contains two disulphide bridges, one of which forms a large loop connecting distant parts of the primary sequence, and the second forms a short loop near the C-terminus. A single conserved tryptophan residue located in the second helix occupies a hydrophobic pocket formed by the hydrophobic faces of the four helix bundle (Abdel-Meguid et al., 1987; Carlacci et al., 1991). The UV absorption and fluorescence properties of this amino acid make it useful as an intrinsic probe for the study of pGH tertiary structure. A recent report of the crystal structure of human growth hormone (hGH) complexed to its receptor (de Vos et al., 1992) has shown that the topography of hGH is similar to that described for pGH. In view of the high degree of conservation of their primary structure, it would be quite reasonable to assume that all members of the growth hormone family have similar three-dimensional structures.

The aim of this chapter is to present the equilibrium denaturation of pGH, a protein that shares 91% and 68% primary sequence identity with bGH and hGH, respectively, using the denaturant GuHCl. The denaturation was followed by UV absorption spectroscopy, intrinsic fluorescence, near- and far-UV circular dichroism and size-exclusion chromatography. The denaturation transitions obtained from each method were non-coincident, indicating a deviation from a two-state denaturation

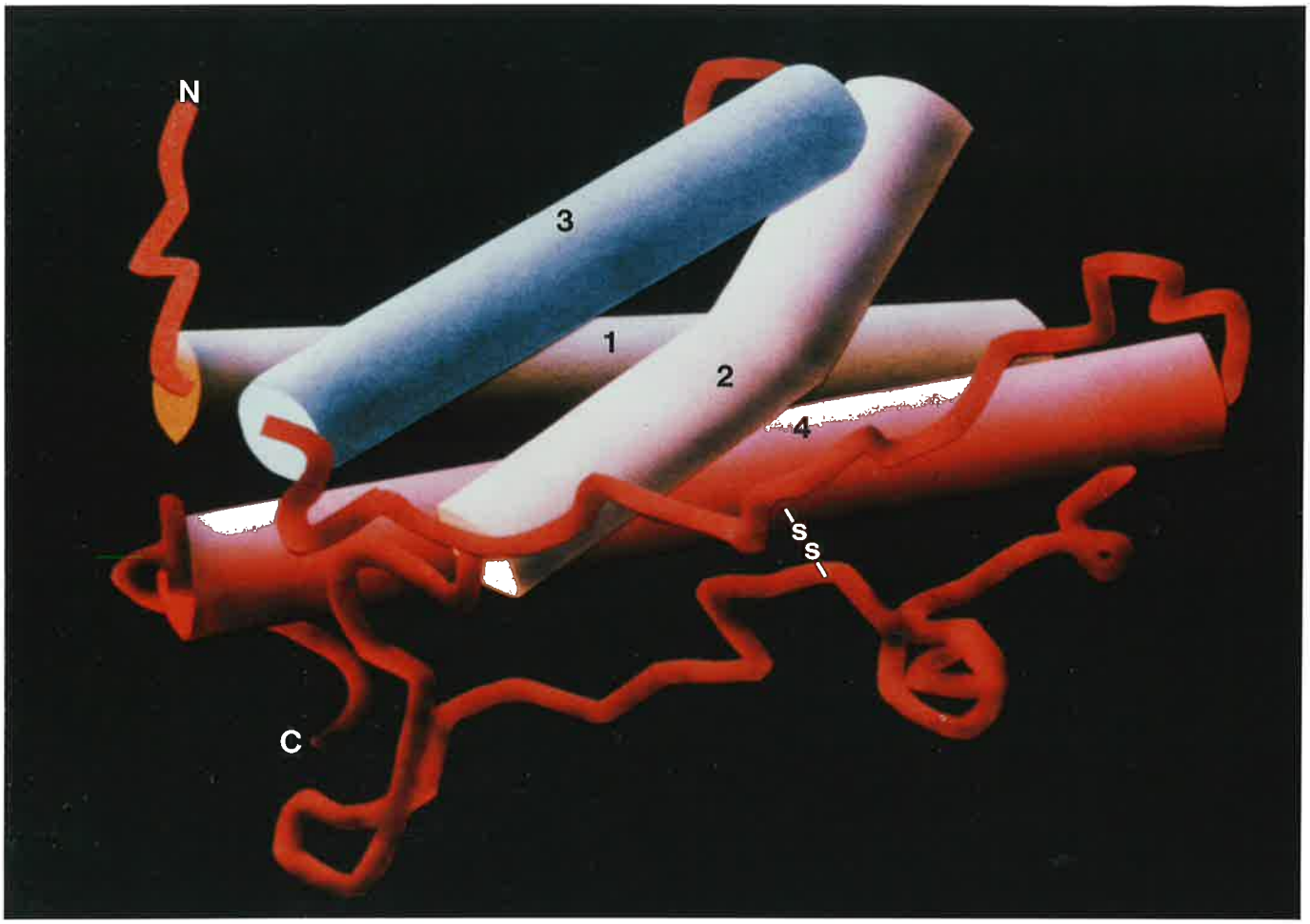

Figure 1. Computer representation of the pGH polypeptide fold.

A computer representation of the pGH fold as seen in the 2.8Å electron density map (*Abdel-Meguid et al., 1987*). Each of the four α-helices (numbered 1 to 4 from the N-terminus) is represented by a cylindrical rod, whereas regions of essentially non-helical polypeptide are shown as a thin tube. The N-terminus is located in the upper left-hand corner, whereas the C-terminus is at the lower left-hand corner. The kink in helix-2 is due to the presence of a proline residue. One of the two disulphide bonds connects the long loop between helix-1 and -2 to helix-4 (just visible in Figure 2). The second disulphide bond, hidden in this view, connects the C-terminal extension to the end of helix-4.

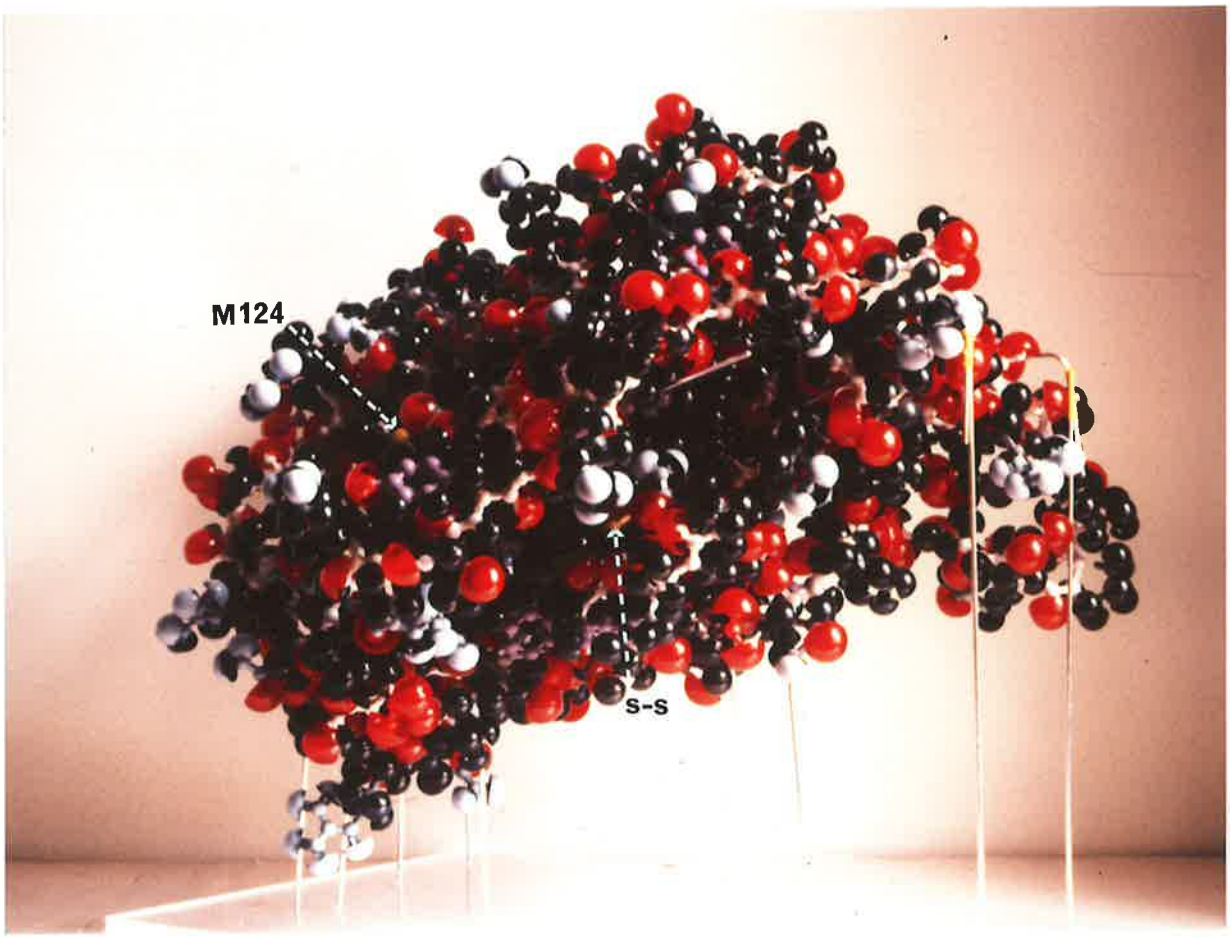

Figure 2. A model of porcine growth hormone.

The model was constructed using the amino acid sequence, helix assignments and the two-dimensional representation of the three-dimensional X-ray structure (as in Figure 1) from Abdel-Meguid et al. (1987) [see 2.2.14 for details]. This view is similar to the one shown in Figure 1 except that the molecule has been tilted upward slightly and rotated about 30° anticlockwise. The long loop disulphide bond is visible as is the sulphur atom of methionine-124. The colour coding is: red, oxygen; black, hydrogen; blue, side-chain amide or amine hydrogen (i.e., arg, lys, gln, asn); yellow, sulphur; white, polypeptide backbone; grey, side-chain "backbone".

mechanism. The presence of an associated folding intermediate similar to that seen in bGH was also detected.

4.2 RESULTS AND DISCUSSION

4.2.1 UV Absorbance Spectroscopy

The UV absorbance spectrum of native pGH was previously described in detail in 3.2.2. The prominent shoulder centred near 290nm is due mainly to the absorption of the single tryptophan residue (Figure 3a). Denaturation of pGH in 6M GuHCl results in a considerable loss in extinction (hypochromicity), with a general blue-shifting of the spectrum toward lower wavelengths (Figure 3a). The GuHCl-induced difference in absorbance at 290nm is indicative of the exposure of the single internalized tryptophan, to the solvent exterior upon unfolding. The absorbance change upon transfer of a particular aromatic residue to an aqueous environment depends upon the hydrophobicity of its environment in the folded protein (Wetlaufer, 1962). Denaturation of pGH results in an extinction loss of 2,400 $M^{-1}cm^{-1}$ at 290nm, similar to that seen in the GuHCl-induced denaturation of bGH (Brems et al., 1985). In addition, Bewley and Li (1984) obtained a similar loss of extinction with hGH when removing all conformational effects on the absorption spectrum by thermolysin digestion and titration of the digest to pH 1.5.

The loss of extinction at 290nm relative to 278nm as a function of GuHCl concentration is shown in Figure 3b. The smoothest transition curves were obtained by using this ratio of absorbances. The absorbance at 278nm was used as an internal standard to monitor any loss of protein due to precipitation. In the initial experiments two stock solutions of pGH at equal concentrations, one in buffer containing no GuHCl and the other in buffer containing 6M GuHCl, were mixed in the appropriate proportions to arrive at each final GuHCl concentration. When measurements of the absorbance at 290nm (A_{290}) were made, a sigmoidal transition with a trough in the 2.5-3.75M GuHCl region was consistently observed. This loss of extinction was later found to be due to a small amount of protein precipitation at these GuHCl

Figure 3. Equilibrium denaturation of pGH monitored by UV-absorbance.

Spectra were recorded on a Cary 3 spectrophotometer as described in 2.2.6.2. The protein concentration was 0.22 mg/ml in buffers containing 25mM sodium borate pH 9.1. (*a*) UV-absorbance spectra of native (—) and 6M GuHCl-denatured (----) pGH. (*b*) The effect of the GuHCl concentration on the absorbance of pGH at 290nm relative to 278nm (i.e., A_{290}/A_{278}) under equilibrium conditions, was determined as described in 2.2.11.1.

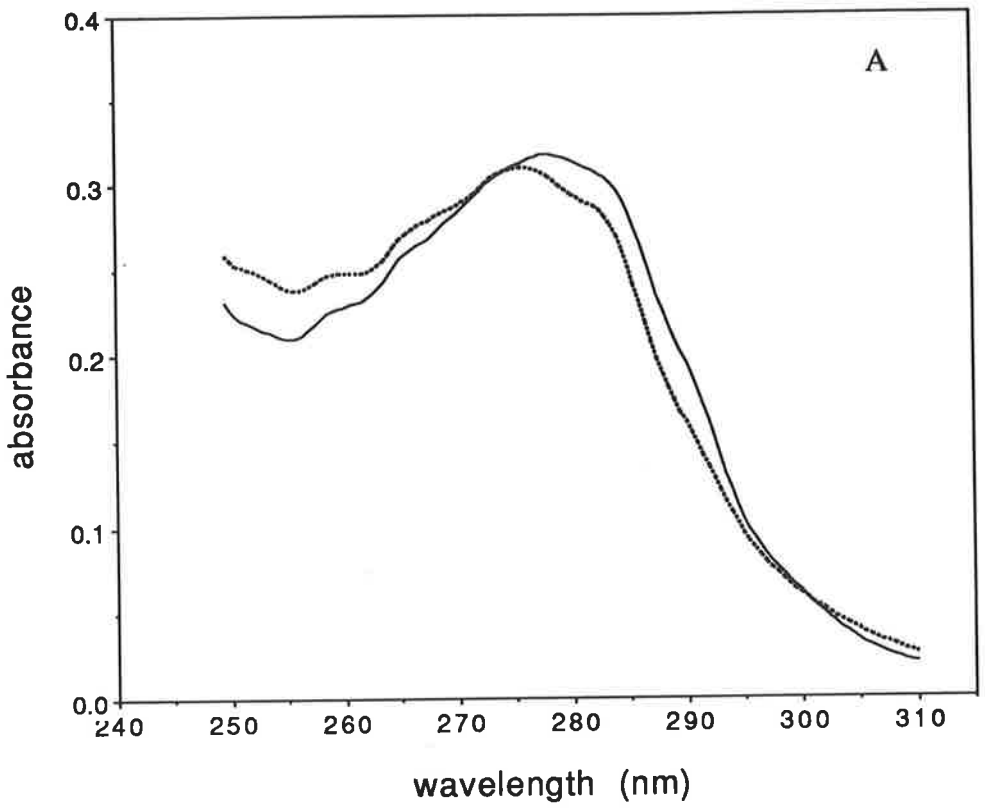
A
absorbance
0.4
0.3
0.2
0.1
0.0
240
250
260
270
280
290
300
310
wavelength (nm)

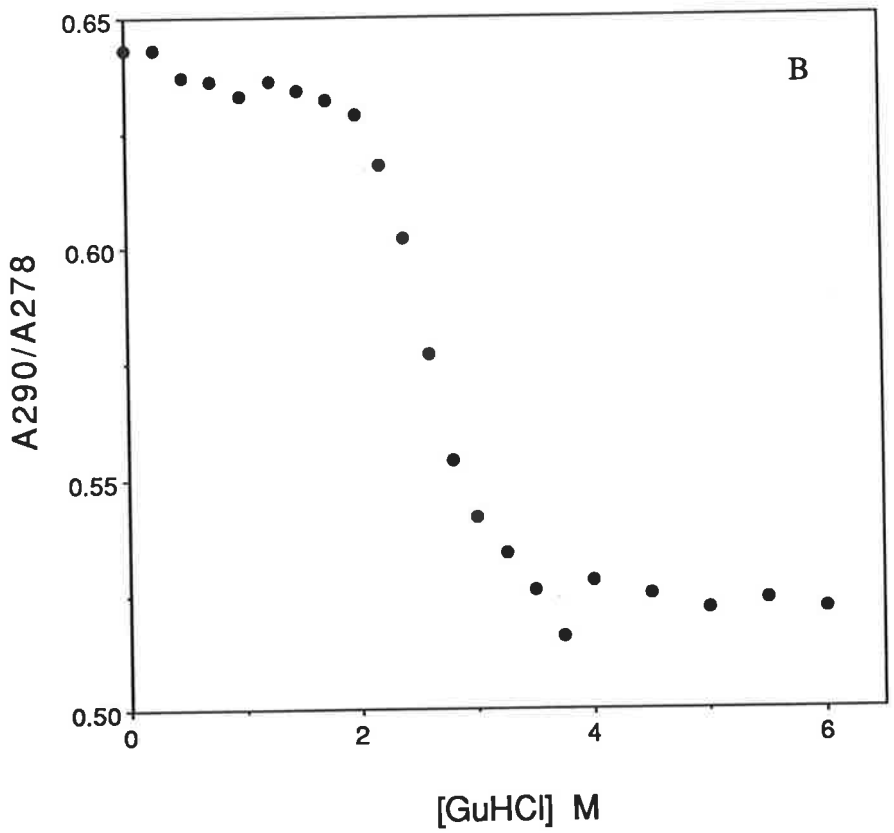
B
A290/A278
0.65
0.60
0.55
0.50
0
2
4
6
[GuHCl] M

concentrations. Fortunately, at the time, I was recording the whole spectrum (310-250nm) for each sample. When the data was re-examined using an A_{290}/A_{278} ratio, a smooth sigmoidal transition was observed (Figure 3b). In subsequent experiments it was found that this complication could be avoided by adding a constant volume of a stock solution of pGH in buffer without GuHCl, to increasing concentrations of GuHCl (see 2.2.11.1). This also avoided the need to measure the whole spectrum of each sample. The pGH UV-absorbance detected denaturation curves generally had a gently downward sloping pre-transition baseline and a flat post-transition baseline (Figure 3b). This was found for all of the mutant pGHs as well (see 5.2.3.2 and Chapter 5, Figures 5-9). The transition begins at about 2.2M GuHCl and is complete by 3.75M GuHCl. The midpoint of the transition, determined from 5 separate experiments, consistently occured at 2.68 ± 0.05 M GuHCl. The transition midpoint was protein concentration independent. Five determinations with protein concentrations ranging from 0.15 - 0.33 mg/ml gave the same result. This compares to a UV-detected transition of 3.1M for bGH (Brems & Havel, 1989) and 4.6M for hGH (Brems et al., 1990).

4.2.2 Fluorescence Spectroscopy

The fluorescence emission spectrum of native pGH upon excitation at 295nm was described in section 3.3.3 as a broad single band with a maximum (λ_{max}) at 338.5 ± 0.5nm (Figure 4a). The λ_{max} of a tryptophan residue is highly sensitive to the polarity of the environment surrounding it (Teale, 1960). An excitation wavelength of 295nm was specifically chosen so that only the tryptophan residue would be excited. Tyrosine residues have negligible absorbance at this wavelength, so their contribution to the fluorescence is also negligible. Excitation of pGH at lower wavelengths such as 278nm results in a similar spectrum characteristic of tryptophan fluorescence, except that the intensity is increased slightly due to the tyrosine contribution (spectrum not shown). The tryptophan dominated emission spectrum is probably due to efficient energy transfer from the tyrosines to the tryptophan in the folded state (Lackowicz,

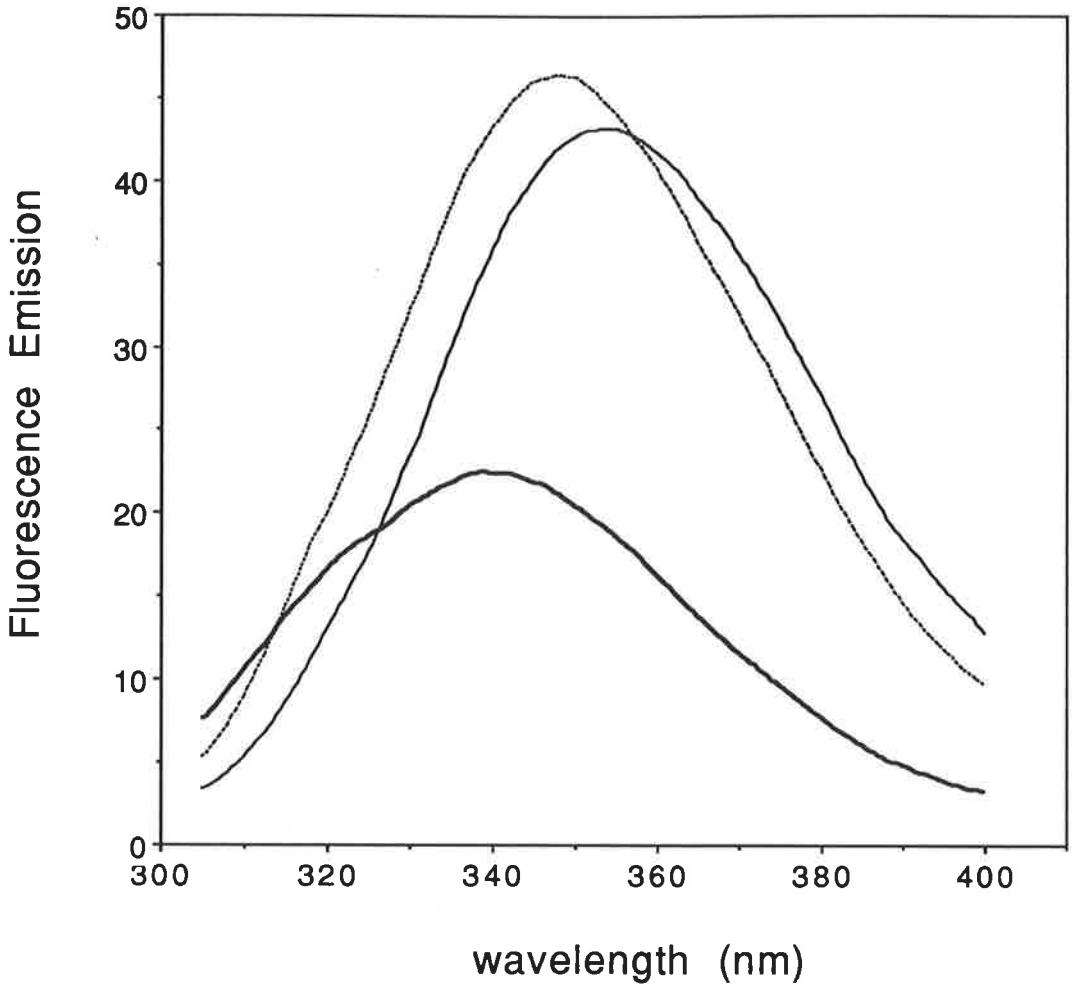

Figure 4a. GuHCl-induced equilibrium denaturation of pGH as measured by intrinsic protein tryptophan fluorescence.

Fluorescence emission spectra were recorded on a Perkin-Elmer model LS-50 fluorescence spectrophotometer using an excitation wavelength of 295nm. Emission spectra were scanned from 305 to 400nm using a scan rate of 60 nm/min with the emission and excitation slit widths set at 5nm. The spectra are corrected for the Raman peak as described in 2.2.8. The protein was dissolved at each concentration of GuHCl in a buffer containing 25mM sodium borate pH 9.1. The final protein concentration was 0.08 mg/ml. Samples were centrifuged at 15,000 × g for 5 min, immediately prior to fluorescence spectroscopy. Emission spectra for native (—), intermediate at 3.25M GuHCl (----), and unfolded in 6M GuHCl (—) pGH.

1983). When the protein is unfolded, the energy transfer is less efficient, because of the increased separation of the tyrosines from the tryptophan, and two emission bands are observed. The first, at 305nm is due to the tyrosine fluorescence and the second at 352nm is due to the solvent-exposed tryptophan fluorescence.

Previous studies have reported values of λ_{max} for native pGH near 330nm (Seely & Hollis, 1986; Kauffman et al., 1989), suggestive of a more non-polar tryptophan environment. The discrepancy in the figures could reflect differences in the recombinant pGH preparations. Seely and Hollis (1986) state that their recombinant pGH was a few residues shorter than the pituitary one. It could also be due to the Raman peak of water overlapping the emission spectrum of pGH, resulting in an apparent blue shift (Schmid, 1989). In my initial fluorescence measurements of pGH, a fluorimeter connected to an analog chart recorder was used. At wide slit widths (10nm), a symmetrical emission band with a λ_{max} of 330nm was observed. Manual subtraction of the Raman water peak proved to be very difficult and so the instrument was abandoned for a computer interfaced model (2.2.8). Nevertheless, native bGH, which shares 91% sequence identity with pGH, has a λ_{max} of 335nm (Havel et al., 1988), similar to that for pGH reported here.

With increasing GuHCl concentration, the fluorescence emission undergoes an increase in intensity, maximal at 3.25M GuHCl, followed by a 15% decrease at higher concentrations of denaturant (Figures 4a). Figure 4b shows the equilibrium denaturation of pGH monitored by fluorescence intensity at 350nm. Similar results were obtained when the entire spectrum was integrated between 305-400nm. This profile is almost identical to that reported for bGH (Havel et al., 1988), except that the pGH curve is shifted to lower concentrations of GuHCl. An almost linear increase in λ_{max} accompanies the unfolding, suggestive of a gradual removal of the tryptophan from the interior of the protein to the solvent exterior (Figure 4c). Like bGH, the native state tryptophan residue in pGH is located close to an intramolecular quenching group, resulting in a quenched native state fluorescence. This quenching group is missing in hGH which has an unquenched native state fluorescence (Kauffman et al.,

Figure 4 (cont.). Equilibrium denaturation of pGH monitored by intrinsic protein tryptophan fluorescence.

The intrinsic fluorescence emission spectra of Figure 4a were analysed in terms of their relative fluorescence intensity at 350nm, and their fluorescence emission maximum, λ_{max}. (*b*) effect of GuHCl concentration on the relative fluorescence intensity at 350nm. (*c*) effect of GuHCl concentration on the λ_{max}.

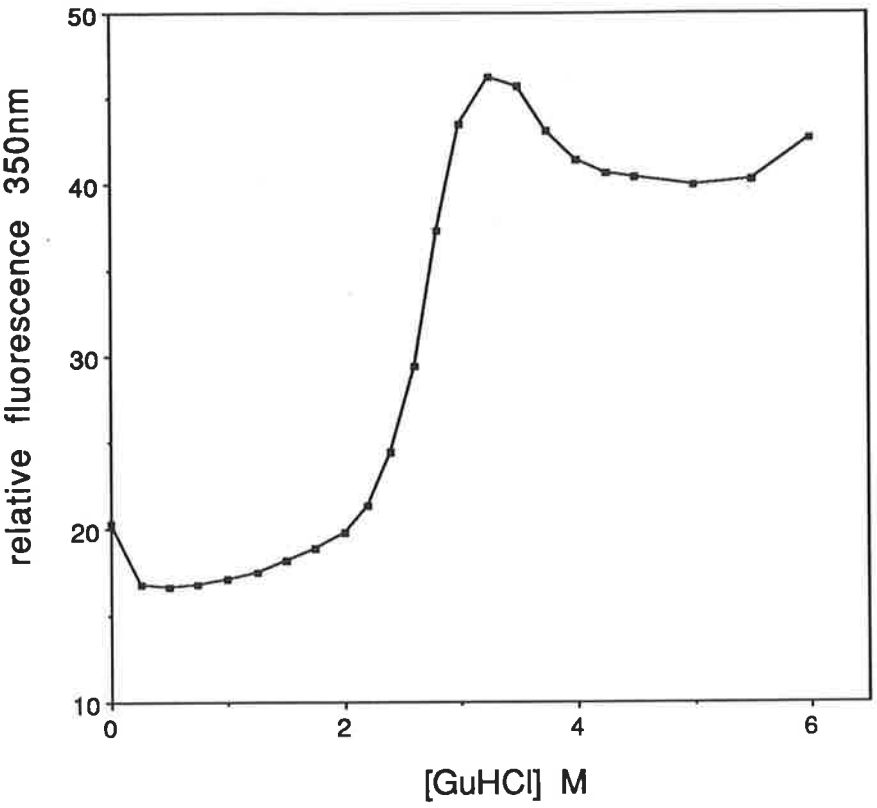
relative fluorescence 350nm
50
40
30
20
10
0
2
4
6
[GuHCl] M

B

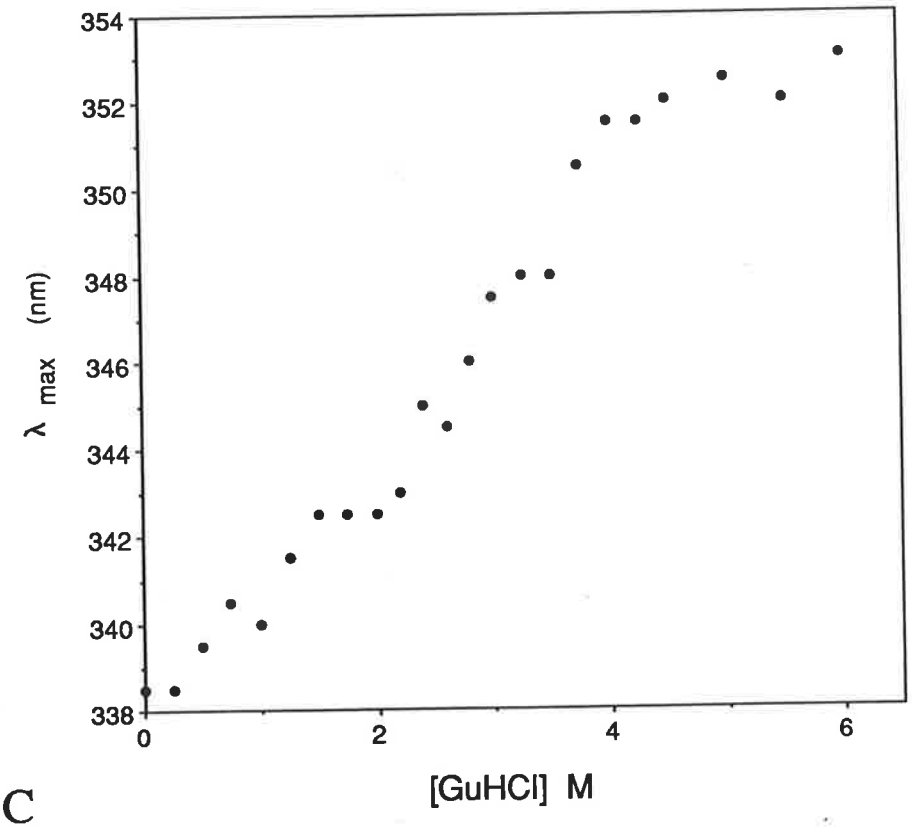
λ max (nm)
354
352
350
348
346
344
342
340
338
0
2
4
6
[GuHCl] M

C

1989). At pre-denaturation concentrations of GuHCl, a 3-4 nm red-shift in the λ_{max} was consistently found. The exact reason for this is not known at present. It is possible that a GuHCl molecule may have diffused into the protein matrix thus altering the conformation slightly. This phenomenon has been observed in apomyoglobin (Bismuto & Irace, 1988) and liver alcohol dehydrogenase (Strambini & Gonnelli, 1986). As seen in the UV absorbance detected denaturation (4.2.1) disruption of the pGH conformation begins at about 2.2M GuHCl. The loosening of the structure slowly moves the quenching group away from the interior tryptophan. At 3.25M GuHCl the intensity is approx. 2.5-fold greater than in the folded state and the λ_{max} has increased to about 347nm. The tryptophan is now in an unquenched state, but is probably near the surface of the protein, partially exposed to the solvent. As the denaturant concentration is increased further, the complete unfolding of the molecule eventually exposes the tryptophan to the aqueous solvent. There is a 15% decrease in the fluorescence intensity between 3.25M and 6M GuHCl. The fluorescence experiments were done at a protein concentration of 0.08 mg/ml, insufficient to result in any aggregation at intermediate GuHCl concentrations (see 4.2.3).

On first examination of the fluorescence denaturation curve for pGH, it appears as if it can not be explained by a simple two-state mechanism. The asymmetrical shape of the curve makes it difficult to analyse if we assume a two-state denaturation mechanism (Pace et al., 1989). For a two-state transition a constantly increasing λ_{max} would be anticipated as the denaturant concentration increased. This is just what has been observed with pGH (Figure 4c). In addition, the observed λ_{max} would be a measure of the relative proportions of native and fully unfolded protein. The midpoint of the λ_{max} vs GuHCl plot is at 2.7M GuHCl, which is also the midpoint of the fluorescence intensity at 350nm vs GuHCl plot. This value is also in agreement with the midpoint for the UV absorbance detected transition. The fact that the midpoints are coincident is not surprising because both techniques are detecting the effects of denaturant on the tryptophan environment.

The asymmetry of the denaturation curve can be mathematically described by two overlapping unevenly weighted sigmoidal plots. The first is the increase in fluorescence intensity due to the removal of the internal quenching group and the second is the decrease in intensity due to quenching of the tryptophan by the bulk solvent. Two theoretical sigmoidal curves were fit to the relative fluorescence at 350nm vs GuHCl plot. The equation for a sigmoidal curve is:

$$y = \frac{n_0 e^{kx}}{1 - \beta n_0 (1 - e^{kx})}$$

where n_0 determines the "lag" of the transition, k determines the rate of increase of the climb and β determines the amplitude of the rise (Bailey & Ollis, 1986). The two theoretical curves fitted to the data are shown in Figure 5a and the sum of the two curves, overlayed on top of the experimental data (Figure 4b) are shown in Figure 5b. The theoretical curves are a simplistic view of the experimental data because the effects of the denaturant on the folded and unfolded states (Schmid, 1989) are not taken into account, i.e., flat baselines have been chosen. However, the curves fit the data reasonably closely. The rising curve modelling the increase in intensity due to removal of the internal quenching group has a midpoint at 2.82M GuHCl. The descending curve modelling the decrease in intensity due to quenching by the bulk solvent has a midpoint of 3.18M GuHCl. A major assumption has been made in fitting these two exponentials to the experimental data. The assumption is the amplitude of the ascending curve. One thing we do know from the experimental data is that the increase in intensity due to removal of the internal quenching group is greater than the decrease in intensity due to bulk solvent quenching, otherwise the fluorescence intensity of the unfolded state would be lower than that for the folded state. When the experimental data is normalised between 0 and 1, the fluorescence intensity levels out at about 0.8 when pGH is unfolded. The ascending curve shown in Figure 5a has an arbitrary maximum set at 2. Because the difference in amplitudes is 0.8, the descending sigmoidal curve drops by 1.2. However, if a higher maximum is

Figure 5. Hypothetical mathematical model to describe the fluorescence intensity plot of pGH denaturation.

The asymmetry of the fluorescence intensity-detected denaturation curve of pGH can be mathematically modelled by two overlapping unevenly weighted sigmoidal curves. The first (shown in blue) is the increase in fluorescence intensity due to the removal of the internal quenching group from the tryptophan residue, while the second (black) is the decrease in intensity due to quenching of the tryptophan by the bulk solvent. The two theoretical curves and their mathematical sum (green) are shown in (*a*). The sum of the two curves is overlayed on top of the experimental data (red squares) from Figure 4b in (*b*). These two curves may not be the only solution to the experimental data. See text for detailed discussion.

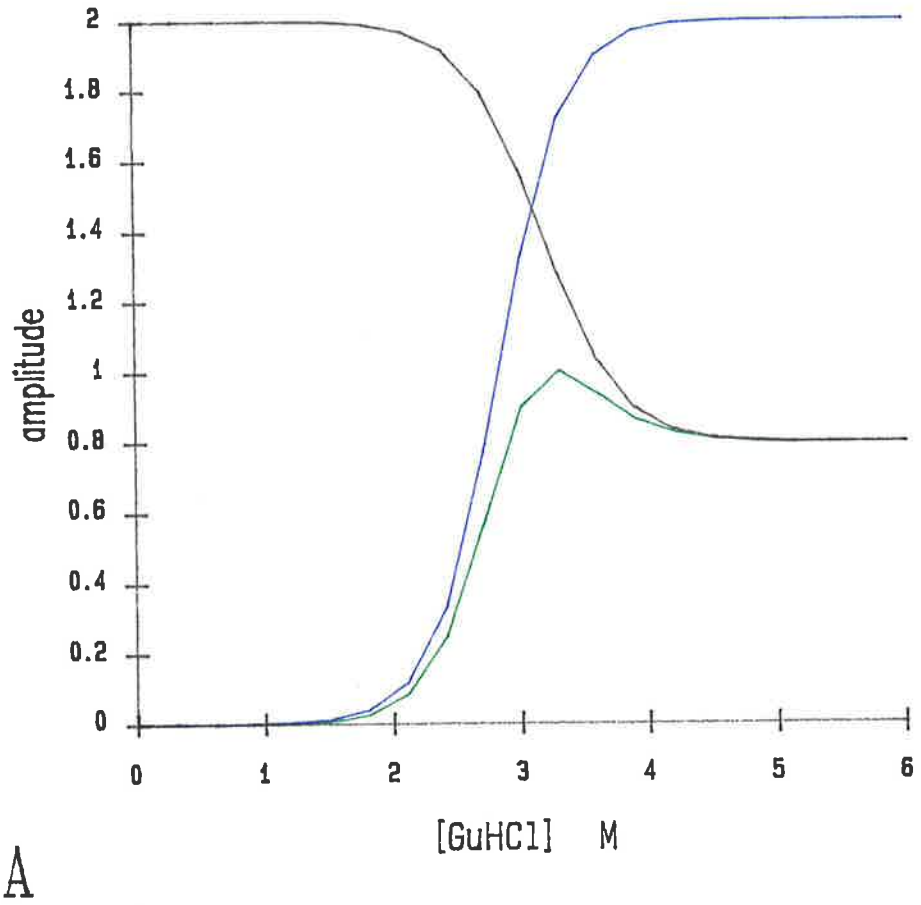
amplitude
2
1.8
1.6
1.4
1.2
1
0.8
0.6
0.4
0.2
0
0
1
2
3
4
5
6
[GuHCl] M

A

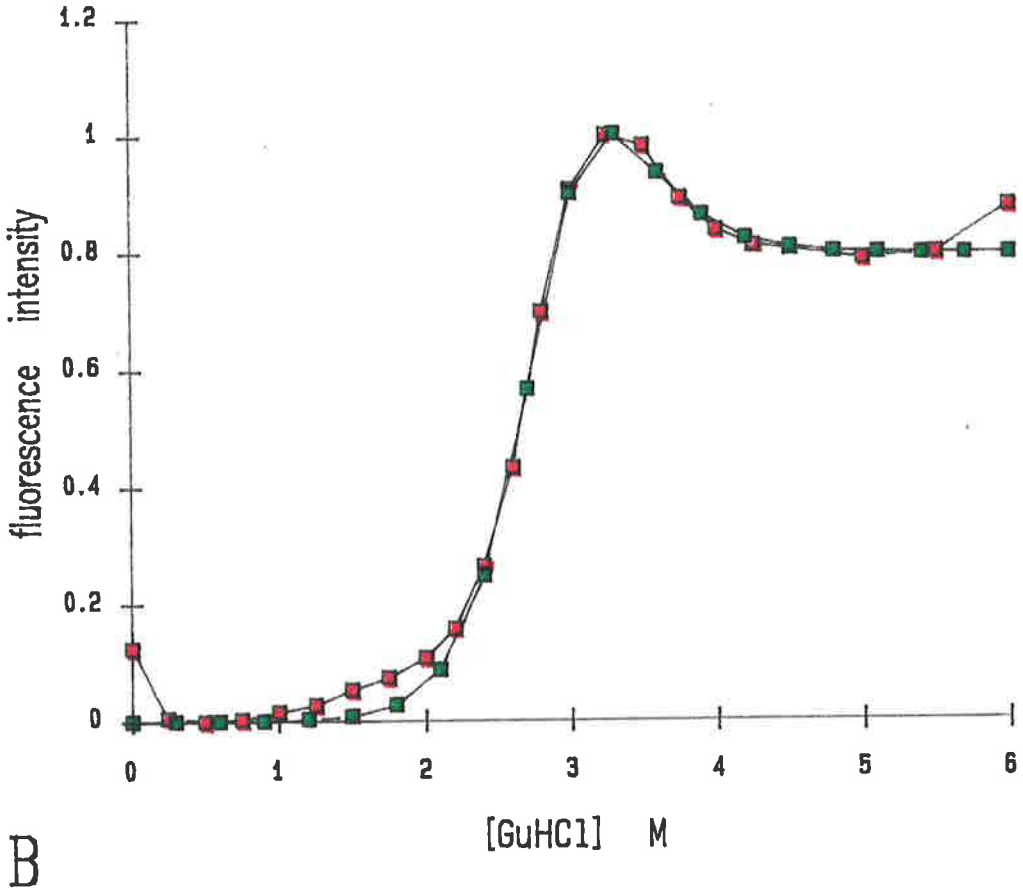
fluorescence intensity
1.2
1
0.8
0.6
0.4
0.2
0
0
1
2
3
4
5
6
[GuHCl] M

B

set for the ascending curve a different pair of sigmoidal curves can fit the data. The higher the maximum set, the closer the midpoints of the two sigmoidal curves approach each other. For example, when the maximum is set at 2, as shown in Figure 5a, the midpoints for the ascending and descending curves are 2.82M and 3.18M, respectively. If the maximum is set at 3, they are 2.79M and 2.98M; a maximum of only 1 results in 2.57M and 3.77M. It is difficult to determine which pair of curves is the "real fit" to the experimental data. Unfolding of hGH, a GH which does not contain a quenched native state tryptophan, results in an approx. two-fold reduction in fluorescence intensity (Brems et al., 1990). If we were to assume a similar effect on the solvent induced quenching of pGH, then perhaps the curves with the maximum set at 2 are correct. However, the obvious anomaly here is that the midpoints of these two theoretical curves are far removed from the UV-detected midpoint of 2.7M (4.2.1). If the internal quenching group in both bGH and pGH is a very efficient quencher [Kauffman et al. (1989) obtained quantum yields of 0.03 and 0.04 for native bGH and pGH, respectively, compared with 0.14 for hGH] then the maximum amplitude of the theoretical ascending curve should be set to a larger number, i.e., 4 or 5. In this case the midpoints of the fitted sigmoidal curves would approach each other, with the descending curve slightly displaced toward higher GuHCl concentrations, somewhere near 2.7M GuHCl.

It is quite obvious that the fluorescence emission of pGH in GuHCl is a very complex process, made up of two opposing intensity effects. The unfolding of the molecule is responsible for both of the observed molecular "events" (removal of the internal quenching group and exposure of the tryptophan to the solvent). These events, probably occuring at very similar GuHCl concentrations in the denaturation transition, are indicative of the breakdown of the tertiary structure of pGH.

4.2.3 Size Exclusion Chromatography

The effect of GuHCl on the hydrodynamic radius of pGH was determined by size-exclusion chromatography on a Superose-12 column (2.2.9).

A calibration curve for the Superose-12 column in 6M GuHCl was determined and utilized to calculate the Stokes radii of pGH at each concentration of GuHCl as described by Corbett & Roche (1984). Horiike et al. (1983) have pointed out that the calibration curve for proteins denatured by GuHCl is identical to that obtained for globular proteins, when plotted as a function of molecular radius (R_s), measured by viscosity measurements (R_η). Proteins used were BSA, ovalbumin, carbonic anhydrase, haemoglobin monomer, ribonuclease, lysozyme and insulin. The resulting calibration curve of R_s vs elution volume is shown in Figure 6b.

The recombinant pGH incubated at each concentration of GuHCl was injected separately onto the Superose-12 column pre-equilibrated at each concentration of GuHCl, at a concentration of 0.66 mg/ml (2.2.9). Figure 6a shows the elution profile of each individual run. From the calibration curve, the hydrodynamic radius of pGH increases from approx. 20Å in the folded state to approx. 40Å in the unfolded state. A similar increase in radius was seen in the GuHCl-induced unfolding of bGH when detected by size-exclusion chromatography (Brems et al., 1985). This increase in size, equivalent to an 8-fold increase in volume, seems rather large. More recently, Lehrman et al. (1991) detected an increase from 19Å to 21Å upon unfolding of bGH using a light scattering technique. A similar increase in radius (10-20%) is seen in the denaturation of lysozyme, ribonuclease, and chymotrypsinogen (Nicoli & Benedek, 1976). The apparently exaggerated increase seen here could be due to the anomalous behaviour of some of the proteins used in the calibration curve. However, the exact hydrodynamic radius is not important, and does not influence the interpretation.

An obvious feature of the chromatograms is the presence of multiple peaks between 2.25M and 3.75M GuHCl. As many as three different peaks are observed in this region. Two of these peaks coincide with those for the folded and unfolded protein, while the third, early eluting peak, appears to be an associated form of pGH wtih a radius of approx. 52Å. Using an expanded monomer radius of 28Å at 3M GuHCl, it would take three to four monomer units to achieve a 52Å radius for the associated form, depending on the shape of the unfolded monomer units and their

Figure 6a. Equilibrium denaturation of pGH as measured by size-exclusion chromatography.

Size exclusion chromatography elution profiles of pGH. The protein was pre-equilibrated at each concentration of GuHCl in a buffer containing 25mM sodium borate pH 9.1. The protein concentration was 0.66 mg/ml. 100µl was injected onto a Superose 12 column pre-equilibrated in the same concentration of GuHCl. The flow-rate was 0.5 ml/min. The A_{280} was monitored (—). The calibration curve in Figure 6b was used to determine the Stokes radius (R_s), according to the peak elution volume (see 2.2.9).

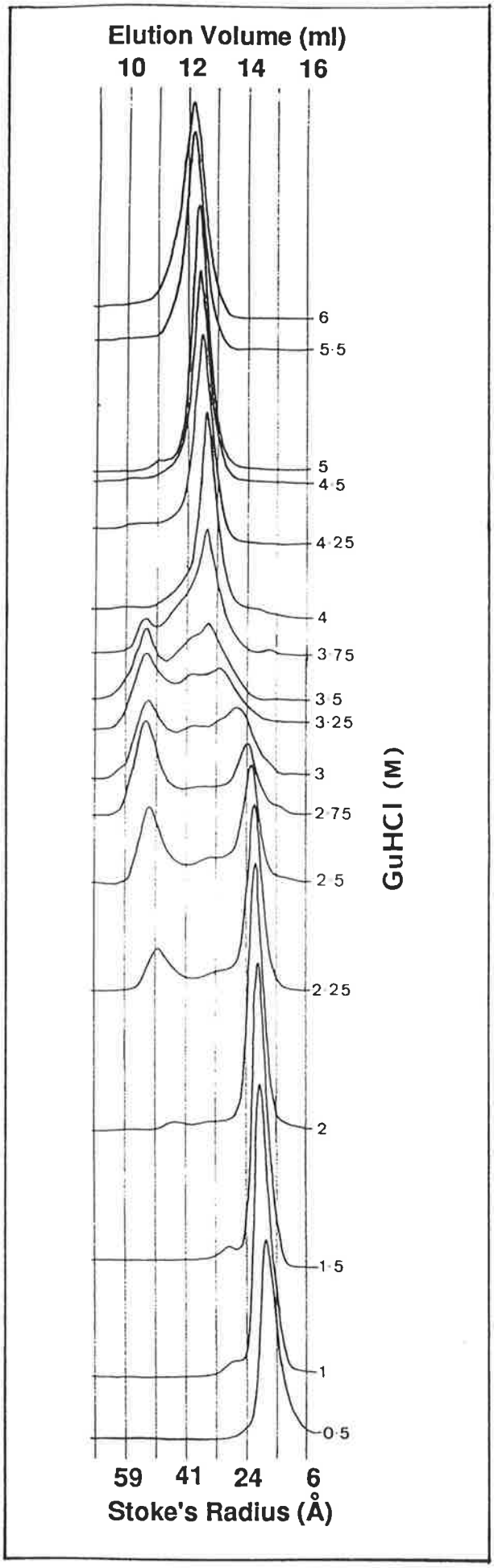
Elution Volume (ml)
10
12
14
16
6
5·5
5
4·5
4·25
4
3·75
3·5
3·25
3
2·75
2·5
2·25
2
1·5
1
0·5
GuHCl (M)
59
41
24
6
Stoke's Radius (Å)

Figure 6b. Molecular weight calibration of the Superose 12 column.

The column was calibrated by recording the elution volume of a series of protein molecular weight standards as described in 2.2.9. The proteins used to calibrate the column were bovine serum albumin (BSA), ovalbumin (OVA), carbonic anhydrase (CAH), haemoglobin monomer (HEM), bovine ribonuclease (RNA), lysozyme (LYS) and insulin (INS). The solid line is a least squares fit of the experimental elution volumes for BSA, ribonuclease and insulin with the Stokes radius (R_S) values for those proteins in non-reducing 6M GuHCl, taken from Corbett & Roche (1984). The equation defining the solid line is: R_S = 147.4 - 8.82[elution volume].

Figure 6c. Equilibrium denaturation of pGH as measured by size-exclusion chromatography.

The effect of GuHCl concentration on the Stokes radius of the monomeric species of pGH seen in Figure 6a. The stokes radius at each GuHCl was determined using the calibration curve in Figure 6b.

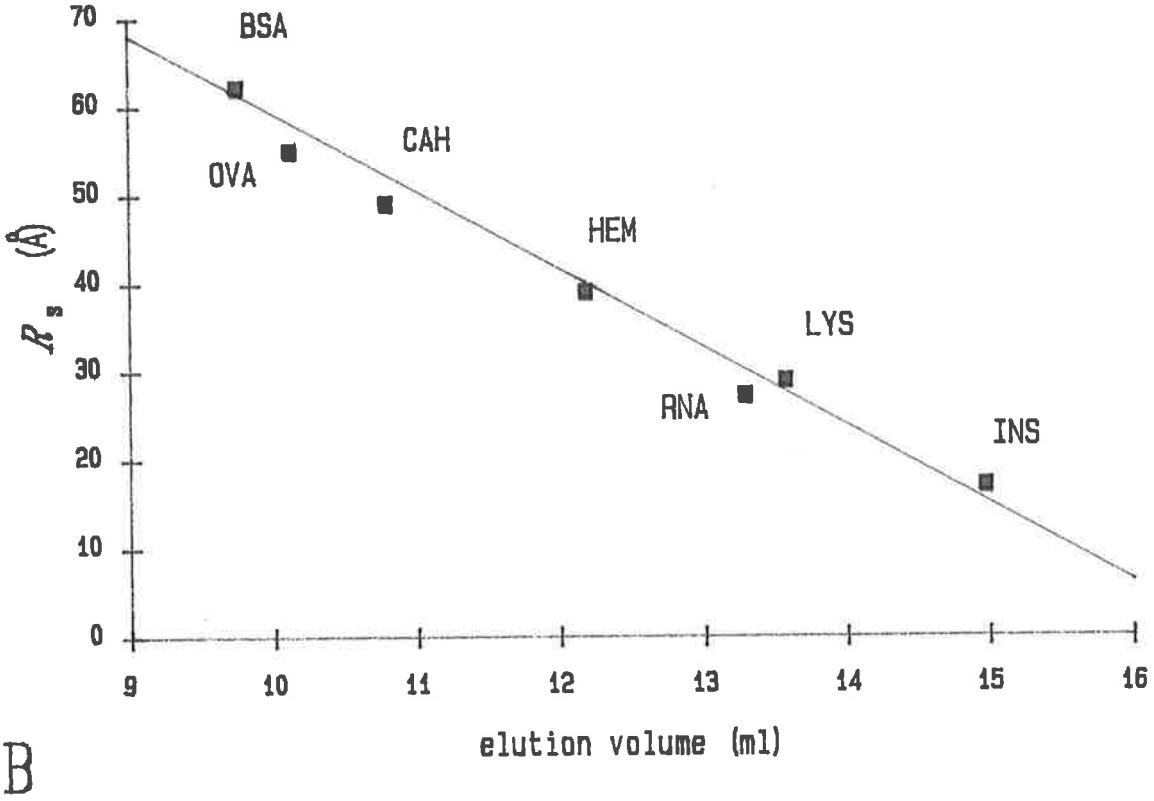
70
60
50
40
30
20
10
0
R_s (Å)
BSA
OVA
CAH
HEM
LYS
RNA
INS
9
10
11
12
13
14
15
16
elution volume (ml)

B

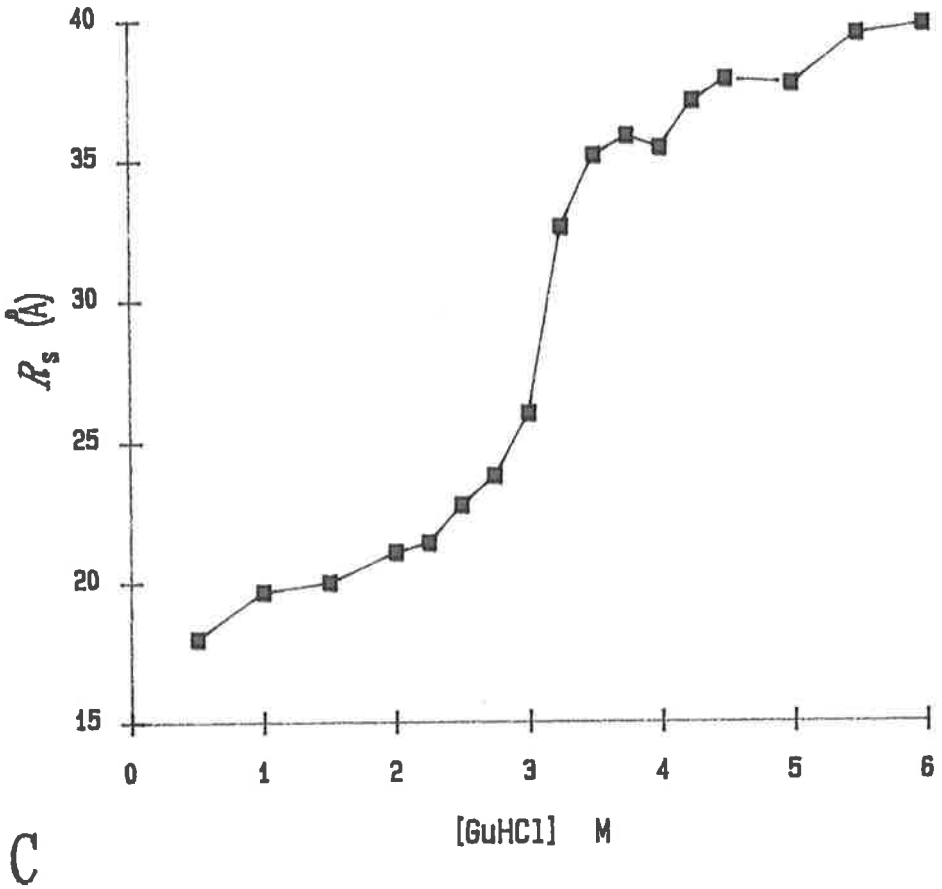
40
35
30
25
20
15
R_s (Å)
0
1
2
3
4
5
6
[GuHCl] M

C

organization in the associated form. The proportion of the associated form is at its highest between 2.75 and 3.25M GuHCl. Size-exclusion chromatography of bGH has also resulted in the presence of a partially denatured self-associated species at intermediate denaturant concentrations (Brems et al., 1985). This associated species is populated at bGH concentrations above 10μM (0.22 mg/ml). A bGH region including the third helix appears to be involved in the association process (Brems et al., 1986). However, unlike pGH, only one peak elutes from the column at each concentration of GuHCl. Multiple peaks were detected during size-exclusion chromatography of a mutant form of bGH and an alkylated form of hGH (Brems et al., 1988, 1990). A lysine-112 to leucine [bGH(K112L)] mutation in the third helix of bGH resulted in a protein which refolds 30-fold slower the wild-type bGH. This mutant of bGH also has a propensity to precipitate upon refolding due to stabilization of an associated folding intermediate via interactions involving the third helix (Brems et al., 1988). Likewise, alkylation of both disulphides in hGH destabilizes the folded state and stabilizes the intermediate, thus resulting in the formation of associated forms at intermediate GuHCl concentrations. Oxidized hGH does not associate: its denaturation clearly follows a two-state mechanism (Brems et al., 1990). The appearance of multiple peaks in a size-exclusion chromatogram is indicative of a slow equilibrium rate between the various molecular forms present. If the conversion rate between the various forms is sufficiently slower than the rate of gel-permeation, that is, in the order of a minute, separate peaks that correspond to each state will appear in the chromatogram (Saito & Wada, 1983). In the transition region, the rate of equilibration of the partially unfolded monomeric, unfolded, and associated forms of pGH is slow, and the three forms are well separated on the column. The fact that the bGH mutant, bGH(K112L), which refolds 30-fold slower than wild-type bGH, results in multiple peaks during size-exclusion chromatography also attests to this. In bGH however, the various species are in fast equilibrium compared to the chromatography time scale. Self-association does not occur at bGH concentrations below 10μM. The

pGH experiments outlined here were done at 30μM, sufficiently high to cause aggregation.

If the Stokes radius of the monomeric pGH form is plotted as a function of GuHCl concentration, a sigmoidal curve with a midpoint at 3.1M GuHCl results (Figure 6c). Increasing the GuHCl concentration causes the folded state to expand slightly (3-4Å) until about 2.5M GuHCl. At this point, increasing the denaturant concentration further causes a rapid increase in the hydrodynamic radius (12-13Å), as the protein unfolds, until about 3.5M GuHCl. Between 3.5M and 6M GuHCl the radius of the unfolded state expands by a further 4Å to a final Stokes radius of about 40Å. The sloping pre- and post-transition baselines may be true increases in the molecular radius, but are most probably due to the influence of the GuHCl on the Superose-12 agarose matrix. This affect of the denaturant on the column matrix may also aid in the separation of the various forms as well. Size-exclusion chromatography detected equilibrium denaturation of bGH results in a midpoint of about 3.7M GuHCl (Brems & Havel, 1989). This means that the compactness of bGH is more resistant to denaturation by GuHCl than pGH.

4.2.4 Circular Dichroism

The far-UV circular dichroism (CD) spectrum of pGH (Chapter 3, Figure 8a, described in detail in 3.3.4), displays minima at 221nm and 209nm, characteristic of the presence of α-helix. By deconvoluting the far-UV CD spectrum, native state pGH was shown to have 47% α-helix. The loss of secondary structure, notably α-helix, upon denaturation with GuHCl, was followed by measuring the relative decrease in negative ellipticity at 222nm ($[\theta]_{222}$). A plot of the change in $[\theta]_{222}$ with increasing GuHCl concentration is shown in Figure 7. The result is a broad sigmoidal curve with a midpoint centred at 3.05M GuHCl. The secondary structure is initially disrupted at 2.2-2.4M GuHCl and is not complete until about 4M GuHCl. Of the four methods used to follow the denaturation thus far, this transition is the broadest at about 1.6-1.8M GuHCl. This compares to 1.2-1.4M GuHCl for the UV and fluorescence

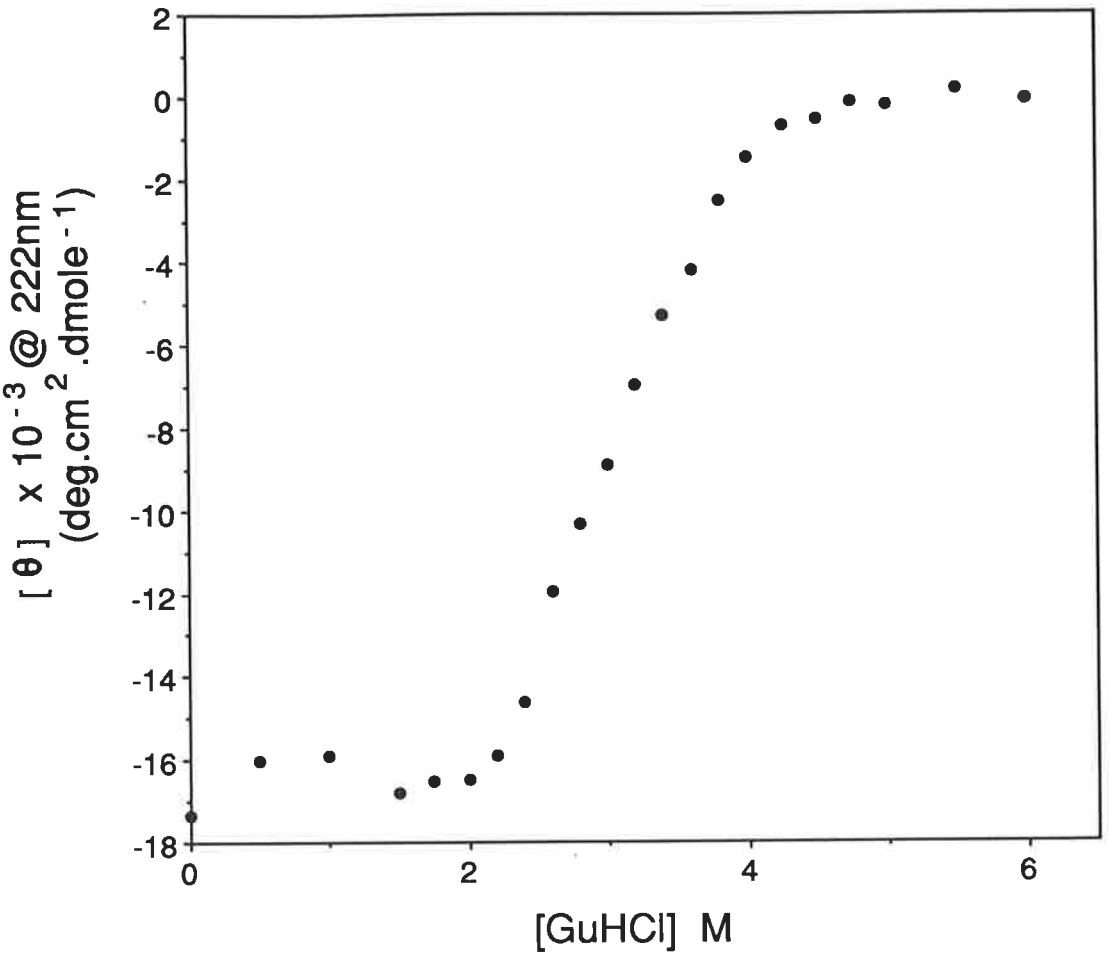

Figure 7.Equilibrium denaturation of pGH monitored by far-UV circular dichroism.

The effect of the GuHCl concentration on the secondary structure of pGH was monitored by measuring the mean residue ellipticity at 222nm. CD spectra were recorded on an AVIV 62DS model spectropolarimeter as described in 2.2.7. pGH was dissolved at each concentration of GuHCl in buffers containing 25mM sodium borate pH 9.1. The concentration of pGH was 0.16 mg/ml. This curve is an average of two independent experiments.

detected transitions and approx. 1M GuHCl for the hydrodynamic radius detected transition (Figures 3b, 4b, 6c). The CD-detected midpoint for bGH at concentations of 0.1 mg/ml or less, is near 3.7-3.8M GuHCl (Brems et al., 1986). Equilibrium denaturation of bGH at 1.6 mg/ml resulted in a biphasic CD-detected transition due to the presence of an associated intermediate (Brems et al., 1986). The inflexion point of the biphasic transition was still at about 3.7M GuHCl. The biphasic transition obtained at high protein concentration was attributed to the presence of two populations of helical structure. Formation of the associated equilibrium intermediate requires a conformational change which decreases the stability of one helix population, yet increases the stability of the other population. The CD equilibrium denaturation measurements of pGH were conducted at 0.16 mg/ml, an insufficient concentration to form the associated intermediate. However, the broadness of the transition may be an indication of the presence of monomeric intermediates.

Whereas far-UV CD can detect the loss in secondary structure of a protein, near-UV CD can be used to detect losses in the tertiary structure. Non-coincidence of the changes in CD at different wavelengths ($[\theta]_{270}$ and $[\theta]_{296}$ aromatic signals vs $[\theta]_{222}$ secondary structure signal) seen in the equilibrium denaturation of α-lactalbumin was early evidence for the framework model of protein folding (Kuwajima et al., 1976). When Havel et al. (1986) examined the near-UV CD spectrum of bGH at various GuHCl concentrations they noticed a prominent band at about 300nm at intermediate concentrations of GuHCl and elevated protein concentrations. Near-UV CD spectra of pGH at a concentration of 1 mg/ml also revealed a prominent band, at about 298nm (Figure 8a). As seen in the UV absorbance spectrum (see 3.3.2), this band is probably due to a trp ^1L_a transition. A similar increase in the negative ellipticity at 298nm assigned to tryptophan-86 was seen in the slow trimerization of an S-carboxymethylated 134 residue amino-terminal fragment of hGH (Bewley & Li, 1978). This fragment was also shown to contain most of its helical structure.

Figure 8. Equilibrium denaturation of pGH monitored by near-UV circular dichroism.

CD spectra were recorded on an AVIV 62DS model spectropolarimeter as described in 2.2.7. pGH was dissolved at each concentration of GuHCl in buffers containing 25mM sodium borate pH 9.1. The protein concentration was 1 mg/ml. A 5mm path length cuvette was used to record the spectra. The mean residue ellipticity, $[\theta]$, has the units $deg.cm^2.dmol^{-1}$.(*a*) Near-UV CD spectra of pGH in 25mM sodium borate pH 9.1 ± 3M GuHCl.(*b*) The effect of GuHCl concentration on the mean residue ellipticity at 300nm, $[\theta]_{300}$.

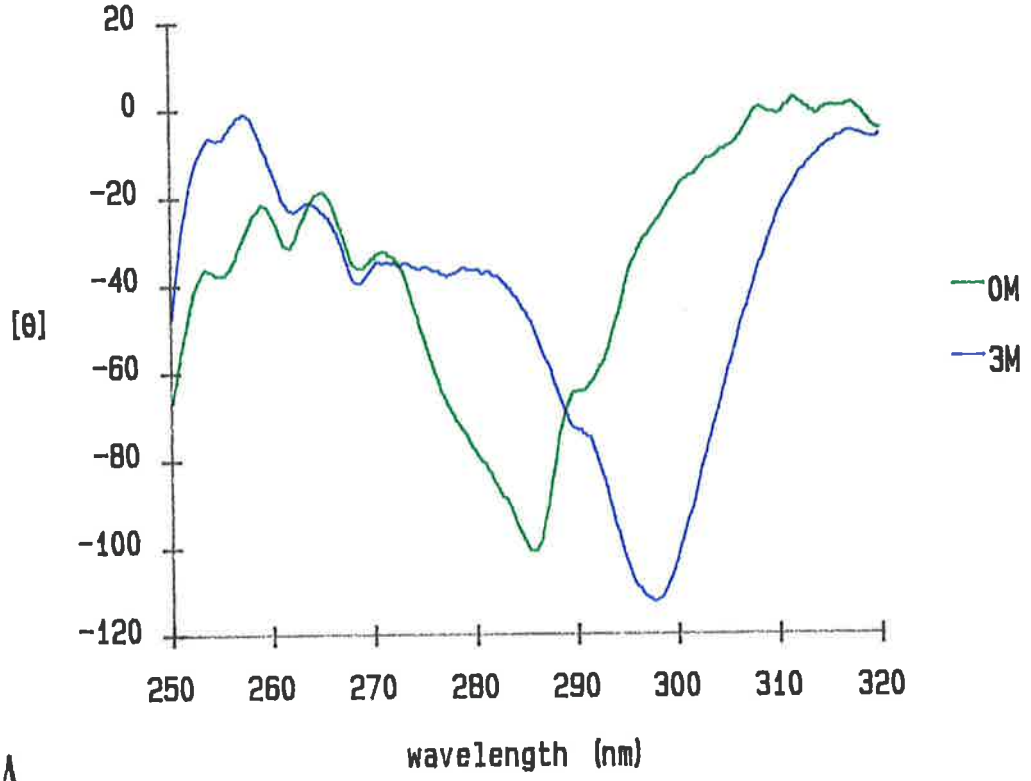
20
0
-20
-40
-60
-80
-100
-120
[θ]
250
260
270
280
290
300
310
320
wavelength (nm)
0M
3M

A

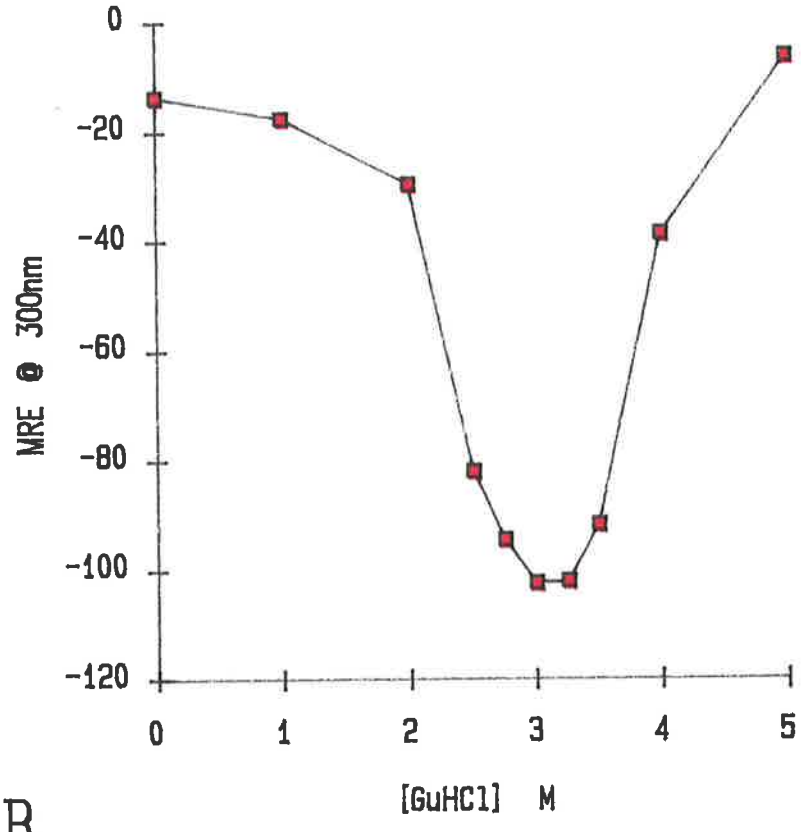
0
-20
-40
-60
-80
-100
-120
MRE @ 300nm
0
1
2
3
4
5
[GuHCl] M

B

The change in intensity (molar ellipticity) of the CD band at 300nm, $[\theta]_{300}$, as a function of the GuHCl concentration is shown in Figure 8b. The band has its greatest optical activity where pGH is partially denatured, i.e., 3-3.25M GuHCl. An almost identical pattern was seen in the $[\theta]_{300}$ vs GuHCl concentration plot in bGH, and once again this pattern only occurred at elevated bGH concentrations (Havel et al., 1986). It is surprising that at a denaturant concentration which is causing major disruption to the conformation as detected by UV and fluorescence signals, such a prominent, spectrum dominating band should appear. From Figure 8a, it can be seen that at 3M GuHCl, much of the tyrosine CD between 270 and 286nm has been lost. Most of the disulphide bond associated optical activity between 255 and 265nm has also been lost, probably due to strain on the bonds as the molecule is distorted by the denaturant. Interestingly, the three phenylalanine bands are still clearly visible. The tryptophan residue responsible for the prominent band at 298nm must be in a unique microenvironment to give such a specific signal. In addition it occurs at protein and denaturant concentrations which promote the formation of an associated form of pGH. Size-exclusion chromatography of pGH detected the presence of an associated species under these conditions (4.2.3). It appears as if the unique environment of the tryptophan residue is a result of the association process. Further discussion on this aspect will be delayed until presentation of the second-derivative spectroscopy results (4.2.5).

Unfortunately, due to insufficient time during my short stay in Dr. Sawyer's laboratory where the CD measurements were carried out, I was unable to record any near-UV CD spectra at lower protein concentrations at the various GuHCl concentrations. At concentrations below 10μM pGH, the ellipticity of the whole spectrum would be expected to generally decrease without the appearance of the 298nm band. This would make it possible to look at the decrease in ellipticity (i.e., at 286nm, the wavelength of maximum ellipticity in the folded state) as a function of the GuHCl concentration. A comparison between the near- and far-UV CD transitions could then be made to determine whether the transitions are coincident or not.

4.2.5 Second Derivative Spectroscopy

Second-derivative absorption spectroscopy in the near-UV region is capable of providing information regarding the polarity of the environment surrounding the aromatic amino acids which absorb in this region (Ragone et al., 1984). The second derivative spectrum of pGH was described in detail in 3.3.2. The changes in the second-derivative spectrum of pGH at 0.22 mg/ml were observed by recording the zero-order absorption spectrum at each GuHCl concentration (2.2.6.2). Shown in Figure 9a are the second-derivative spectra in the transition region where pGH unfolds. Although the tyrosine and tryptophan absorption bands overlap, the spectral changes between 291 to 295nm are principally due to tryptophan. The peak to trough difference in the second-derivative spectrum at 291 and 295nm is a measure of the polarity of the environment surrounding the tryptophan. A large peak to trough difference is indicative of a non-polar tryptophan environment. The behaviour throughout the denaturation transition is shown in Figure 9b by measuring the peak (295nm) to trough (291nm) intensity. As pGH unfolds there is a rapid decrease in the intensity indicating the tryptophan environment changing from non-polar to polar. The intensity is at its lowest at 3-3.25M GuHCl, before it rises again. Exposure of the tryptophan to the solvent upon unfolding would normally be seen as a smooth decrease in intensity as the tryptophan environment changes from non-polar to polar. However, pGH unfolding causes the intensity to go through a minimum at 3-3.25M GuHCl, indicating a more polar tryptophan environment at these partially denaturing concentrations than in the unfolded state. Again, this result is identical to that obtained in the second-derivative analysis of bGH at 0.3 mg/ml (Havel et al., 1986). In addition, they claim that at low bGH concentrations (0.05 mg/ml) a smooth transition without the minimum is observed. When the pGH denaturation experiments were repeated using urea as the denaturant and pGH at 0.33 mg/ml, the 291-295nm peak to trough intensity difference minimum was not so prominent (Figures 10a,b).

Closer examination of the spectra in Figure 9a reveals that the decrease in intensity of the minimum at 291nm is accompanied by a red shift of this band by

Figure 9. GuHCl-induced equilibrium denaturation of pGH as monitored by second-derivative spectroscopy.

(*a*) second-derivative spectra of pGH. This illustrates the change in the spectrum in the tryptophan (288-300nm) and tyrosine (275-282nm) absorbing regions of pGH, in the unfolding region of the GuHCl-induced denaturation. Spectra were recorded on a Cary 3 spectrophotometer and the second-derivative spectra were determined as described in 2.2.6.2. The protein was dissolved at each GuHCl concentration in a buffer containing 25mM sodium borate pH 9.1. The protein concentration was 0.22 mg/ml.

(*b*) the 291nm to 295nm peak-to-trough difference of the second-derivative spectra shown in (*a*).

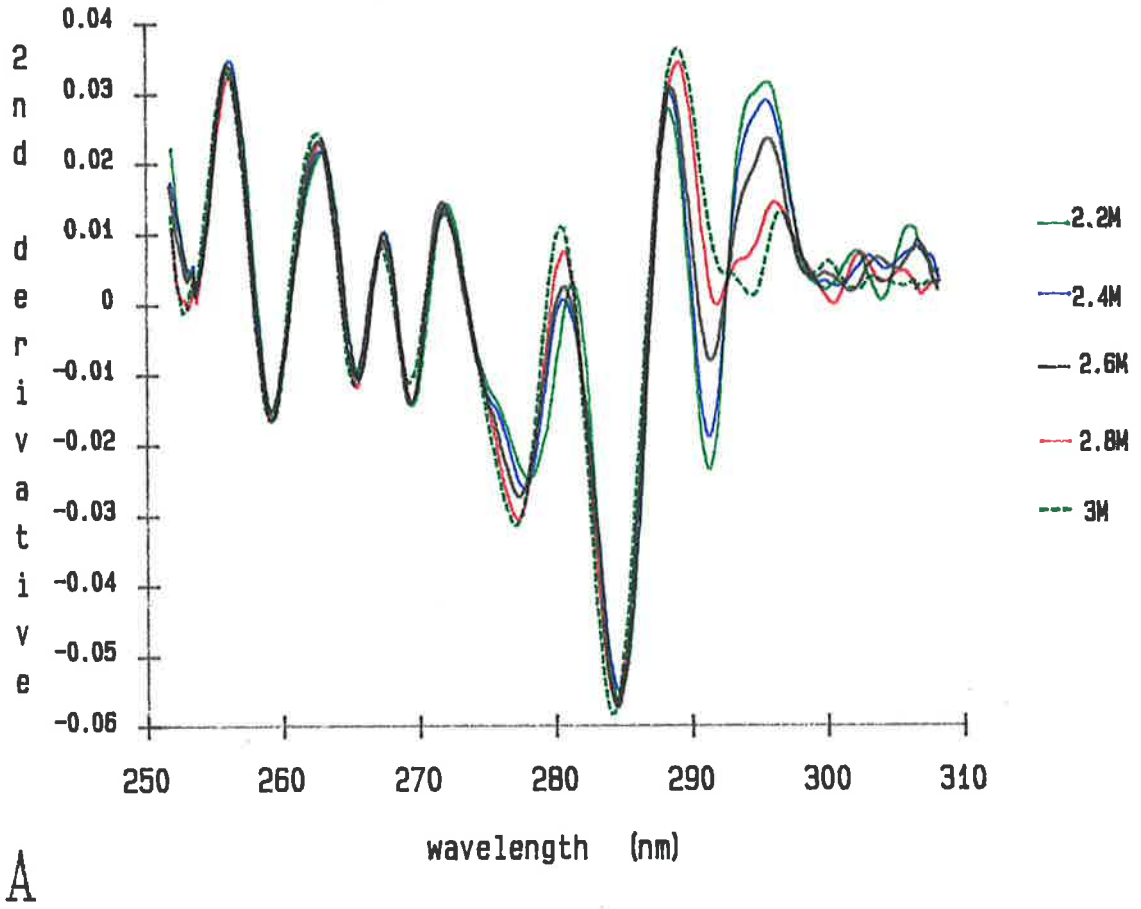
2nd derivative
0.04
0.03
0.02
0.01
0
-0.01
-0.02
-0.03
-0.04
-0.05
-0.06
250
260
270
280
290
300
310
wavelength (nm)
2.2M
2.4M
2.6M
2.8M
3M

A

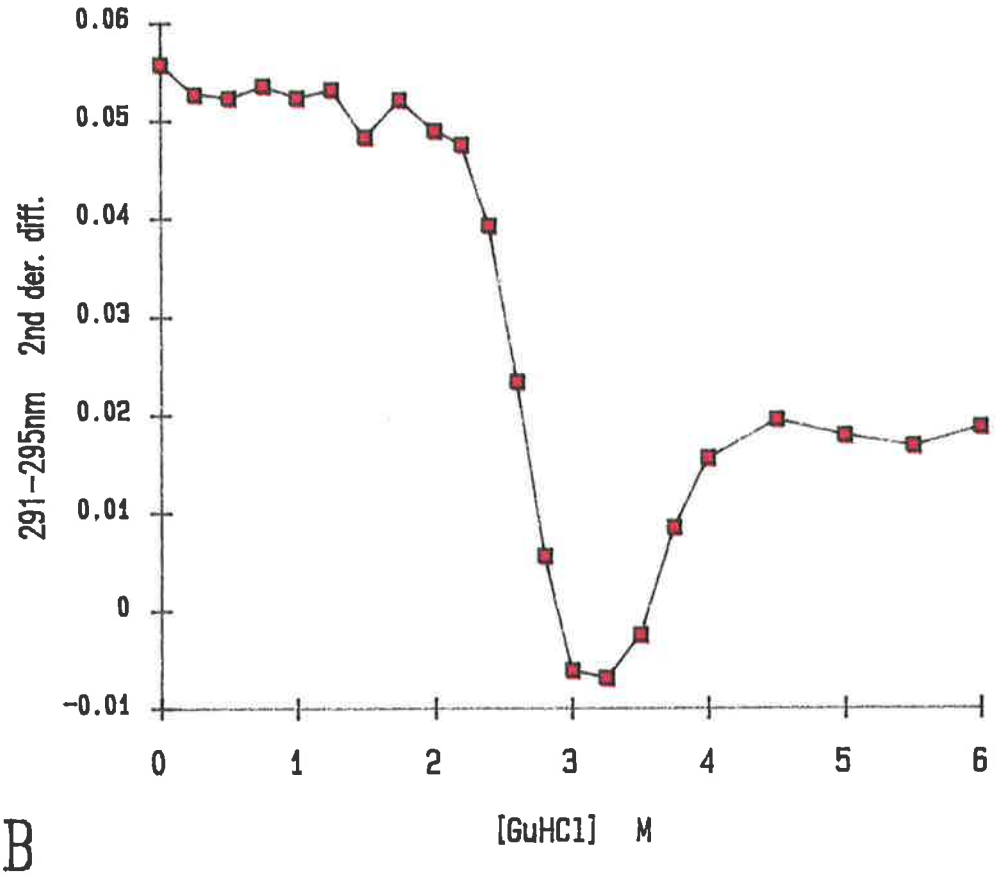
291-295nm 2nd der. diff.
0.06
0.05
0.04
0.03
0.02
0.01
0
-0.01
0
1
2
3
4
5
6
[GuHCl] M

B

Figure 10. Urea-induced equilibrium denaturation of pGH as monitored by second-derivative spectroscopy.

(*a*) expanded view of the tryptophan absorption region of the second-derivative spectra of pGH, in the transition region of the urea-induced denaturation. Spectra were recorded on a Cary 3 spectrophotometer and the second-derivative spectra were determined as described in 2.2.6.2. The protein was dissolved at each urea concentration in a buffer containing 25mM sodium borate pH 9.1. The protein concentration was 0.35 mg/ml.

(*b*) the 291nm to 295nm peak-to-trough difference of the second-derivative spectra shown in (*a*).

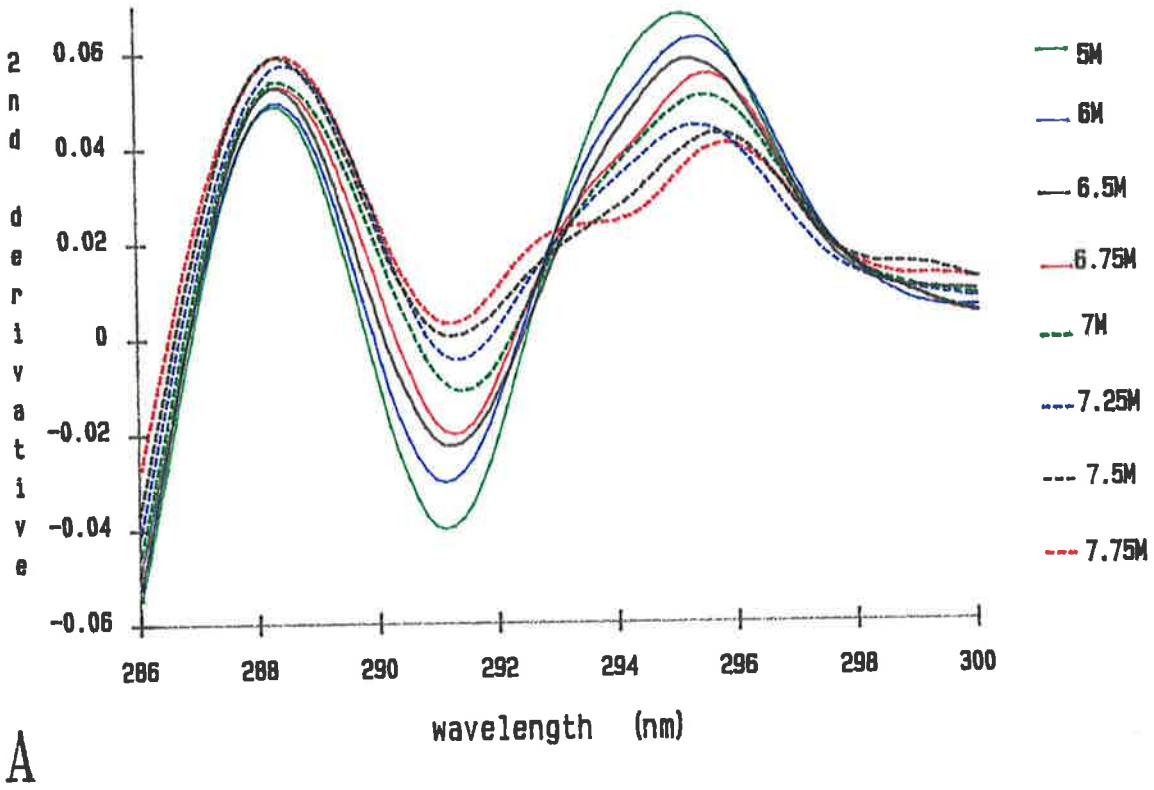
2nd derivative
0.06
0.04
0.02
0
-0.02
-0.04
-0.06
286
288
290
292
294
296
298
300
wavelength (nm)
5M
6M
6.5M
6.75M
7M
7.25M
7.5M
7.75M

A

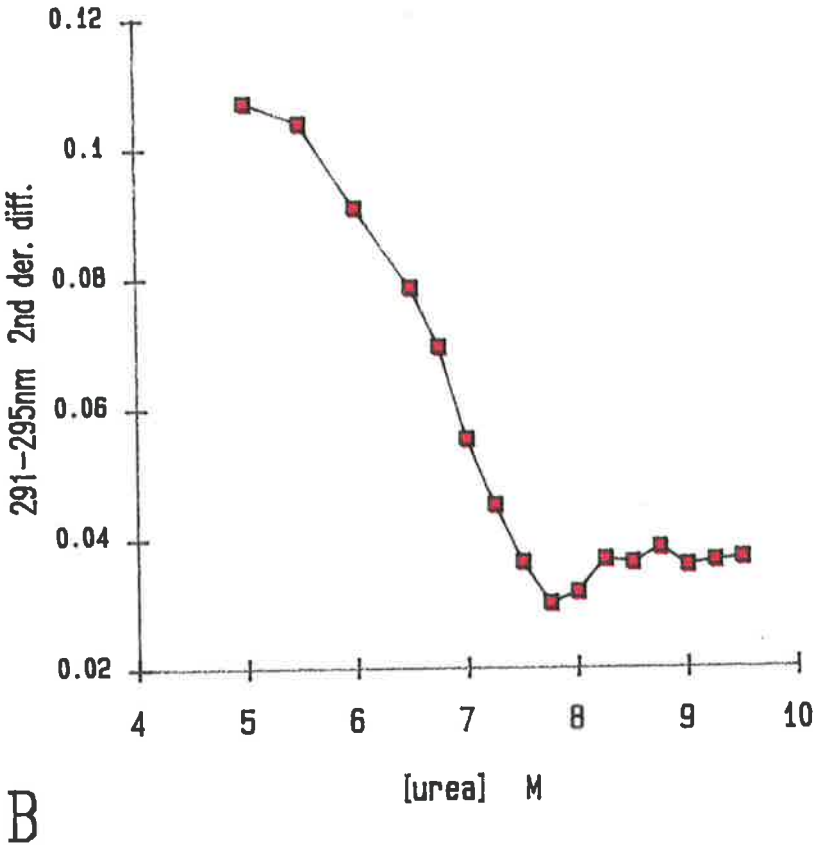
291-295nm 2nd der. diff.
0.12
0.1
0.08
0.06
0.04
0.02
4
5
6
7
8
9
10
[urea] M

B

about 2nm. As the denaturant begins to perturb the protein conformation, the intensity of the 291nm minima decreases, without red-shifting (2.2-2.6M GuHCl). The maximum at 295nm also decreases in intensity, along with the weak shoulder minimum at approx. 294nm. Between 2.8 and 3.0M GuHCl all of these bands red-shift slightly by about 1.5nm, but return to their initial wavelengths by 4M GuHCl. The minimum at 291nm in the second-derivative spectrum is due to the trp^1L_b [0-0] transition whereas the weak shoulder at 294nm is probably a higher vibronic band of the trp^1L_a transition (3.3.2). This latter minimum is so weak it is hardly visible in the native spectrum (see Chapter 3, Figure 6b), but becomes noticeable in the transition region. Unfortunately, due to the low signal to noise ratio, it is not possible to determine the extent of wavelength shifts of the trp^1L_a bands near 300nm.

In contrast to GuHCl, denaturation of pGH by urea does not result in a pronounced 291-295nm peak to trough intensity minimum (Figure 10b). There is a slight increase in the intensity after the minimum at 7.75M urea. In addition there is no obvious red-shifting of the tryptophan second-derivative bands (Figure 10a). This is contrary to the result seen in bGH where GuHCl and urea give similar results (Havel et al., 1986). Why urea did not produce the same effect as GuHCl in the pGH denaturation is not known. The red-shift seen in the GuHCl-induced denaturation occurs very near the UV-detected midpoint of 2.7M. The midpoint of the urea-induced denaturation transition as detected by UV, is 6.9M (see Chapter 5). It appears that the two denaturants may have slightly different effects on the molecular structure of the self-associated state of pGH.

The GuHCl-induced red-shifting of the tryptophan second-derivative bands near 291-295nm could provide an explanation for the apparently "highly polar" environment observed in Figure 9b between 3-3.25M GuHCl. From the results seen in the size-exclusion chromatography it appears as if the formation of an associated form of pGH at intermediate GuHCl concentrations, could be responsible for the effects seen on the tryptophan absorption and CD signals. The red-shifting seen in the second-derivative spectroscopy and the prominent 298nm CD band suggest a specific

interaction between partially folded monomers of pGH, involving tryptophan interacting with an electron-rich centre. This interaction could be a specific hydrogen bond between the tryptophanyl >NH and a proton acceptor (resulting in red-shifting), and/or interaction of the tryptophan with neighbouring aromatic residues of the associated state.

4.2.6 Precipitation of The Associated State of pGH

Size-exclusion chromatography of pGH incubated at elevated protein concentrations and intermediate GuHCl concentrations (2.25-3.75M) results in the formation of an associated form of pGH. From the size-exclusion chromatograms (Figure 6b), it can be seen that more than 50% of the protein is in the associated form between 2.75-3.25M GuHCl. Brems (1988) showed that the associated intermediate for bGH is less soluble than the native or denatured states. This was demonstrated using a two-step assay: (*i*) the various conformers including the associated intermediate are populated at each GuHCl concentration, at a protein concentration sufficient to induce the formation of the associated intermediate (*ii*) the various conformers are introduced, by a simple dilution, into solvent conditions that induce precipitation (2.2.12). Following centrifugation to remove precipitates, the remaining soluble protein is quantitated by UV absorbance at 278nm. This assay was used to detect the presence of the associated intermediate in pGH solutions.

Figure 11 illustrates the percentage of soluble pGH as a function of GuHCl concentration following the precipitation step. The protein concentration in the first step of the assay was 2 mg/ml. Results from incubations at 21°C and 2°C are shown for comparison. The plot indicates that at 21°C the native (<2M GuHCl) and denatured (>4M GuHCl) forms of pGH are soluble when diluted into non-denaturing concentrations of GuHCl (0.8M final). At 3M GuHCl as much as 80% of the protein precipitates when diluted to non-denaturing concentrations of GuHCl. At 2°C the extent of precipitation is decreased and the maximum is shifted slightly to lower GuHCl concentrations (2.75M GuHCl). The decreased precipitation at lower

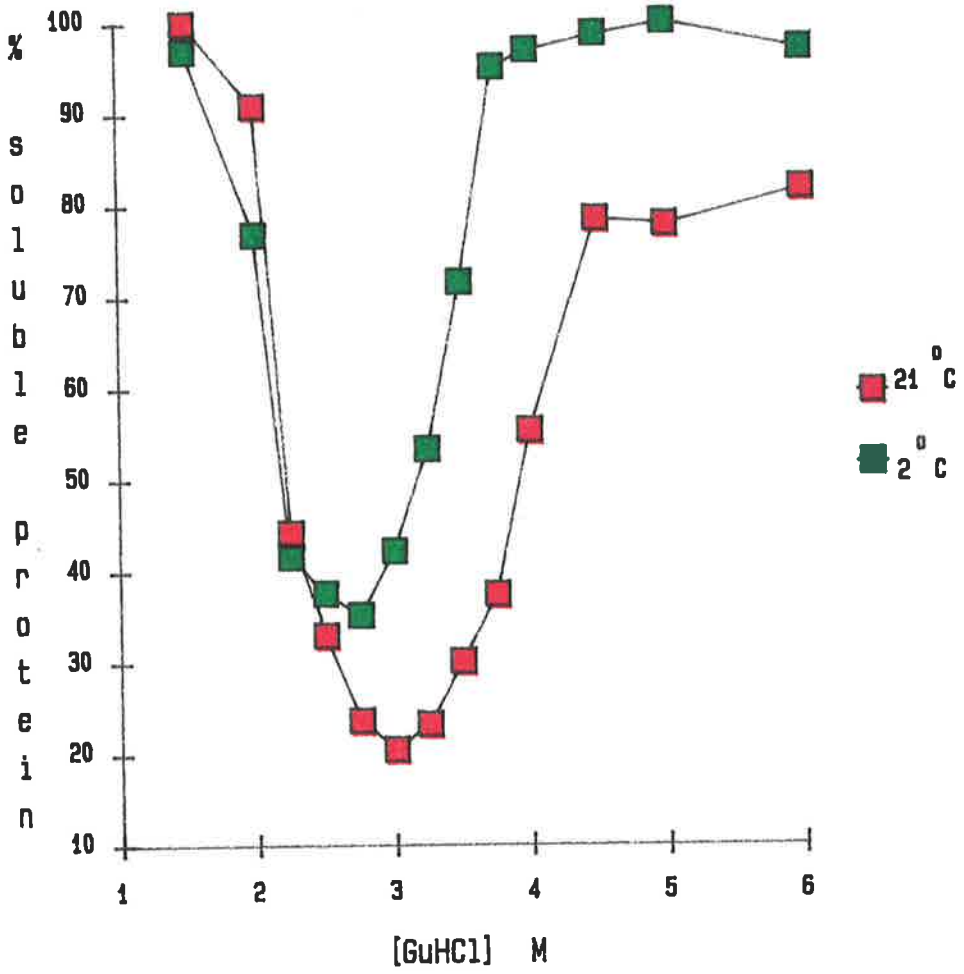

Figure 11. The effect of temperature on the precipitation of the associated state of pGH.

The results were obtained by using the two-step procedure described in 2.2.12. In the first step, protein, at 2 mg/ml, was incubated in varying concentrations of GuHCl for 30min at each temperature. In the second step, the samples were diluted to 0.8M GuHCl and 0.2 mg/ml protein in order to induce precipitation. The amount of precipitate was determined by measuring the absorbance at 278nm of the remaining soluble protein.

temperatures suggests that hydrophobic interactions are involved in the formation of the associated state, as hydrophobic interactions increase with increasing temperature. The shape of the curve in Figure 11 is reminiscent of the $[\theta]_{300}$ vs GuHCl plot (Figure 8b). The associated state of pGH is characterized by its negative ellipticity at 300nm and by its insolubility upon dilution into non-denaturing concentrations of GuHCl.

The results for pGH are very similar to those obtained for bGH, except that the maximum precipitation occurs at slightly higher GuHCl concentrations in bGH (Brems, 1988). Formation of the associated intermediate prevents the correct refolding of the partially denatured states. When denatured forms of pGH are diluted into non-denaturing solvent conditions, they are able to refold to the native conformation quantitatively. The denatured state is stabilized as a monomer by the high denaturant conditions whereas partially denatured pGH self-associates in order to minimize exposure of hydrophobic side-chains to the solvent. Rapid dilution into solutions that do not solubilize the associated intermediate results in the formation of the insoluble aggregate.

4.2.7 Analysis of The Denaturation Curves

The equilibrium unfolding transitions of most small, globular proteins are highly cooperative, and the two-state approximation ($N \leftrightarrow U$) is usually applicable in the analysis. There are two tests for an equilibrium intermediate based on the use of probes: (*i*) a biphasic transition measured by a single probe and (*ii*) noncoincident transitions as measured by different probes. Either one of these observations is sufficient evidence for an equilibrium intermediate (Kim & Baldwin, 1982).

A two-state approximation was assumed in the analysis of pGH denaturation, even though the denaturation deviates from a two-state mechanism. The changes in the observed parameters of pGH were compared by normalizing each transition curve to the apparent fraction of the unfolded form, F_{app}:

$$F_{app} = (Y_{obs} - Y_{nat})/(Y_{unf} - Y_{nat})$$

where Y_{obs} is the observed A_{290nm}/A_{278nm}, fluorescence intensity, molar ellipticity at 222nm or Stokes radius at a given GuHCl concentration and Y_{nat} and Y_{unf} are the observed values for the native and unfolded forms, respectively, at the same denaturant concentration (Pace, 1986). The latter two values are obtained by extrapolating the pre- and post-transition baselines into the transition region. The above four probes were used in this analysis because the denaturation as detected by each of these probes followed a near-symmetrical sigmoidal curve. The $[\theta]_{300}$ and second-derivative data have not been included due to their asymmetric transitions.

A plot of the apparent fraction of unfolded protein, F_{app}, for each of the four detection methods is shown in Figure 12. The effect of the analysis of the raw data from each probe using the above equation, is the levelling of the pre- and post-transition baselines. This figure illustrates that denaturation of pGH results in absorbance- and fluorescence-detected transitions which are coincident, but CD- and hydrodynamic radius- detected transitions which occur at higher concentrations of denaturant, indicative of a greater stability towards denaturation. In terms of protein folding, the results are in agreement with the framework model of protein folding. If we consider what is happening on a molecular level as the protein refolds from 6M GuHCl to native state conditions, the helices begin to form near 4M GuHCl. When approx. 60% of the helix is recovered, the conformation begins to collapse into a more compact configuration. This is seen as the initial decrease in hydrodynamic radius at approx. 3.5M GuHCl. By 3M GuHCl, 50% of the helix is present and the molecule is 25% larger than the native state (Figure 12 & 6c), yet the tertiary structure is yet to form as seen by absence of recovery of the fluorescence and absorbance probes. The tryptophan residue is probably near the surface of the protein, only partially shielded from the bulk solvent. This state of pGH is "molten-globule" like in that it is largely α-helical and compact, yet has packing of the aromatic side-chains that is similar to the unfolded state. Eventually as the denaturant concentration

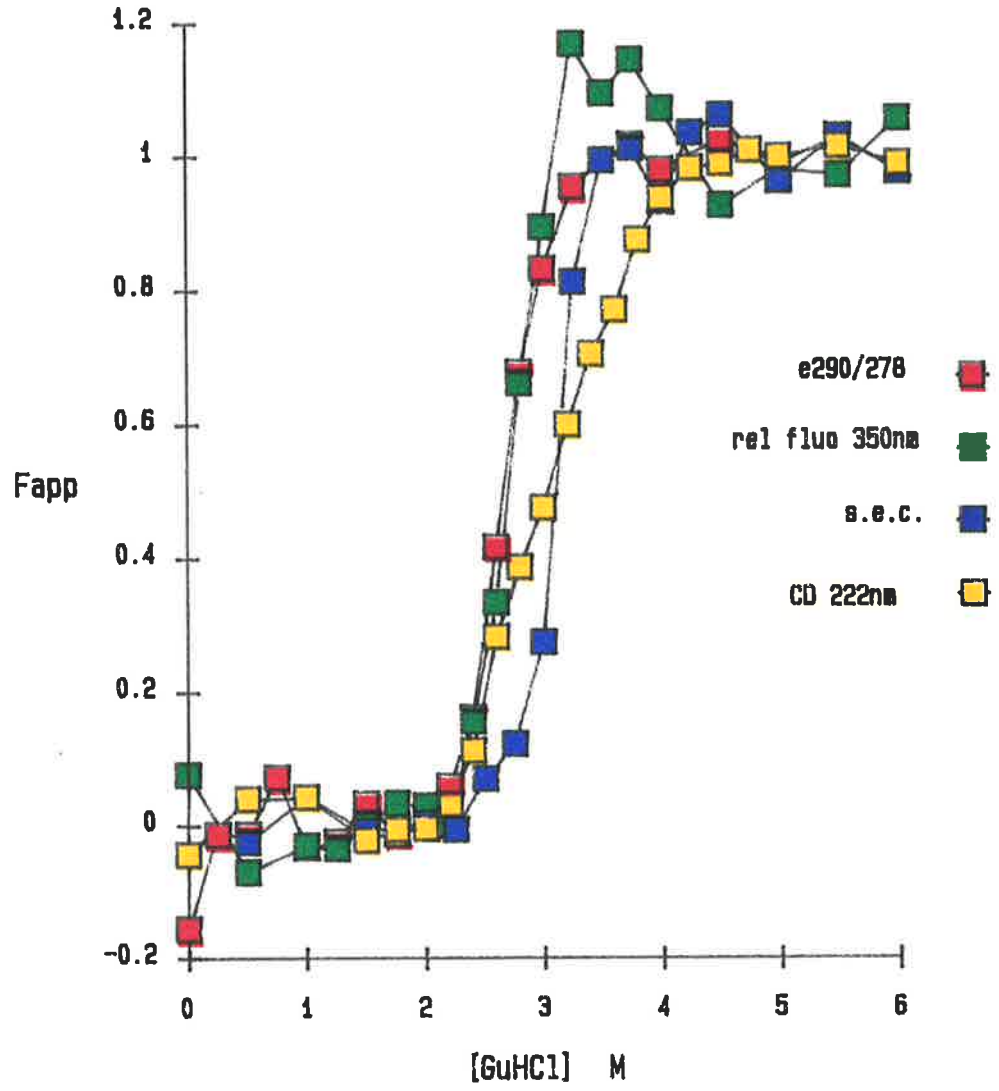

Figure 12. The apparent fraction of unfolded pGH as a function of GuHCl concentration.

The apparent fraction of unfolded protein, F_{app}, as measured by the four probes, UV-absorbance, fluorescence, size-exclusion chromatography and far-UV CD. $F_{app} = (Y_{obs} - Y_{nat})/(Y_{unf} - Y_{nat})$ where Y_{obs} is the value of the measured observable, and Y_{nat} and Y_{unf} are the observed values for the native and unfolded forms, respectively. (see 4.2.7 for details).

decreases further to about 2.2M GuHCl, these aromatic residues are locked into their native state configuration. The gradual recovery of helix as evidenced by CD is suggestive of a biphasic transition; the initial loss of helix upon unfolding accompanies the tertiary structure disruption (Figure 12).

4.3 CONCLUSIONS

Earlier equilibrium denaturation studies of several members of the GH family detected the presence of stable intermediates in the bovine, ovine and rat growth hormones (Burger et al., 1966; Holladay et al., 1974). More recently, the thorough equilibrium and kinetic examination by Brems and Havel et al. (summarized in Brems & Havel, 1989) has shown that denaturation of bGH is a multistate process in which at least two folding intermediates have been identified. However, hGH has been shown to follow a two-state denaturation mechanism with no detectable intermediates (Brems et al., 1990). A comparison of the unfolding transition midpoints for these two proteins and pGH is shown in Table I. hGH is more resistant to chemical denaturation than bGH or pGH and folds cooperatively with all transition midpoints at 4.6M GuHCl. The tertiary structure of bGH is less stable than the secondary structure as evidenced by the lower denaturation midpoints detected by UV absorbance and fluorescence, compared to that for CD. The denaturation of pGH follows a similar pattern to that for bGH, except that the transitions are shifted to lower concentrations of GuHCl and they occur over a narrower range of denaturant concentration. The fact that the denaturation midpoints of pGH are shifted to lower concentrations of GuHCl does not necessarily mean that pGH is less stable than bGH. The conformational stability ($\Delta G(H_2O)$) of a protein is dependent on the steepness of the denaturation transition (m value; Chapter 5) as well as the denaturation midpoint (Greene & Pace, 1974). The UV absorbance-detected transition of pGH results in a $\Delta G(H_2O)$ of about 7 kcal/mol (Chapter 5). Published values of $\Delta G(H_2O)$ for bGH vary between 5-7 kcal/mol (Brems et al., 1985). It would be reasonable to say that

proteins	far-UV circular dichroism	fluorescence	size-exclusion chromatography	UV-absorbance
pGH	3.1	2.7	3.1	2.7
bGH[a]	3.8	3.3	3.7	3.1
hGH[b]	4.6	4.6	4.6	4.6

Units are in molar (M). [a]Results for bGH were obtained from Brems & Havel (1989) and Lehrman et al. (1991).[b]Results for hGH were obtained from Brems et al. (1990).

Table I: GuHCl Denaturation Midpoints of pGH, bGH, and hGH as Determined by Different Spectral/Physicochemical Methods

pGH and bGH have comparable stabilities but are less stable than hGH which has a $\Delta G(H_2O)$ value of 14.5 kcal/mol (Brems et al., 1990).

The similarities in the equilibrium denaturation of pGH and bGH are echoed in the similar fluorescence and size-exclusion chromatography results. Both proteins possess a single tryptophan residue located in a moderately non-polar environment with a quenched native-state fluorescence. As with bGH, size-exclusion chromatography experiments of pGH have detected the presence of a partially denatured self-associated species at intermediate denaturant concentrations. The properties of this species include increased near-UV CD at 300nm, a polar tryptophan environment (second derivative spectroscopy) and a propensity to precipitate when diluted to non-denaturing concentrations of denaturant. However, unlike bGH, size-exclusion chromatography of pGH at GuHCl concentrations between 2.25M and 3.75M resulted in chromatograms displaying multiple peaks (Figure 6a). This phenomenon, previously seen in a destabilized mutant of bGH containing a single mutation in the third helix (Brems et al., 1988) and an alkylated form of hGH (Brems et al., 1990) is indicative of a slow equilibrium rate between the various forms present. The most favourable condition for self-association of pGH was in buffers containing 3-3.25M GuHCl.

The similarity in the equilibrium denaturation of bGH and pGH is not surprising considering their sequence similarity. It has been shown previously that the third helix is directly involved in the association of the partially unfolded bGH (Brems et al., 1986). This helix is unusually stable even in the absence of the rest of the bGH structure (Brems et al., 1987b). As bGH unfolds, initial disruption of the tertiary structure exposes the hydrophobic face of the amphiphilic helix. Association is stabilized by the hydrophobic interactions resulting from the intermolecular packing of the lipophilic faces of partially exposed helices. The third helix of pGH is identical in sequence to that for bGH except for a leu→gln substitution at residue 121. Figure 13 compares the helical wheel projections for the third helix of pGH, bGH and hGH. The amphipathic nature of helix-3 is evident as is the sequence similarity

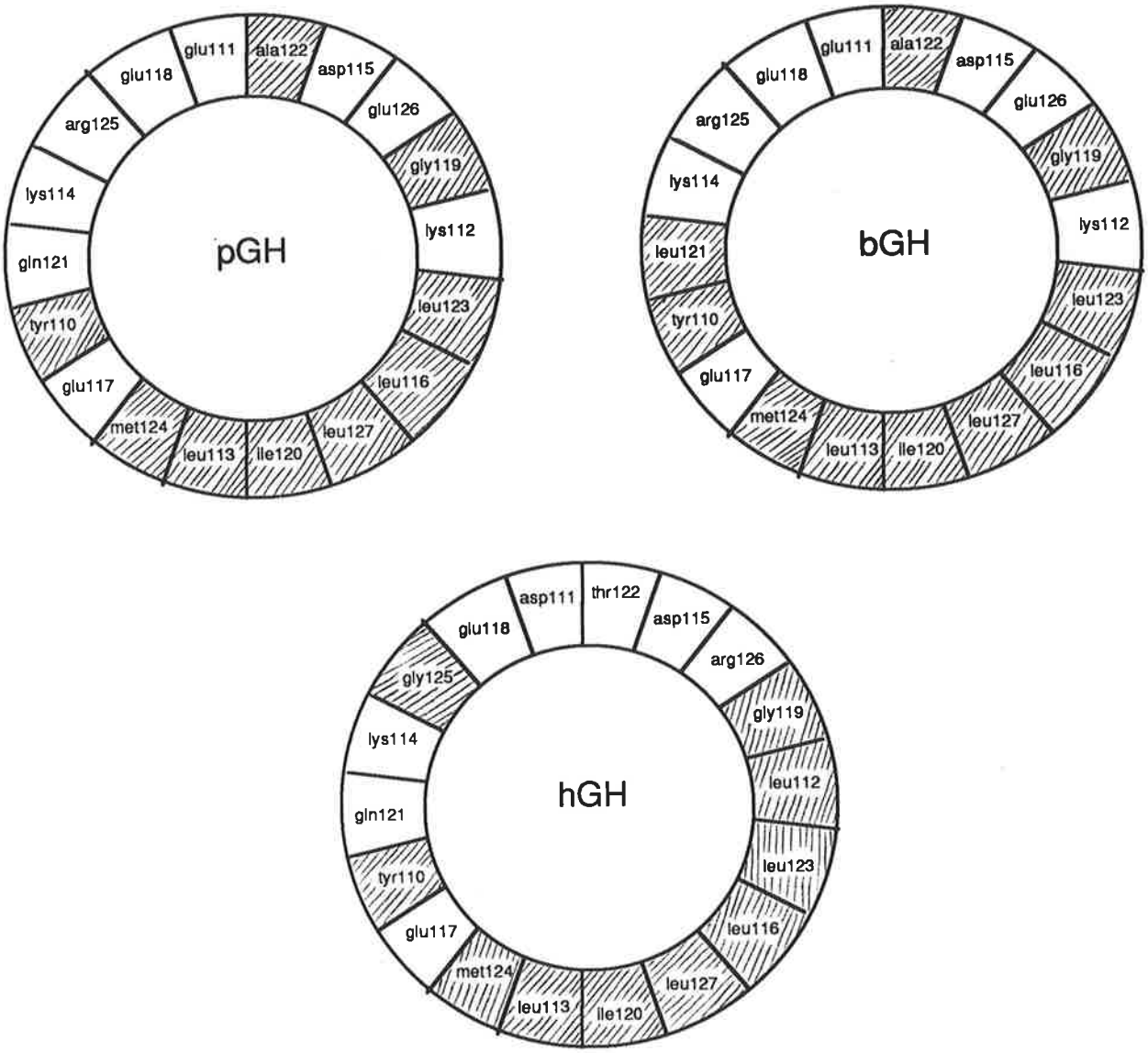

Figure 13. Helical wheel analysis of helix-3 of pGH, bGH and hGH.

Helical wheel analysis of residues 110-127 of pGH, bGH and hGH. Hydrophobic amino acids, noted by shading, are designated as described by Eisenberg et al. (1984). Note that pGH and bGH differ only by one residue, gln121→leu.

between species. It is quite possible that helix-3 of pGH may be involved in the self-association process. Figure 14 illustrates the pGH model with helix-3 hinged upward showing the hydrophobic face (black carbons and hydrogens) and the "hydrophobic pocket" formed by the packing together of the other helices. Denaturant-induced loosening of tertiary structure could expose these hydrophobic patches thus promoting the association process.

The association phenomenon in non-human GHs cannot be solely attributed to interactions between partially unfolded helix-3. Recently, a mutant bGH containing the helix-3 sequence of hGH substituted for the wild-type sequence, was shown to result in a significant decrease in aggregation compared to wild-type bGH, when incubated under conditions favouring self-association (Lehrman et al., 1991). Aggregation was not completely abolished however, suggesting other partially exposed hydrophobic sites are involved. In addition the close similarity between helix-3 of hGH with that for pGH and bGH (Figure 13) implies a similar aggregation phenomenon should occur in hGH, which is not the case. From equilibrium denaturation studies of hGH, it was concluded that hGH does not form an associated state because the relatively greater stability of native hGH compared to the non-human GHs precludes the observation of hGH folding intermediates (Brems et al., 1990). The general topography of hGH is very similar to that for pGH (Abdel-Meguid et al., 1987; de Vos et al., 1992) suggesting that the molecular interactions contributing to the presence of intermediates and the subsequent self-association seen in non-human GHs are very specific. Specific residues present in the internal architecture of hGH but absent in non-human GHs, may be involved in conferring greater stability to the native state. These residues could participate in maintaining a compact configuration of the four α-helix bundle.

Without the atomic coordinates of the previously published pGH structure (Abdel-Meguid et al., 1987) available, Carlacci and coworkers' (1991) heuristic approach in predicting the three-dimensional structure of bGH, resulted in a structure very similar to that of pGH. Using energy minimization models, they predicted that

Figure 14. Model of pGH showing "helix-3 hinge".

A "Peloponnesian"* view of the pGH model showing exposure of the hydrophobic face of helix-3 (arrow) and the hydrophobic centre of the molecule. It became apparent in the construction of the model, how easy it was to literally "pick up" helix-3 and manoeuvre it up and down on the "hinge" peptide connecting it to helix-4, without "disturbing" the rest of the model (see Figure 1 also). It is unlikely that partially-denaturing concentrations of denaturant will only affect this region of the molecule. However, general loss of stabilizing tertiary interactions may lead to exposure of hydrophobic regions as shown in this example. Colour coding of the atoms is described in Figure 2. The yellow sphere is the sulphur atom of met179.

*From this angle, the bottom half of the model resembles the Peloponnesian peninsula of Greece, the ancestral origin of the author.

the four α-helix bundle of bGH is stabilized considerably by the connecting loops between the helices. This stabilization was principally due to hydrophobic and electrostatic interactions between the α-helices and loops. When the hGH/receptor complex X-ray structure was revealed by the Genentech group (de Vos et al., 1992), several interesting differences between the porcine and human structures were observed. Firstly, two short helices (residues 38-47 and 64-70) present in the connecting loop between helix-1 and helix-2 of hGH are absent in pGH. This region of hGH is involved in receptor binding and it is thought that these short helices may represent conformational changes upon receptor binding. In addition, another short helix (residues 94-100) is present in hGH in the short connection between helix-2 and helix-3 which has an omega-loop conformation in pGH. This probably represents a true structural difference between the two hormones since this connection is not involved in receptor binding. It is possible that this short helix present in hGH bestows greater rigidity to the connection between the two helices, and thus by stabilizing the interaction between helix-3 and the hydrophobic pocket "below" it (as in Figure 14), may confer a greater overall stability to this hormone. We are currently in the process of constructing a mutant pGH with the hGH sequence between helix-2 and -3 substituted in place of the pGH sequence to test this hypothesis. This involves three pGH sequence changes: T98A, F103Y and T105A.

Considering that the greatest sequence divergence between the human and non-human GHs is in the connecting loops (Chapter 1, Table I; Nicoll et al., 1986), these regions may hold the key to explaining why hGH is more stable. Reduction and alkylation of both the disulphide bridges of hGH with iodoacetate (2-RCOM hGH) greatly decreases its stability, such that the denaturation behaviour is similar to the non-human GHs with well-populated intermediates (Brems et al., 1990). The denaturation midpoint for UV and fluorescence decreases from 4.6M to 3M GuHCl, while that for CD decreases to 3.45M GuHCl. Reduction of the disulphide bonds removes the covalent links between the long connecting loop and helix-4 (disulphide bond 53-164), and the short C-terminal extension and helix-4, thus decreasing the

loop-helix interactions. Obviously oxidized pGH and bGH still contain these covalent bonds, but the fluidity of the connecting loops in these hormones may be similar to that of alkylated hGH. Tight packing of the connecting loops against the helices could be important in stabilizing the structure of the molecule as a single entity. Interactions (hydrophobic and electrostatic) between specific helix residues and the connecting loops would contribute to this stabilization process.

What does this tell us about the porcine growth hormone folding pathway?

Equilibrium denaturation of pGH using the denaturant GuHCl has resulted in non-coincidence of the transition curves of various spectroscopic and hydrodynamic probes. These findings show that pGH does not follow a simple two-state folding mechanism, but is consistent with the framework model of folding (Kim & Baldwin, 1982). From equilibrium and kinetic folding studies of bGH, Brems and coworkers have summarized the folding pathway of bGH with the following model:

$$N \leftrightarrow I \leftrightarrow U$$
$$\updownarrow$$
$$I_{\text{assoc}}$$

where N, I, U , and I_{assoc} are the native, monomeric intermediate, unfolded and associated intermediate states, respectively (Brems et al., 1988). The model illustrates that the folding of bGH is a multistate process involving at least one folding intermediate and that formation of the monomeric intermediate precedes aggregation. The intermediate I is populated at equilibrium in denaturation studies and transiently during kinetic folding (Brems et al., 1987a). The structure of I has been likened to the "molten globule state", and is characterized as having a compact structure, mostly helical, flexible, yet possessing a tertiary structure similar to the denatured state. The associated intermediate, I_{assoc}, is present only at elevated protein concentrations and has an association constant of 10μM.

The equilibrium denaturation of pGH described in this chapter is very similar to that of bGH in many respects. The above model for bGH could also describe the folding pathway of pGH. There is the unquestionable presence of an associated intermediate which originating from a monomeric intermediate, verifies the existence of the monomeric intermediate. This intermediate, populated at equilibrium in intermediate concentrations of denaturant is difficult to quantitate at low protein concentrations. However, at elevated protein concentrations, the intermediate is the predominant species, amounting to as much as 80% of all species present at 3.0M GuHCl.

Although the denaturation mechanism of bGH has been described as a multistate folding process involving a molten globule like intermediate, a recent review has stated that the bGH data is also consistent with the *variable two-state model* (Dill & Shortle, 1991). The variable two-state model involves a mechanism in which the denatured state changes continuously from a compact form to an unfolded form with increasing denaturant concentration. The compact denatured form in the case of bGH is the molten globule-like intermediate, *I*. To verify the existence of a discrete intermediate species it is necessary to establish that there is a free energy barrier between the compact and unfolded denatured states for these transitions in GuHCl. The folding of pGH is definitely not a simple two-state mechanism, but fits the variable two-state model also. Whether the species present near 3M GuHCl having the characteristics of a molten globule or *compact* denatured state is a discrete intermediate remains to be verified. The fact that the equilibrium rate at this concentration of denaturant is slower than that seen in bGH may make it easier to isolate the intermediate. At this stage, very little kinetic examination has been made on the pGH folding process. Further studies in this area in combination with the use of mutant pGHs should shed some light on the stability and lifetime of the proposed intermediate in the pGH folding pathway.

CHAPTER 5

THE CONFORMATIONAL STABILITY OF THE GROWTH HORMONES

5.1 INTRODUCTION

5.1.1 The Concept of Conformational Stability

Under physiological conditions, most proteins attain a compact, globular conformation that is essential for their biological function. This three-dimensional conformation, determined by the primary amino acid sequence, is usually referred to as the native state, *N*. The native state is only marginally stable over the array of unfolded or denatured states of the protein, *D*, in equilibrium with the native state. The conformational stability of a protein is defined as the free energy change for the equilibrium reaction:

$$N \quad \Leftrightarrow \quad D \qquad (1)$$

under ambient conditions such as in water at 25°C. Thus, the conformational stability of a protein is concerned with the stability of the folded state, in the absence of covalent changes. By measuring the equilibrium constant, *K* (the ratio of the fraction of molecules in the *D* state against the fraction in the *N* state), the free energy change (ΔG) on conversion of *N* to *D* can be calculated from the equation:

$$\Delta G = -RT \ln K \qquad (2)$$

A number of different methods are employed for determining the conformational stability of a protein. These include reversible denaturation by temperature, pH or chemical denaturants. Measurements of the conformational stability from urea or guanidine hydrochloride (GuHCl) denaturation curves are designated $\Delta G(H_2O)$, and those from thermal denaturation curves are designated $\Delta G(25^{\circ}C)$. All methods used to determine the conformational stability give only the *difference* in free energy between the *N* and *D* states. Therefore it is not possible to assign changes in conformational stability, $\Delta(\Delta G)$, between two similar proteins, i.e., wild-type and a site-directed mutant, with any certainty to changes in the free energy of either the *D* or the *N* state. However, recent studies using truncated and site-directed mutants of

staphyloccocal nuclease have shown that it is possible to obtain some information on the effect of a mutation on the stability of the denatured state (Shortle & Meeker, 1989; Shortle et al., 1990).

The difference in free energy between the *N* and *D* states for most proteins is generally quite small, being typically some 5 to 15 kcal/mol (Pace, 1975; Privalov, 1979). This is the difference between two large numbers that are delicately balanced; the free energy of the non-covalent interactions in the folded state of the protein, mainly arising from interactions between the atoms of the protein, minus the free energy of the non-covalent interactions in the unfolded state, which arises mainly from solvation energies. More specifically, this refers to the balance of forces primarily contributing to stabilization of the native state, namely hydrophobic interactions, hydrogen-bonding, van der Waals interactions and electrostatics (classical ion pairing), and those opposing stabilization, namely conformational entropy and classical charge repulsions (Dill, 1990).

This chapter is concerned with determining the conformational stability of various isolated pGH mutants using chemical denaturation (GuHCl and urea). Because of this, I shall from here on refer to the conformational stability of a protein as $\Delta G(H_2O)$. The determination of $\Delta G(H_2O)$ is useful in comparing stabilities of proteins differing slightly in chemical structure. Such a structural change might be a single change in amino acid sequence made by site-directed mutagenesis, or a change in the structure of a side-chain made by chemical modification. Determining the effects a mutation can have on the conformational stability of a protein will help us to understand the interactive forces involved in the acquisition of the unique fold of the native state. The effects of the mutation on the cooperativity of the folding event can also be examined. Finally, it should then be possible to optimize these interactions in order to construct stable proteins with varying functional specificities, for pharmaceutical and industrial applications.

5.1.2 Selecting a Technique to Monitor the Unfolding of a Protein.

The physical and biological properties of a protein change substantially upon unfolding, making it relatively simple to monitor the extent of unfolding. Denaturation is generally induced by either a chemical denaturant or by temperature. It is absolutely essential that the denaturation process is completely reversible because the conformational stability measurements are made on the assumption that the *N* and *D* states are in equilibrium (Pace et al., 1989). Urea- and GuHCl-induced unfolding are more likely to be completely reversible than thermal unfolding. Extremes of temperature can have irreversible effects on the physicochemical integrity of proteins due to damage to the covalent structure. However, minimizing the time spent in unfolding conditions increases the reversibility of the thermally-induced unfolding process. Because of the possibility of incomplete reversibility of thermal denaturation, I decided to use GuHCl- and urea-induced denaturation to examine the effects of site-directed mutations on the stability of pGH. Once the denaturation mechanism has been chosen it is necessary to select a technique to monitor the extent of unfolding. The techniques most often used are UV difference spectroscopy (Herskovits, 1967), fluorescence (Brand & Witholt, 1967) and circular dichroism (Adler et al., 1973). As well as these spectroscopic techniques, size-exclusion chromatography is also commonly used to monitor unfolding (Saito & Wada, 1983; Fridman et al., 1990). Obviously, the greater the change in the physical property when the protein unfolds, the better the technique is for monitoring unfolding.

5.1.3 Denaturation Curve Analysis

A typical denaturation curve shows how the value of the physical parameter being measured, *y*, changes with increasing denaturant concentration. For example, Figure 1a illustrates the effect of the GuHCl concentration on the measured parameter, the A_{290}/A_{278} absorbance ratio for pGH. The denaturation curve can be conveniently divided into three regions:(*i*) the pre-transition region, which shows how *y* for the folded protein, y_N , depends upon denaturant, (*ii*) the transition region, which

shows how y varies as unfolding occurs, and (*iii*) the post-transition region, which shows how y for the unfolded protein, y_D, varies with denaturant (Pace et al., 1989). Denaturant-induced perturbation of the folded and unfolded states often result in pre- and post-transition baselines with significant slopes (Schmid, 1989). These denaturant effects must be taken into account when defining y_N and y_D. From equation 1, it follows that for a two-state mechanism, $f_N + f_D = 1$, and $y = y_N f_N + y_D f_D$ where f_N and f_D represent the fraction of the protein present in the native and denatured states, respectively. Combining these equations, we obtain

$$f_D = (y_N - y)/(y_N - y_D) \tag{3}$$

and

$$f_N = (y - y_N)/(y_N - y_D) \tag{4}$$

The equilibrium constant, K, and the free energy change, ΔG, can be calculated using

$$K = f_D/f_N = (y_N - y)/(y - y_D) \tag{5}$$

and

$$\Delta G = -RT \ln K = -RT \ln [(y_N - y)/(y - y_D)] \tag{6}$$

where R is the gas constant (1.987 cal/deg/mol) and T is the absolute temperature (°Kelvin). Using only K values (range of 0.1-10) near the midpoint of the denaturation curve, the resulting plot of ΔG versus denaturant concentration is linear. The simplest method of estimating the conformational stability in the absence of denaturant, $\Delta G(H_2O)$, is to assume that this linear dependence continues to zero concentration and to use a least-squares analysis to fit the data to the equation

$$\Delta G = \Delta G(H_2O) - m[\text{denaturant}] \tag{7}$$

where m is a measure of the dependence of ΔG on the denaturant concentration. Note that at the midpoint of the transition, where the concentration of folded and unfolded states is equal, the equilibrium constant, K, is equal to 1, and ΔG is equal to 0. Therefore, at the midpoint of the unfolding curve, $[\text{denaturant}]_{½} = \Delta G(H_2O)/m$. This

implies that $\Delta G(H_2O)$ is dependent on both the midpoint of the denaturation curve, [denaturant]$_{½}$, and on the dependence of the free energy of unfolding on the denaturant concentration, m.

There are other methods currently available for determining the conformational stability of proteins using chemical denaturation. Santoro and Bolen (1988) stated that the error in $\Delta G(H_2O)$ and m is underestimated in the linear extrapolation method described above, because no error is assumed for the pre- and post-transition baselines. They devised a non-linear, least-squares program to fit the entire unfolding curve to an equation containing six parameters. However, if sufficient data points are taken in the pre- and post-transition regions, as well as the transition region, the values of $\Delta G(H_2O)$ and m obtained by both of these methods are generally in good agreement (Pace et al., 1992). An alternative method makes use of transfer free energies for side chains and peptide units from water to the particular denaturant concentration, to fit the various ΔG_{app} (i.e., experimentally determined) points to Equation 8 below, by summing over the number of peptide units and the various side chains using $\Delta\alpha_{app}$ and $\Delta G(H_2O)$ as adjustable parameters (Tanford, 1964, 1970; Puett, 1972).

$$\Delta G_{app} = \Delta G(H_2O) + \Delta\alpha_{app} \Sigma_i n_i \Delta G_i^t \qquad (8)$$

The parameters $\Delta\alpha_{app}$, n_i , and ΔG_i^t refer to the apparent average difference in the degree of exposure of the side chains and peptide groups in the denatured and native conformation, the total number of groups of type i present in the protein, and the transfer free energy of these groups, respectively. Finally, the denaturant binding model makes use of the assumption that there are a greater number of denaturant binding sites on the unfolded conformation than there are on the folded conformation. It follows that

$$\Delta G = \Delta G(H_2O) - \Delta nRT \ln (1+ka) \qquad (9)$$

where Δn is the difference in the number of denaturant binding sites, k is the equilibrium constant for binding at each site, and a is the activity of the denaturant (Tanford, 1970). Estimates of $\Delta G(H_2O)$, Δn, and k are obtained by fitting the data to Equation 9.

Using each of these methods leads to different estimates of $\Delta G(H_2O)$, with the linear extrapolation method always resulting in the lowest estimate. The difference in results is more pronounced in GuHCl-induced denaturation. Which is the best method to use? Due to its relative simplicity, the linear extrapolation method is the most commonly used, even if the estimates of $\Delta G(H_2O)$ from urea and GuHCl denaturation curves may prove to be too low. Schellman (1978) has suggested that a linear dependence of ΔG on denaturant concentration may be reasonable based on theoretical grounds. More recently Santoro and Bolen (1992) have shown experimentally that the dependence of unfolding ΔG on GuHCl concentration for "stable proteins" is linear over the full denaturant concentration range. In addition, $\Delta G(H_2O)$ values obtained using the linear extrapolation method have also been shown to agree very closely with those obtained using differential scanning calorimetry (Santoro & Bolen, 1992; Hu et al., 1992). Furthermore, if the comparison of $\Delta G(H_2O)$ values between various mutants of a protein is made under a standard set of conditions, the absolute value is not essential.

5.2 RESULTS AND DISCUSSION

5.2.1 Assumptions and Standard Conditions

In Chapter 4, it was shown that the denaturation of pGH does not follow a simple two-state mechanism, but is consistent with a variable two-state model (Dill & Shortle, 1991). One of the conditions necessary for calculation of $\Delta G(H_2O)$ using the linear extrapolation model is that the denaturation mechanism closely approaches a two-state mechanism. However, there have been several stability studies on mutant proteins which clearly deviate from two-state denaturation mechanisms, even if the wild-type protein approaches a two-state mechanism (Lim et al., 1992; Shortle &

Meeker, 1986). In these cases the qualitative results of the effects of the mutations on protein stability has allowed some basic conclusions to be made about protein folding and stability. The analysis of denaturation curves in terms of a two-state approximation is useful even when denaturation deviates substantially from a two-state mechanism. Because intermediates are present in pGH, I will refer only to the apparent equilibrium constant, K_{app}, and the apparent free energy of unfolding, ΔG_{app}, rather than K and ΔG.

Of the four probes used in the equilibrium denaturation studies described in Chapter 4, I decided to use UV absorbance spectroscopy to monitor the denaturation of pGH and mutants, hGH and brGH. The reasons for this were (*i*) removal of the single tryptophan buried in the hydrophobic core of pGH to the solvent exterior is a good indicator of the general unfolding of the molecule, i.e., the cooperative breakdown of the native structure. However, it is not indicative of the complete unfolding of the protein i.e., loss of all secondary structure, (*ii*) unfolding produced a smooth sigmoidal denaturation profile (unlike fluorescence), (*iii*) the technique was relatively simple and fast (compared to size-exclusion chromatography), (*iv*) the denaturation profile was protein concentration independent (unlike size-exclusion chromatography), (*v*) protein sample usage was "low" (10 mg/determination), and (*vi*) I had ready access to a sensitive, thermostatted spectrophotometer.

A standard set of conditions were used in all $\Delta G(H_2O)$ determinations for all GHs. The pH of the buffers was pH 9.1 (25mM sodium borate) and the temperature of incubation and spectrophotometer readings was 25°C (see 2.2.11.1). The same conditions were employed for both GuHCl and urea determinations. To test the reversibility of the denaturation, samples were initially prepared by mixing two stock solutions of an equal concentration of pGH, one in buffer containing no GuHCl and the other in buffer containing 6M GuHCl, at the appropriate volumes, to arrive at each final GuHCl concentration. This method of sample preparation gave identical results to the alternative method in which the samples were prepared by adding a constant volume of a stock solution of pGH in buffer without GuHCl, to increasing

concentrations of GuHCl (see 2.2.11.1 & 4.2.1). Upon completion of recording the absorbance values (290nm and 278nm) for each concentration of GuHCl, the data was typed into an Excel spreadsheet on the computer. Table I illustrates an example of the Excel format for calculating the A_{290}/A_{278}, y_N, y_D, F_{app} and ΔG_{app} values.

5.2.2 Conformational Stability of Wild-Type Porcine Growth Hormone

The $\Delta G(H_2O)$ of pGH was determined using both GuHCl and urea as denaturants. This was done to compare the effects of ionic and non-ionic denaturants on the unfolding and stability of pGH.

5.2.2.1 Denaturation with Guanidine Hydrochloride

Table I gives an example of the data set and calculations for a typical pGH denaturation curve using GuHCl as the denaturant. To obtain a good average, five $\Delta G(H_2O)$ determinations were performed on pGH with GuHCl as the denaturant. Figure 1a illustrates the A_{290}/A_{278} ratio as a function of GuHCl concentration. As explained in 4.2.1, the smoothest transition curves were obtained using this ratio of absorbance at two wavelengths. The denaturation curve has a gently downward sloping pre-transition baseline and an essentially flat post-transition baseline. A least-squares analysis of the experimental data was used to determine the baselines. With most proteins, a slight linear increase in absorbance is detected in the pre- and post-transition phases as a result of the hyperchromic effect of the denaturant on surface exposed aromatic residues in the folded state, and all of the aromatics exposed in the unfolded state, respectively (Donovan, 1969). The downward trend observed in the pre-transition phase of pGH can be explained by the ratio of absorbances. At 290nm, only tryptophan would be absorbing significantly, and being buried in the core of the protein, would not be perturbed by the increase in denaturant concentration. However, at 278nm the 7 tyrosines present in pGH would be absorbing strongly. Previous experiments using second derivative spectroscopy (Ragone et al., 1984) have shown that three of these are exposed near the surface of the protein (Vu, 1988) and would

[GuHCl]	A290/A278	A290	A278	yf	yu	Fapp	dGapp
0	0.6432749	0.11	0.171	0.642243	0.521793	-0.00857	#NUM!
0.25	0.6433121	0.101	0.157	0.640664	0.52184	-0.02228	#NUM!
0.5	0.636646	0.1025	0.161	0.639086	0.521886	0.020817	2280.248
0.75	0.6358025	0.103	0.162	0.637507	0.521933	0.014749	2487.94
1	0.6328358	0.106	0.1675	0.635928	0.521979	0.027141	2119.337
1.25	0.6363636	0.105	0.165	0.63435	0.522026	-0.01793	#NUM!
1.5	0.6339286	0.1065	0.168	0.632771	0.522073	-0.01045	#NUM!
1.75	0.6315789	0.108	0.171	0.631193	0.522119	-0.00354	#NUM!
2	0.6287425	0.105	0.167	0.629614	0.522166	0.008112	2845.95
2.2	0.6181818	0.102	0.165	0.628351	0.522203	0.095804	1329.171
2.4	0.6024845	0.097	0.161	0.627088	0.52224	0.234662	699.9931
2.6	0.5772871	0.0915	0.1585	0.625825	0.522278	0.468754	74.10316
2.8	0.5537459	0.085	0.1535	0.624563	0.522315	0.6926	-480.986
3	0.5424837	0.083	0.153	0.6233	0.522352	0.800576	-822.995
3.25	0.534202	0.082	0.1535	0.621721	0.522399	0.881165	-1186.33
3.5	0.5263158	0.08	0.152	0.620142	0.522446	0.960386	-1887.78
3.75	0.5164474	0.0785	0.152	0.618564	0.522492	1.06292	#NUM!
4	0.5279503	0.085	0.161	0.616985	0.522539	0.942703	-1658.25
4.5	0.525	0.084	0.16	0.613828	0.522632	0.974034	-2146.26
5	0.5216049	0.0845	0.162	0.610671	0.522725	1.012739	#NUM!
5.5	0.523511	0.0835	0.1595	0.607514	0.522818	0.991824	-2841.22
6	0.5216049	0.0845	0.162	0.604356	0.522912	1.016045	#NUM!
yfs	yfi	yus	yui		midpoint	m	dG(H2O)
-0.00631	0.6422429	0.000186	0.521793		2.681768	-2428.25	6512.001

Table I. Excel worksheet of experimental data and calculations for a typical pGH denaturation curve.

On completion of recording the absorbance values (290nm and 278nm) for each concentration of GuHCl (or urea), the data was typed into an Excel spreadsheet on the computer. [GuHCl] is the molar concentration of GuHCl, A290 and A278 are the experimentally determined absorbance values at 290nm and 278nm, respectively, and A290/A278 is the ratio of the absorbance values. y_F and y_U are the values of A290/A278 for the folded and unfolded states, respectively, at each GuHCl concentration. yfs and yfi are the slope and intercept terms, respectively, for the equation defining how A290/A278 for the folded state changes with GuHCl concentration. Likewise, yus and yui are the analogous parameters for the unfolded state. Fapp is the apparent fraction of unfolded protein, dGapp is the apparent change in free energy of unfolding (ΔG_{app} in cal/mol), dG(H_2O) is the free energy of unfolding in the absence of denaturant, i.e., $\Delta G(H_2O)$ in cal/mol, m is the dependence of ΔG_{app} on the GuHCl concentration, i.e. m, in cal/mol/M, and 'midpoint' refers to the midpoint of the denaturation transition, in units of molarity, M. #NUM! is an Excel error code. This occurs when the experimental A290/A278 ratio is above the pre-transition baseline or below the post-transition baseline.

Figure 1a. GuHCl-induced equilibrium denaturation of pGH monitored by UV-absorbance.

The effect of the GuHCl concentration on the absorbance of pGH at 290nm relative to 278nm (i.e., A_{290}/A_{278}) under equilibrium conditions was determined as described in 2.2.11.1. The protein concentration was 0.22 mg/ml in buffers containing 25mM sodium borate pH 9.1. The equations for y_F and y_U give the value of A_{290}/A_{278} for the folded and unfolded states, respectively, where [GuHCl] is the molar concentration of GuHCl.

Figure 1b. ΔG_{app} for pGH unfolding as a function of GuHCl concentration.

The UV-absorbance data was transformed to give a linear plot of the apparent free energy change (ΔG_{app}) versus GuHCl concentration around the midpoint of the unfolding transition. ΔG_{app} was calculated at each GuHCl concentration as described in 2.2.11.2. The solid line indicates the best fit of the data to eq. 7, where [GuHCl] is the molar concentration of GuHCl. Linear extrapolation of this plot to 0M GuHCl results in the free energy change of denaturation in the absence of denaturant, i.e., $\Delta G(H_2O)$. In this case, $\Delta G(H_2O)$ is 6.51 kcal/mol and m, the slope of the solid line, is 2.43 kcal/mol/M.

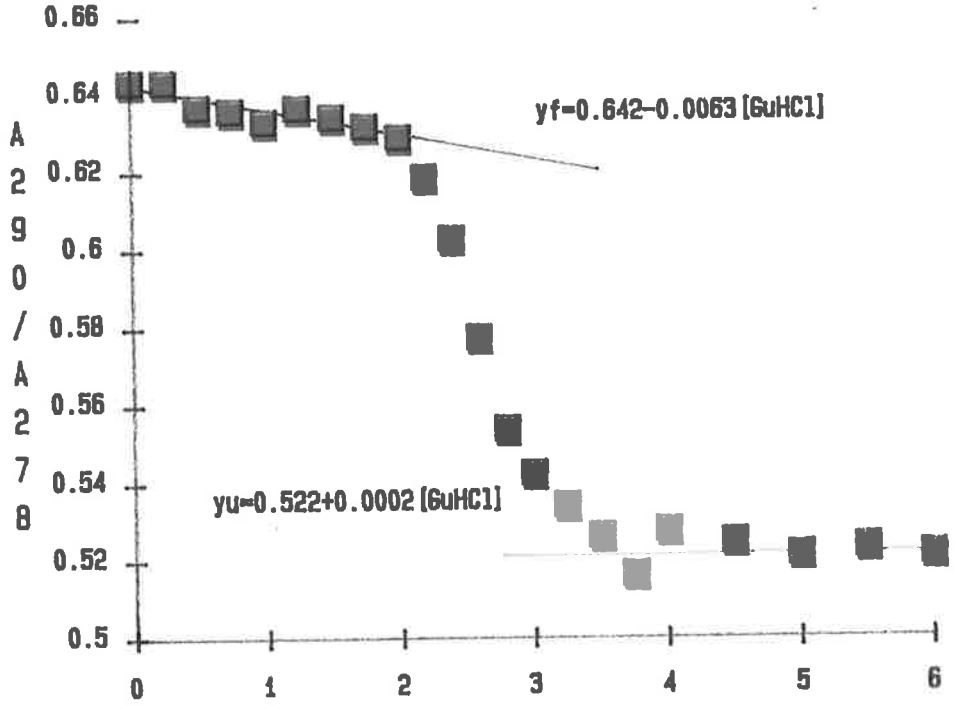
0.66
0.64
0.62
0.6
0.58
0.56
0.54
0.52
0.5
A 2 9 0 / A 2 7 8
yf=0.642-0.0063 [GuHCl]
yu=0.522+0.0002 [GuHCl]
0
1
2
3
4
5
6
[GuHCl] M

A

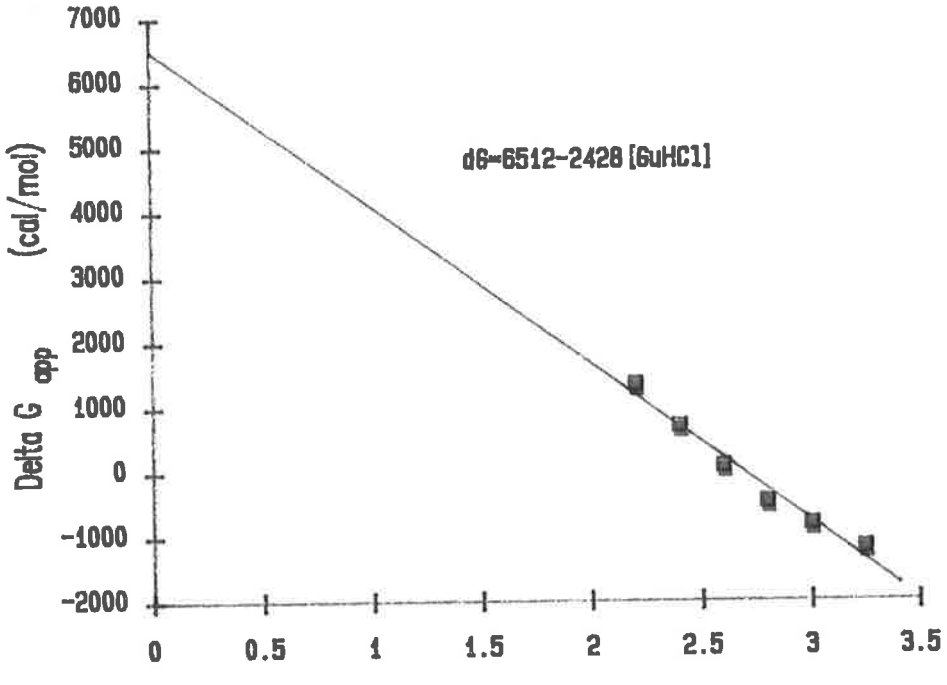
7000
6000
5000
4000
3000
2000
1000
0
-1000
-2000
Delta G app (cal/mol)
dG=6512-2428 [GuHCl]
0
0.5
1
1.5
2
2.5
3
3.5
[GuHCl] M

B

therefore undergo an increase in extinction with increasing denaturant. Therefore the downward slope in the ratio is due to the increase in absorbance at 278nm (relative to 290nm). The sigmoidal decrease from 2.2 to 3.5M GuHCl represents the unfolding transition. The flat post-transition baseline suggests that the denaturant perturbation of the exposed tryptophan (290nm) and tyrosines (278nm) results in roughly equal extinction increases in the unfolded state.

Using only ΔG_{app} values of ± 1.5 kcal/mol, Figure 1b shows that ΔG_{app} varies linearly with denaturant concentration in the limited region where ΔG_{app} can be measured. In this particular determination, least-squares analysis of the data to fit to Equation 7 (above) resulted in a $\Delta G(H_2O)$ of 6.51 kcal/mol and an m value of 2.43 kcal/mol/M. The midpoint of the denaturation was at 2.68M GuHCl. Table II shows the results of the five $\Delta G(H_2O)$ determinations of pGH. From five determinations an average $\Delta G(H_2O)$ of 7.06 kcal/mol was obtained with an average m value of 2.63 kcal/mol/M and midpoint of 2.68M GuHCl. The average includes the result from the second determination which gave a much higher m value even though the midpoint was similar. It is not known why this particular experiment gave such a high m value. The more $\Delta G(H_2O)$ determinations I performed, the smoother the denaturation curves became, and therefore the error decreased. The standard deviation of $\Delta G(H_2O)$ for the five determinations was approx. 0.7 kcal/mol. Omission of the result from the second experiment lowers the $\Delta G(H_2O)$ average to 6.76 kcal/mol and the standard deviation to 0.2 kcal/mol.

5.2.2.2 Denaturation with Urea

The pGH denaturation curve using urea as the denaturant was performed twice. Figure 2 illustrates the A_{290}/A_{278} denaturation curves for both experiments. The pre-transition baselines were flat while the post-transition baselines were sloping downward. The perturbation of the exposed surface tyrosines is not as great in urea as it is in GuHCl (Schmid, 1989), so the downward slope is not observed in the pre-transition baseline. In the denatured state the hyperchromicity of the exposed tyrosine

GuHCl	$\Delta G(H_2O)$ §	m¥	midpoint*
1	6.92	2.68	2.59
2	8.27	3.07	2.69
3	6.80	2.44	2.78
4	6.51	2.43	2.68
5	6.79	2.54	2.68
Average	7.06±0.69	2.63±0.26	2.68±0.07

Urea	$\Delta G(H_2O)$ §	m¥	midpoint*
1	8.33	1.20	6.93
2	6.71	0.97	6.92
Average	7.52±1.15	1.09±0.16	6.92±0.01

Table II. Results of Denaturation Curve Analysis for Wild-Type pGH in GuHCl and urea.
§units are in kcal/mol; ¥units are kcal/mol/M; *units are in molarity (M).

Figure 2. Urea-induced equilibrium denaturation of pGH monitored by UV-absorbance.

The effect of the urea concentration on the absorbance of pGH at 290nm relative to 278nm (i.e., A_{290}/A_{278}) under equilibrium conditions was determined as described in 2.2.11.1. (*a*) and (*b*) are the results of two separate experiments. The protein concentration was (*a*) 0.34 mg/ml and (*b*) 0.32 mg/ml, in buffers containing 25mM sodium borate pH 9.1. The equations for y_F and y_U give the value of A_{290}/A_{278} for the folded and unfolded states, respectively, where [urea] is the molar concentration of urea.

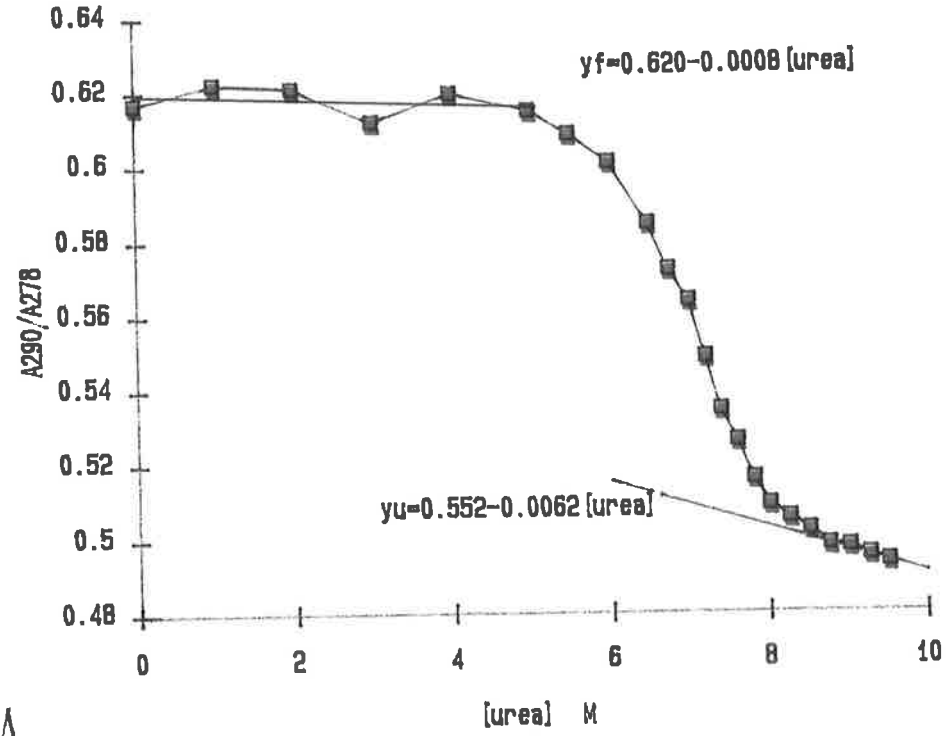
yf=0.620-0.0008 [urea]
yu=0.552-0.0062 [urea]
A290/A278
0.64
0.62
0.6
0.58
0.56
0.54
0.52
0.5
0.48
0
2
4
6
8
10
[urea] M

A

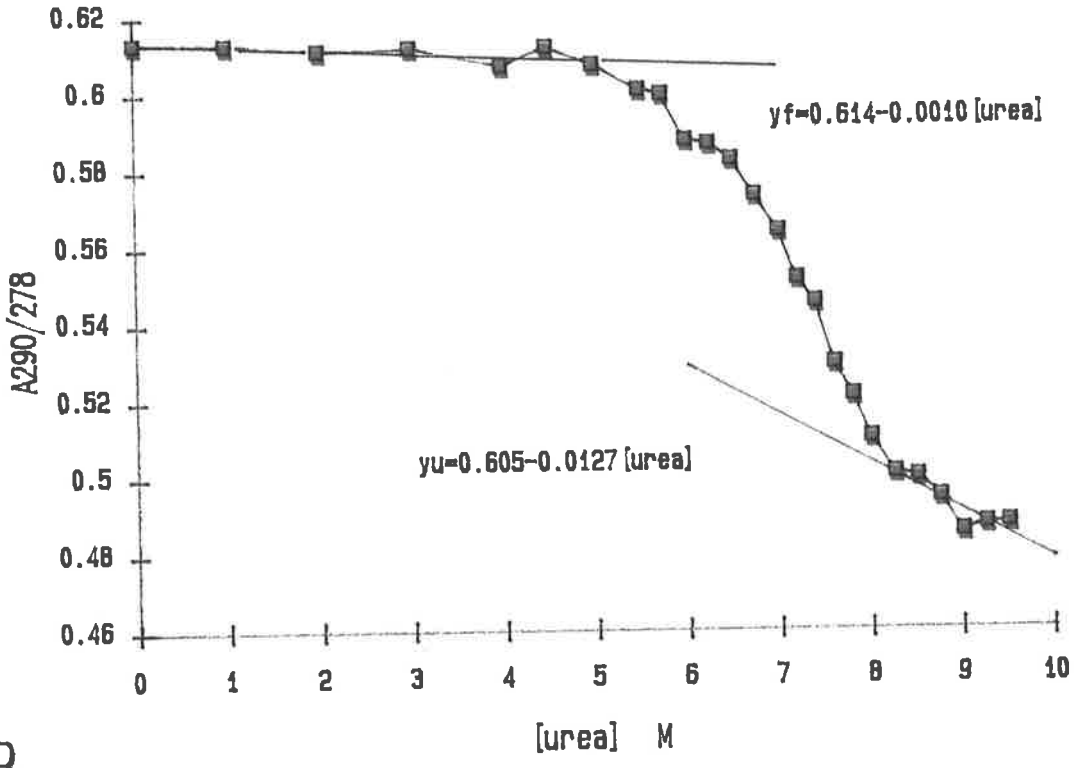
yf=0.614-0.0010 [urea]
yu=0.605-0.0127 [urea]
A290/278
0.62
0.6
0.58
0.56
0.54
0.52
0.5
0.48
0.46
0
1
2
3
4
5
6
7
8
9
10
[urea] M

B

residues (278nm) is greater than that for the tryptophan residue (290nm), as the refractive index (i.e. polarity) of the solvent increases. This results in the observed decreasing A_{290}/A_{278} ratio. The post-transition baseline was flat in the GuHCl denaturation curve (Figure 1a). It is possible that even at high urea concentrations (>9M), pGH is not completely denatured and some remnants of structure (hydrophobic clusters) could be protecting the tryptophan from complete solvation. Concentrations of urea up to 9.5M were not sufficient to completely denature bGH (Holzman et al., 1986). Even though bGH has a higher denaturation midpoint than pGH (in both GuHCl and urea), it is possible that pGH is not completely denatured at 9-9.5M urea. GuHCl is a much stronger denaturant than urea having up to 2.5 times greater denaturing power (Greene & Pace, 1974). Denaturation of pGH with GuHCl is complete by about 4M GuHCl.

Table II shows the results of the urea denaturation experiments. The average of the two determinations results in a $\Delta G(H_2O)$ of 7.52 kcal/mol with an m value of 1.09 kcal/mol/M. The midpoints for both experiments were very close indeed (6.93M and 6.92M). The $\Delta G(H_2O)$ value for the first experiment may be an overestimate because of the flatter post-transition baseline chosen. In general, m values (and therefore $\Delta G(H_2O)$ values) are about 10 ± 5% greater when flat baselines are used (Pace et al., 1992).

5.2.2.3 Comparison of GuHCl and Urea Denaturation of pGH

The $\Delta G(H_2O)$ value obtained in urea is in reasonable agreement with that obtained in GuHCl (Table II). This result was encouraging since the value of the $\Delta G(H_2O)$ of a protein should be independent of the denaturant used. Figure 3a shows how the ΔG_{app} for the unfolding of pGH varies linearly for both GuHCl and urea. Greene and Pace (1974) have shown that the ability of a denaturant to unfold a protein is more directly reflected in the m value rather than the midpoints of the respective denaturation curves. The ratio of m values for the two denaturants, m_{GuHCl}/m_{urea}, is 2.43 for pGH. This compares to m ratio values of 2.82 for

Figure 3a. ΔG_{app} for the denaturation of pGH as a function of GuHCl and urea molarity at pH 9.1.

Comparison of the ΔG_{app} for the denaturation of pGH as a function of GuHCl (blue line) and urea (red line) molarity at pH 9.1. ΔG_{app} was determined at each concentration of denaturant as described in 2.2.11.2. The equations defining the solid lines are the average of five separate $\Delta G(H_2O)$ determinations in GuHCl and of two determinations in urea (see Table II).

Figure 3b. Analysis of the denaturation of pGH using Tanford's model.

ΔG_{app} is plotted as a function of $\Sigma_i n_i \Delta G_i^t$ (see text in 5.1.3 and 5.2.2.3). In order to estimate the $\Delta G(H_2O)$, the transfer free energies for side chains and peptide units from water to the particular denaturant concentration, were used to fit the experimental ΔG_{app} values to eq. 8, by summing over the number of peptide units and the various side chains, and using $\Delta\alpha_{app}$ and $\Delta G(H_2O)$ as adjustable parameters (*Tanford, 1970; Nozaki & Tanford, 1970*). The blue line is the best fit to the urea data while the red line is the best fit to the GuHCl data. The resulting $\Delta G(H_2O)$ and $\Delta\alpha_{app}$ values are shown in Table III.

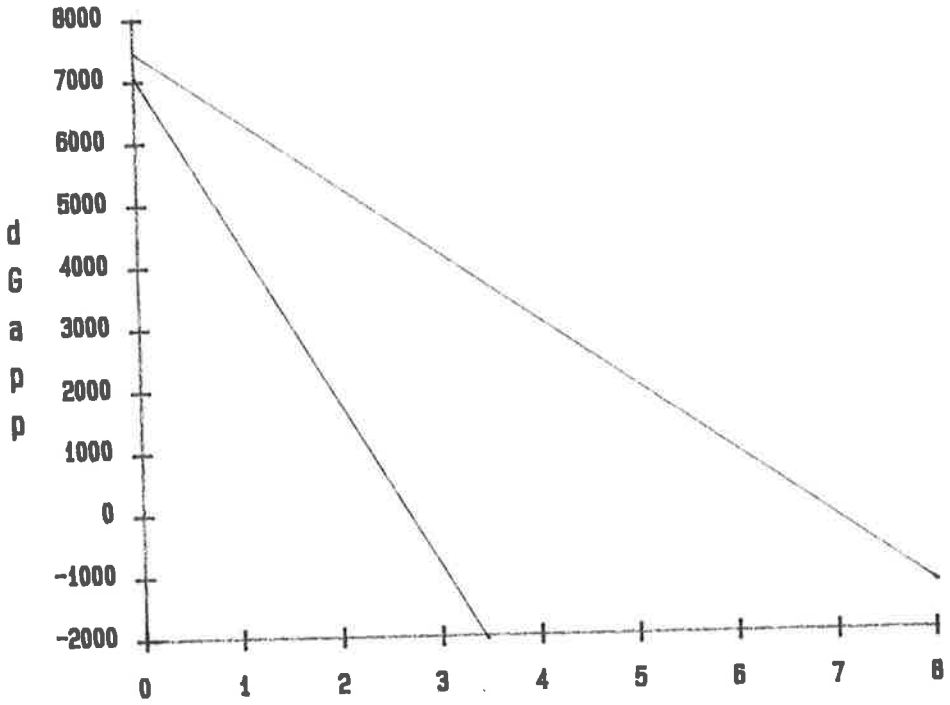
8000
7000
6000
5000
4000
3000
2000
1000
0
-1000
-2000
d G a p p
0 1 2 3 4 5 6 7 8
molarity (M)

A

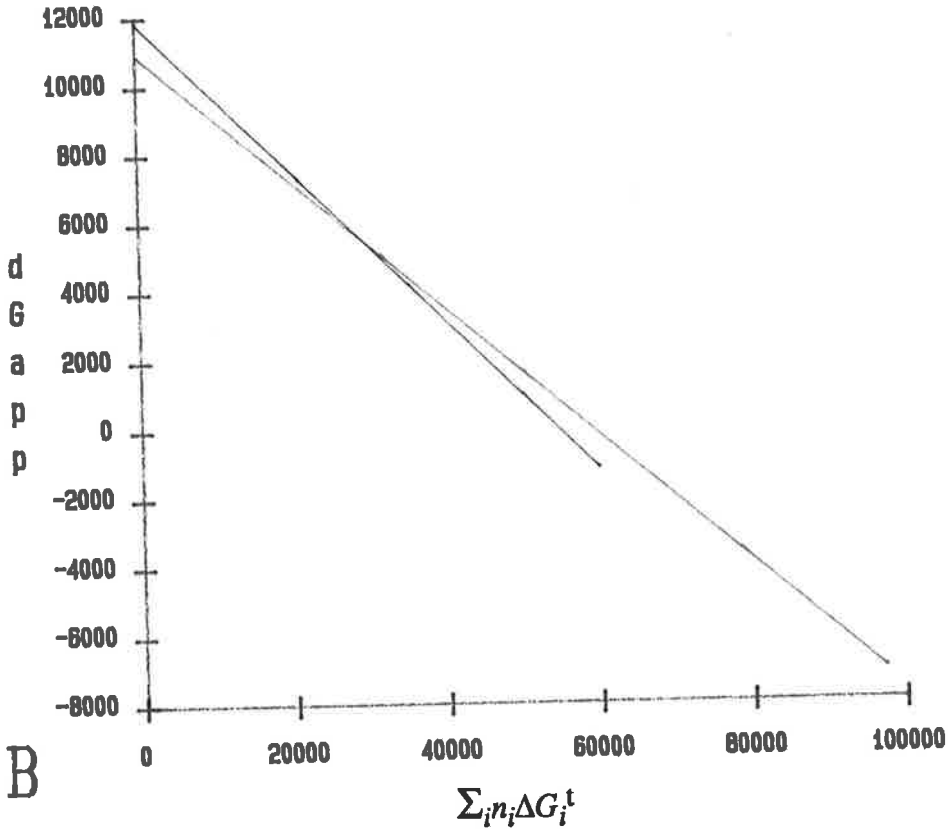
12000
10000
8000
6000
4000
2000
0
-2000
-4000
-6000
-8000
d G a p p
0 20000 40000 60000 80000 100000
$\Sigma_i n_i \Delta G_i^t$

B

ribonuclease and 1.68 for lysozyme (Greene and Pace, 1974). The magnitude of the m ratio has been correlated with the polarity of the unfolding unit, i.e., the unit which unfolds in pGH is less polar than that which unfolds in ribonuclease, but is less non-polar than that which unfolds in lysozyme. This is derived from the fact that GuHCl unfolds polar side chains more efficiently than non-polar ones.

Applying Tanford's denaturation model (Tanford, 1970) to the experimental ΔG_{app} data using Equation 8, above, higher values of $\Delta G(H_2O)$ are obtained for both urea and GuHCl denaturation. By using the free energy of transfer data of Nozaki and Tanford (1970), values for $\Delta G(H_2O)$ and $\Delta\alpha_{app}$ were obtained by plotting ΔG_{app} as a function of $\Sigma_i n_i \Delta G_i^t$ as shown in Figure 3b. The best fit to the experimental data gave $\Delta G(H_2O)$ values of 10.99 kcal/mol and 11.85 kcal/mol, and $\Delta\alpha_{app}$ values of 0.19 and 0.22 for the GuHCl and urea denaturation curves, respectively (Table III & Figure 3b). The Tanford model for determining $\Delta G(H_2O)$ of proteins consistently gives higher values than the linear extrapolation method. The value of $\Delta\alpha_{app}$ is chosen so that the dependence of ΔG_{app} on denaturant concentration calculated with Equation 8 equals the experimentally determined value, i.e., the m value in the linear extrapolation method. $\Delta\alpha_{app}$ is a measure of the apparent average difference in the degree of exposure of the side chains and peptide groups in the denatured and native conformations. Studies comparing the accessibility to solvent of various proteins in their native and denatured states, with model compounds have shown that unfolding from the native state to a completely denatured state (6M GuHCl) results in a $\Delta\alpha_{app}$ of 0.35 (Tanford, 1970). An α_{app} value of 1 indicates that the side-chain or peptide is as fully exposed to solvent as a similar group on a simple model compound of low molecular weight whereas a value of 0 indicates that the group is completely buried inside an ordered region and has no contact with the solvent at all. The presence and location of disulphide bonds in the protein structure restricts the accessibility of side-chains in the denatured state thus lowering the $\Delta\alpha_{app}$ value. The low $\Delta\alpha_{app}$ value for pGH suggests that the denatured state still retains a proportion of residues in a solvent-excluded configuration. Obviously, removing the disulphide bonds would

	$\Delta G(H_2O)^{\S}$	$\Delta\alpha_{app}$
GuHCl	11.85	0.22
urea	10.99	0.19

Table III. $\Delta G(H_2O)$ and $\Delta\alpha_{app}$ values of pGH_{wt} in GuHCl and urea calculated using Tanford's procedure (see text for explanation).
§units are in kcal/mol.

detected transition has a low *m* value (1.53 kcal/mol/M), and is suggestive of a biphasic transition: the initial loss of helix accompanies the tertiary structure disruption (4.2.7). Since the tertiary structure of pGH(M8) is more stable than that in wild-type pGH, it is expected that the CD-detected transition of pGH(M8) will have a higher *m* value than wild-type pGH. The three probes used to follow the denaturation of pGH(M8) are coincident within experimental error. This suggests that the denaturation of pGH(M8) closely approaches a two-state mechanism.

In comparison to wild-type pGH, the presence of the associated intermediate during the equilibrium denaturation of pGH(M8) is greatly diminished. Only trace amounts of the associated state were detected in size-exclusion chromatography experiments. The increase in molar ellipticity at 300nm, $[\theta]_{300}$, a convenient measure of the associated intermediate, was also significantly less in pGH(M8). These two measurements were conducted at protein concentrations of 45μM and 31μM, for wild-type pGH and pGH(M8), respectively. At higher protein concentrations (91μM), a maximum of 53% of the total protein present in solutions containing 3M GuHCl was in the form of the associated intermediate, as judged by the two-step precipitation assay. Second-derivative spectroscopy of pGH(M8), at a protein concentration of 10μM, detected a smooth unfolding transition indicative of the trp86 environment changing from non-polar to polar. In wild-type pGH, an asymmetric transition was observed with the trp86 environment being apparently more polar at intermediate concentrations of GuHCl, than in the unfolded state. This pattern of the denaturation transition was attributed to the population of a stable associated intermediate. From these results it is apparent that pGH(M8) does possess a monomeric equilibrium intermediate, but greater protein concentrations are required to stabilize it in a self-associated form. The dissociation constant for the associated intermediate of pGH(M8) is greater than 50μM.

The UV absorbance-detected denaturation transition of pGH(M8) resulted in a $\Delta G(H_2O)$ much higher than the wild-type pGH value (Chapter 5). This was due to the combined increase in the *m* value and the denaturation midpoint. Due to its increased

conformational stability, it was predicted that the folding/unfolding of pGH would more closely approach a two-state mechanism than wild-type pGH. The coincidence of the denaturation curves and the lack of significant amounts of the associated intermediate, both indicative of a two-state denturation mechanism, support this conclusion.

How could the insertion of a tryptophan residue in place of the wild-type methionine, in helix-3, have such an effect on the stability and folding mechanism of pGH? It has been shown that helix-3 is involved in the self-association process seen in bGH (Brems et al., 1986). Due to the sequence similarity, helix-3 of pGH is very likely to be involved in pGH self-association. Unlike the non-human GHs examined thus far, human growth hormone (hGH) does not form an associated intermediate, and is consistent with a two-state folding mechanism. A mutant bGH, referred to as 8H-bGH, containing the helix-3 sequence of hGH substituted for the wild-type sequence, was shown to result in a significant decrease in aggregation compared to wild-type bGH, when incubated under conditions favouring self-association (Lehrman et al., 1991). The results obtained with 8H-bGH are very similar to those obtained with pGH(M8). There was a reduction in the $[\theta]_{300}$ CD signal and reduced precipitation of the associated intermediate in the two-step assay. Aggregation was not completely abolished however, suggesting other partially unfolded sites are involved in the aggregation process. Lehrman et al. (1991) suggested that the diminished aggregation of 8H-bGH is due primarily to local structural changes in helix-3, rather than effects on overall protein conformation. Far-UV CD studies of peptide fragments of bGH and hGH containing helix-3, indicate that helix-3 of hGH has significantly less α-helical potential than the corresponding helix in bGH. Stabilization of helix-3 increases its resistance to denaturation at partially denaturing concentrations of GuHCl. This in turn increases the possibility of interactions between the exposed hydrophobic faces of helices in adjacent molecules, resulting in the observed self-association. Hydrophobic interactions are crucial in stabilizing the associated species as illustrated in the K112L mutation in bGH (Brems et al., 1988).

This mutation enhanced the hydrophobic effect without diminishing the α-helical potential of helix-3. How would a met→trp mutation affect helix-3 stability? From a number of hydrophobicity scales, methionine and tryptophan have similar hydrophobicities (Janin,1979; Wolfenden et al., 1981; Rose et al., 1985). The hydrophobic moment of the helix would not be affected by the mutation. In wild-type pGH, met124 is situated four residues from the C-cap. In a sample of 215 helices from 45 crystal structures, the C_4 position (being 4 residues from the C-cap) was the most common position for methionine residues in an α-helix (Richardson & Richardson, 1989). Tryptophan, however, is most prevalent in the N_4 position (4 residues from the N-cap). On these statistical considerations, helix-3 in pGH(M8) may be fractionally less stable than the corresponding helix in wild-type pGH. This would decrease the possibility of aggregation of partially denatured states. In this case, however, helix stabilization may not play a key role in the stability and folding effects observed.

Aromatic side chains primarily provide interactions between separate segments of secondary structure (Richardson & Richardson, 1989). The geometry is such that aromatics cannot pack well against their own local backbone in a helical conformation, but they are able to pack against the backbone or side-chains of a neighbouring helix. In wild-type pGH the side chain of met124 contributes to a hydrophobic pocket composed of several leucine side chains of helix-2 and helix-3. Insertion of the bulky tryptophan residue may have been sufficient to pry open this hydrophobic pocket between the two helices. The pGH(M8) native state λ_{max} of 345nm is indicative of a near-surface tryptophan (Burstein et al., 1973). Trp124 may have its planar indole ring packed against side chains of helix-2 but its polar >NH group in contact with the surrounding water. Tight packing of side chains in the interiors of proteins play a crucial role in stabilizing the native conformation. The deleterious effects of cavity creation in the cores of proteins when large residues are replaced by small ones has been well documented (Eriksson et al., 1992a; Shortle et al., 1990; Kellis et al., 1988). Lim et al. (1992) have recently characterized some

extreme volume mutants of the N-terminal domain of the λ repressor. These mutants involved changes in which the core volume was increased dramatically. Although destabilizing, the protein is able to accommodate these large changes in volume with the same overall fold. However, significant structural rearrangements decreased their biological activity and affinity towards antibodies. The mutation in pGH(M8) has caused some alteration to the surface of the protein. The binding affinity towards its receptor has decreased two-fold (Chapter 3, Table III). However, contrary to the λ repressor mutants, insertion of the bulky tryptophan in pGH(M8) has increased the stability of the protein.

From the experimental data, we know that the tertiary structure of pGH(M8) is more stable than the equivalent structure in wild-type pGH. Yet we also know that pGH(M8) acquires a more expanded state at lower GuHCl concentrations in the denaturation process (Figure 6b). These two findings appear to be contradictory. However, pGH (and pGH(M8)) contains only one tryptophan located in the hydrophobic core of the molecule and the UV signal at 290nm is due to this aromatic residue (we have already seen that trp124 does not contribute to any extinction loss upon protein unfolding). The UV absorbance-detected transition (at 290nm) in the case of growth hormones, is more likely to represent core disruption rather than gross tertiary structure disruption. Therefore it is more correct to say that the core of pGH(M8) is disrupted at higher concentrations of denaturant. The disruption of other side-chains, e.g., peripheral helix and loop side-chains, may result in an expanded state before the core itself is ruptured. The increased cooperativity of the disruption in the core (as seen by the high UV-detected *m* value) results in a sudden expansion of the molecule. This intermediate state is more expanded than the wild-type pGH intermediate state and higher protein concentrations are required to stabilize it as an associated form. From the size-exclusion chromatography experiments, the associated state also had a slightly more expanded form than that seen in wild-type pGH (Figure 5, 58Å vs 52Å). The pGH(M8) intermediate state is likely to be more transient than the wild-type equivalent. Concentrations of about 50μM are necessary before the

associated state can be stabilized significantly. Similar intermolecular interactions to those which occur in the formation of the wild-type pGH associated state must be involved, since the 298nm CD band is still present though the intensity is somewhat diminished. The met→trp mutation in pGH(M8) results in the apparent interference of the self-association reaction at low protein concentrations. It is not clear at present how this mutation causes this interference. Steric hindrance may be involved if intermolecular helix-helix contact is necessary to stabilize the associated state.

In summary, the single mutation in pGH(M8) has altered the stability and folding behaviour of pGH. The coincidence of the UV-, fluorescence- and hydrodynamic radius-detected equilibrium denaturation curves and the absence of significant amounts of associated forms suggest that pGH(M8) folding/unfolding is more closely approximated by a two-state mechanism than wild-type pGH.

CHAPTER 7

CONCLUDING REMARKS

CONCLUDING REMARKS

The experiments outlined in this thesis have shown that the equilibrium denaturation of pGH deviates from a simple two-state mechanism, but is consistent with the framework model of protein folding. Conformations intermediate to the folded and fully unfolded states are stable at equilibrium under partially denaturing conditions. These intermediate forms have the characteristics of *molten-globule* or *compact denatured states;* a compact structure with considerable helix content, yet possessing a tertiary structure similar to that of the fully unfolded state. Similar intermediates have been observed in the denaturation of bGH (Brems & Havel, 1989), a protein which shares 91% amino acid sequence identity with pGH. However, hGH, a protein which shares 68% amino acid sequence identity with pGH, has been shown to follow a two-state denaturation mechanism with no detectable intermediates (Brems et al., 1990).

It has been suggested previously that the relative stability of native hGH precludes the observation of folding intermediates (Brems et al., 1990). hGH has an apparent stability greater than that for bGH (Brems et al., 1985) and pGH (this thesis). However, the stabilities of these three proteins have been determined with the assumption that folding follows a two-state mechanism, which is clearly not the case in the latter two. Both pGH and bGH have lower apparent stabilities because they possess stable equilibrium intermediates which tend to lower the slope (*m* value) of the denaturation transition, i.e., decrease the rate of change of free energy with respect to the denaturant concentration; this in turn results in their relatively lower apparent stabilities. The intermediate or compact denatured state of pGH and bGH is the result of the cooperative breakdown of the native structure upon denaturation. What forces contribute to the stability of the compact denatured states of pGH and bGH and what features of hGH prevent their formation? Proteins with a higher non-polar content are expected to preferentially form a compact denatured state over a more expanded fully unfolded state (Alonso et al., 1991). Using a consensus hydrophobicity scale (Horne, 1988), the relative hydrophobicities of the GHs are

ranked in order: bGH > pGH > hGH. However, the differences in the hydrophobicities are very small and can be accounted for by the replacement of one or two polar residues with non-polar residues. Hydrophobicity is an important factor in determining the form of the denatured state, but in this case, other forces must be involved in the stabilization of the compact denatured states of the pGH and bGH. It was suggested in Chapter 4 that tight packing of the connecting loops between the helices may aid in stabilizing the native state of hGH. These interactions would involve the combined stabilizing contributions of the hydrophobic effect, hydrogen bonding, van der Waals interactions and to a lesser extent electrostatic interactions.

Single amino acid changes in the sequence of pGH have been shown to alter the *m* value substantially, resulting in either higher or lower apparent stabilities. Similar changes in *m* have been observed in mutants of other proteins (Shortle & Meeker, 1986; Lim et al., 1992). Mutants of pGH which result in an increase in the *m* value are more likely to behave like 'classical two-state' proteins. The M124W mutation of pGH(M8) increased the *m* value significantly; monitoring the equilibrium denaturation of pGH(M8) by spectroscopic and hydrodynamic probes resulted in coincident denaturation transitions, suggestive of a two-state mechanism. In pGH(M10), the deletion of 8 residues near the C-terminus, had the opposite effect: relative to wild-type pGH, the *m* value was lower [the magnitude of the change was the same as for pGH(M8)] resulting in a lower apparent stability. It was also suggested that the solvent-accessible surface area of the denatured state is proportional to *m* (Schellman, 1978); mutants with higher *m* values denature to more expanded states. This was observed in size-exclusion chromatography of pGH(M8). It appears that these changes in stability may reflect changes in the free energy of the denatured state rather than the native state. Finally, mutants which involved pGH to hGH alterations in the sequence [except for pGH(M13)] generally resulted in increased *m* values.

Work currently in progress is aimed at several major areas: (*i*) what feature of the hGH structure is responsible for its greater apparent stability? This involves the

use of site-directed mutagenesis of pGH to construct mutants with regions of hGH sequence e.g., mutagenesis of the short omega-loop sequence between helix-2 and -3, which forms a short helix in hGH (de Vos et al., 1992). This involves three pGH sequence changes: T98A, F103Y and T105A. The increased rigidity of the connection between the two helices may stabilize the tertiary structure. (*ii*) examine the equilibrium denaturation of pGH(M10) using various spectroscopic and hydrodynamic probes. Due to its inherent instability, this mutant may provide an opportunity to examine the denatured state under mildly denaturing conditions. (*iii*) examine the kinetics of folding and unfolding of wild-type pGH and mutants. Kinetic studies can reveal whether the changes in stability measured in equilibrium experiments most likely result from changes in the free energy of the native or of the unfolded states. In addition, kinetic studies are capable of demonstrating the existence of transient intermediates or multiple unfolded forms that cannot be detected in equilibrium studies. (*iv*) continue investigating the effects of mutations on the stability of pGH by means of systematically replacing residues of a certain type, e.g., non-polar, with residues of another type. For example, what effects would decreasing the hydrophobicity (to the level of hGH) of pGH have on its folding characteristics?

The growth hormones provide a useful system for examining the effects of alterations in the amino acid sequence on protein folding and stability. The intrinsic marginal stability of the non-human GHs in comparison to hGH exemplifies the fact that changes in sequence can have large effects on folding and stability. Perhaps the subtle differences in the sequences of the non-human GHs may provide some clues as to which residues are critical in determining the folding and stability of the GH family of proteins.

REFERENCES

Abdel-Meguid, S. S., Shieh, H.-S., Smith, W. W., Dayringer, H. E., Violand, B. N., & Bentle, L. A. (1987) *Proc. Natl. Acad. Sci. U.S.A. 84*, 6434-6437.

Adler, A. J., Greenfield, N. J., & Fasman, G. D. (1973) *Methods Enzymol. 27*, 675.

Alber, T. (1989) in *Prediction of Protein Structure and the Principles of Protein Conformation* (Fasman, G. D., Ed.) pp. 161-192, Plenum Press, New York.

Alonso, D. O. V., Dill, K. A., & Stitger, D. (1991) *Biopolymers 31*, 1631-1649.

Akke, M., & Forsén, S. (1990) *Proteins: Struct., Funct., Genet. 8*, 23-29.

Anfinsen, C. B. (1973) *Science 181*, 223.

Anfinsen, C. B., & Scheraga, H. A. (1975) *Adv. Protein Chem. 29*, 205-300.

Bailey, J. E., & Ollis, D. F. (1986) *Biochemical Engineering Fundamentals*, (2nd ed.) pp.403-404, McGraw-Hill, New York.

Baker, E. N., & Hubbard, R. E. (1984) *Prog. Biophys. Mol. Biol. 44*, 97-179.

Baldwin, R. L. (1986) *Proc. Natl. Acad. Sci. U.S.A. 83*, 8069.

Baldwin, R. L., & Eisenberg, D. (1987) in *Protein Engineering* (Oxender, D. L., & Fox, C. F., Eds.) pp. 127-148, Alan R. Liss, Inc., New York.

Baldwin, J., & Chothia, C. (1979) *J. Mol. Biol. 129*, 175-220.

Balestrieri, C., Colonna, G., Giovane, A., Irace, G., & Servillo, L. (1978) *Eur. J. Biochem. 90*, 433-440.

Barlow, D. J., & Thornton, J. M. (1983) *J. Mol. Biol. 168*, 867-885.

Barnard, R., Rowlinson, S. W., & Waters, M. J. (1989) *J. Theor. Biol. 140*, 355-367.

Baum, J., Dobson, C. M., Evans, P. A., & Hanley, C. (1989) *Biochemistry 28*, 7-13.

Bazan, J. F., (1990) *Immunol. Today 11*, 350-355.

Bello, J. (1978) *Int. J. Peptide Res. 12*, 38-41.

Bennett, W. F., Chloupek, R., Harris, R., Canova-Davis, E., Keck. R., Chakel, J., Hancock, W. S., Gellerfors, P., & Pavlu, B. (1987) in *Advances in Growth Hormone and Growth Factor Research*, (Müller, E. E., Cocchi, D., & Locatelli, V., eds.), pp. 29-50, Pythagora Press, Milan.

Bentle, L. A., Mitchell, J. W., & Storrs, S. B. (1987) *U.S. Patent 4652630.*

Bewley, T. A. (1982) *Anal. Biochem. 123*, 55-65.

Bewley, T. A., Brovetto-Cruz, J., & Li, C. H. (1969) *Biochemistry 8*, 4701-4708.

Bewley, T. A., & Li, C. H. (1970) *Arch. Biochem. Biophys. 138*,338-346.

Bewley, T. A., & Yang, J.-T. (1980) in *Hormonal Proteins and Peptides*, (Li, C. H., ed.), Vol. IX, pp. 175-238.

Bewley, T. A., & Li, C. H. (1978) *Biochemistry 17*, 3315-3320.

Bewley, T. A., & Li, C. H. (1984) *Arch. Biochem. Biophys. 233*, 219-227.

Bewley, T. A., & Li, C. H. (1987) *Int. J. Peptide Protein Res. 29*, 589-595.

Bewley, T. A., & Papkoff, H. (1987) *Int. J. Peptide Protein Res. 29*, 568-573.

Bierzynski, A., & Baldwin, R. L. (1982) *J. Mol. Biol. 162*, 173-186.

Bismuto, E., & Irace, G. (1988) *Int. J. Peptide Protein Res. 32*, 312-325.

Blagdon, D. E., & Goodman, M. (1975) *Biopolymers 14*, 241-245.

Brand, L., & Witholt, B. (1967) *Methods Enzymol. 11*, 776.

Brandts, J. F. (1964a) *J. Am. Chem. Soc. 86*, 4291.

Brandts, J. F. (1964b) *J. Am. Chem. Soc. 86*, 4302.

Brandts, J. F., Halvorson, H. R., & Brennan, M. (1975) *Biochemistry 14*, 4953-4963.

Brazhnikov, E. V., Chirgadze, Y. N., Dolgikh, D. A., & Ptitsyn, O. B. (1985) *Biopolymers 24*, 1899-1907.

Brems, D. N. (1988) *Biochemistry 27*, 4541-4546.

Brems, D. N., Plaisted, S. M., Havel, H. A., Kauffman, E. W., Stodola, J. D., Eaton, L. C., & White, R. D. (1985) *Biochemistry 24*, 7662-7668.

Brems, D. N., Plaisted, S. M., Kauffman, E. W., & Havel, H. A. (1986) *Biochemistry 25*, 6539-6543.

Brems, D. N., Plaisted, S. M., Dougherty, J. J., Jr., & Holzman, T. F. (1987a) *J. Biol. Chem. 262*, 2590-2596.

Brems, D. N., Plaisted, S. M., Kauffman, E. W., Lund, M., & Lehrman, S. R. (1987b) *Biochemistry 26*, 7774-7778.

Brems, D. N., & Havel. H. A. (1989) *Proteins: Struct., Funct.,Genet. 5*, 93-95.

Brems, D. N., Brown, P. L., & Becker, G. W. (1990) *J. Biol. Chem. 265*, 5504-5511.

Brown, L. R., DeMarco, A., Richarz, R., Wagner, G., & Wüthrich,K. (1978) *Eur. J. Biochem. 88*, 87-95.

Buckwalter, B. L., Cady, S. M., Shieh, H.-M., Chaudhuri, A. K., & Johnson, D. F. (1992) *J. Agric. Food. Chem. 40*, 356-362.

Burger, H. G., Edelhoch, H., & Condliffe, P. G. (1966) *J. Biol. Chem. 241*,449-457.

Burstein, E. A., Vedenkina, N. S., & Ivkova, M. N. (1973) *Photochem. Photobiol. 18*, 263-279.

Carlacci, L., Chou, K.-C., & Maggiora, G. M. (1991) *Biochemistry 30*, 4389-4398.

Chaffotte, A. F., Cadieux, C., Guillou, Y., & Goldberg, M. E. (1992) *Biochemistry 31*, 4303-4308.

Chan, H. S., & Dill, K. A. (1990) *J. Chem. Phys. 92*, 3118.

Chan, H. S., & Dill, K. A. (1991) *J. Chem. Phys. 95*, 3775-3787.

Chen, B., Baase, W. A., & Schellman, J. A. (1989) *Biochemistry 28*, 691-699.

Chou, P. Y., & Fasman, G. D. (1974) *Biochemistry 13*, 211-221.

Cohen, F. E., & Kuntz, I. D. (1987) *Proteins: Struct., Funct., Genet. 5*, 162-166.

Cohn, E. J., & Edsall, J. T. (1943) in *Proteins, Amino Acids and Peptides as Ions and Dipolar Ions*, Reinhold, New York.

Colombo, M. F., & Rau, D. C. (1992) *Biophys. J. 61*, A1980.

Corbett, R. T., & Roche, R. S. (1984) *Biochemistry 23*, 1888-1894.

Creighton, T. E. (1983) in *Proteins*, W. H. Freeman, New York.

Creighton, T. E. (1990) *Biochem. J. 270*, 1-16.

Cunningham, B. C., Jhurani, P., Ng, P., & Wells, J. A. (1989) *Science 243*, 1330-1336.

Cunningham, B. C., Ultsch, M., de Vos, A. M., Mulkerrin, M. G., Clauser, K. R., & Wells, J. A. (1991) *Science 254*, 821-825.

Dao-pin, S., Liao, D.-I., & Remington, S. J. (1989) *Proc. Natl. Acad. Sci. U.S.A. 86*, 5361-5365

Dao-pin, S., Anderson, D. E., Baase, W. A., Dahlquist, F. W., & Matthews, B. W. (1991) *Biochemistry 30*, 11521-11529.

Dayhoff, M. O. (1976) *Atlas of Protein Sequence and Structure*, Vol. 5 [suppl 2]:120, National Biomedical Research Foundation, Washington DC.

DeNoto, F. M., Moore, D. D., & Goodman, H. M. (1981) *Nucleic Acids Res. 9*, 3719-3730.

de Vos, A. M., Ultsch, M., & Kossiakoff, A. A. (1992) *Science 255*, 306-312.

Dill, K. A. (1985) *Biochemistry 24*, 1501-1509.

Dill, K. A. (1987) in *Protein Engineering* (Oxender, D. L., & Fox, F. C., Eds.) pp. 187-192, Alan R. Liss, Inc., New York.

Dill, K. A. (1990) *Biochemistry 29*, 7133-7155.

Dill, K. A., & Shortle, D. (1991) *Annu. Rev. Biochem. 60*, 795-825.

Dobson, C. M., Evans, P. A., & Williamson, K. L. (1984) *FEBS Lett. 168*, 331-334.

Doig, A. J., & Williams, D. H. (1991) *J. Mol. Biol. 217*, 389-398.

Donovan, J. W. (1969) in *Physical Principles and Techniques of Protein Chemistry*, (Leach, S. J., ed.), Part A, pp. 101-170, Academic Press, New York.

Edelhoch, H., & Burger, H. G. (1966) *J. Biol. Chem. 241*, 458-463.

Eisenberg, D., Weiss, R. M., & Terwilliger, T. C. (1984) *Proc. Natl. Acad. Sci. U.S.A. 81*, 140-144.

Ellis, R. J., & van der Vies, S. M. (1991) *Annu. Rev. Biochem. 60*, 321-347.

Eriksson, A. E., Baase, W. A., Zhang, X.-J., Heinz, D. W., Blaber, M., Baldwin, E. P., & Matthews, B. W. (1992a) *Science 255*, 178-183.

Eriksson, A. E., Baase, W. A., Wozniak, J. A., & Matthews, B. W. (1992b) *Nature 355*, 371-373.

Farmer, S. W., Papkoff, H., Hayashida, T., Bewley, T. A., Bern, H. A., & Li, C. H. (1976) *Gen. Comp. Endocrinol. 30*, 91-100.

Fauchère, J.-L., & Pliska, V. (1983) *Eur. J. Med. Chem. Chim. Ther. 18*, 369-375.

Fersht, A. R. (1972) *J. Mol. Biol. 64*, 497-509.

Fersht, A. R., Shi, J. P., Knill-Jones, J., Lowe, D. M., Wilkinson, A. J., Blow, D. M., Brick, P., Carter, P., Waye, M. M. Y., & Winter, G. (1985) *Nature 314*, 235-238.

Fischer, G., & Schmid, F. X. (1990) *Biochemisty 29*, 2205-2212.

Flynn, G. C., Pohl, J., Flocco, M. T., & Rothman, J. E. (1991) *Nature 353*, 726-730.

Fridman, M., Aguilar, M. I., & Hearn, M. T. W. (1990) *J. Chromatogr. 512*, 57-75.

Garrett, D. S., Powers, R., March, C. J., Frieden, E. A., Clore, G. M., & Gronenborn, A. M. (1992) *Biochemistry 31*, 4347-4353.

Garvey, E. P., Swank, J., & Matthews, C. R. (1989) *Proteins: Struct., Funct., Genet. 6*, 259-266.

Gill, S. C., & von Hippel, P. H. (1989) *Anal. Biochem. 182*, 319-326.

Gilmanshin, R. I., & Ptitsyn, O. B. (1987) *FEBS Lett. 223*, 327-329.

Gilson, M. K., Rashin, A., Fine, R., & Honig, B. (1985) *J. Mol. Biol. 184*, 503-516.

Goldberg, M. E. (1985) *Trends Biochem. Sci. 10*, 388-391.

Gooley, P. R., Plaisted, S. M., Brems, D. N., & MacKenzie, N. E. (1988) *Biochemistry 27*, 802-809.

Goto, Y., & Fink, A. L. (1989) *Biochemistry 28*, 945-952.

Goto, Y., Calciano, L. J., & Fink, A. L. (1990) *Proc. Natl. Acad. Sci. U.S.A. 87*, 573-577.

Graf, L., & Li, C. H. (1974) *Biochem. Biophys. Res. Commun. 56*, 168-176.

Greene, R. F., Jr., & Pace, C. N. (1974) *J. Biol. Chem. 249*,5388-5393.

Haas, E., McWherter, C. A., & Scheraga, H. A. (1988) *Biopolymers 27*, 1-21.

Hartley, R. W. (1968) *Biochemistry 7*, 2401.

Havel, H. A., Kauffman, E. W., Plaisted, S. M., & Brems, D. N. (1986) *Biochemistry 25*, 6533-6538.

Havel, H. A., Kauffman, E. W., & Elzinga, P. A. (1988) *Biochim. Biophys. Acta 955*, 154-163.

Haynie, D. T., & Freire, E. (1992) *Biophys. J. 61*, A2753.

Hecht, M. H., Richardson, J. S., Richardson, D. C., & Ogden, R. C. (1990) *Science 249*, 884-891.

Herning, T., Yutani, K., Taniyama, Y., & Kikuchi, M. (1991) *Biochemistry 30*, 9882-9891.

Herskovits, T. T. (1967) *Methods Enzymol. 11*,748.

Hol, W. G. J. (1985) *Prog. Biophys. Molec. Biol. 45*, 149-195.

Holladay, L. A., Hammonds, R. G., & Puett, D. (1974) *Biochemistry 13*, 1653-1661.

Holzman, T. F., Brems, D. N., & Doughterty, J. J., Jr. (1986) *Biochemistry 25*, 6907-6917.

Holzman, T. F., Dougherty, J. J., Jr., Brems, D. N., & MacKenzie, N. E. (1990) *Biochemistry 29*, 1255-1261.

Honeycutt, J .D., & Thirumalai, D. (1992) *Biopolymers 32*, 695-709.

Horiike, K., Tojo, H., Yamano, T., & Nozaki, M. (1983) *J. Biochem. 93*, 99-106.

Horne, D. S. (1988) *Biopolymers 27*, 451-477.

Horovitz, A., Serrano, L., Avron, A., Bycroft, M., & Fersht, A. R. (1990) *J. Mol. Biol. 216*, 1031-1044.

Hu, C.-Q., Sturtevant, J. M., Thomson, J. A., Erickson, R. E., & Pace, C. N. (1992) *Biochemistry 31*, 4876-4882.

Hulmes, J. D., Miedel, M. C., Li, C. H., & Pan, Y.-C. E. (1989) *Int. J. Peptide Protein Res. 33*, 368-372.

Isaksson, O. G. P., Eden, S., & Jansson, J. O. (1985) *Annu. Rev. Physiol. 47*, 483-499.

Jacobson, R. H., Matsumura, M., Faber, H. R., & Matthews, B.W. (1992) *Protein Sci. 1*, 46-57.

Jaenicke, R. (1987) *Prog. Biophys. Molec. Biol. 49*, 117-237.

Jaffé, H.H., & Orchin, M. (1962) *Theory and Applications of Ultraviolet Spectroscopy*, John Wiley & Sons, Inc., New York.

Janin, J. (1979) *Nature 277*, 491-492.

Jones, B. E., & Matthews, C. R. (1992) *Biophys. J. 61*, A2751.

Kane, J. F., & Hartley, D. L. (1988) *Trends in Biotech. 6*, 95-101.

Karplus, M., & Weaver, D. L. (1976) *Nature 260*, 404-406.

Kauffman, E. W., Thamann, T. J., & Havel, H. A. (1989) *J. Am. Chem. Soc. 111*, 5449-5456.

Kauzmann, W. (1959) *Adv. Protein Chem. 14*, 1-63.

Kellis, J. T., Jr., Nyberg, K., Sali, D., & Fersht, A. R. (1988) *Nature 333*, 784-786.

Kiefhaber, T., Quaas, R., Hahn, U., & Schmid, F. X. (1990) *Biochemistry 29*, 3061-3070.

Kim, P. S., & Baldwin, R. L. (1982) *Annu. Rev. Biochem. 51*,459-489.

Kim, P. S., & Baldwin, R. L. (1990) *Annu. Rev. Biochem. 59*, 631-660.

Knibb, W., Robins, A., Crocker, L., Rizzon, J., Heyward, A., & Wells, J. (1991) *DNA Sequence 2*, 121-123.

Kossiakoff, A. A. (1983) *Annu. Rev. Biophys. Bioeng. 12*, 159-182.

Kuroki, R., Taniyama, Y., Seko, C., Nakamura, H., Kikuchi, M., & Ikehara, M. (1989) *Proc. Natl. Acad. Sci. U.S.A. 86*, 6903-6907.

Kuwajima, K., Nitta, K., Yoneyama, M., & Sugai, S. (1976) *J. Mol. Biol. 106*, 359-373.

Kuwajima, K. (1989) *Proteins: Struct., Funct., Genet. 6*, 87-103.

Kuwajima, K., Mitani, M., & Sugai, S. (1989) *J. Mol. Biol. 206*, 547-561.

Kuwajima, K., Garvey, E. P., Finn, B. E., Matthews, C. R., & Sugai, S. (1991) *Biochemistry 30*, 7693-7703.

Kyte, J., & Doolittle, R. F. (1982) *J. Mol. Biol. 157*, 105-132.

Laemmli, U. K. (1970) *Nature 227*, 680-685.

Lackowicz, J. R. (1983) *Principles of Fluorescence Spectroscopy*, Plenum Press.

Langer, T., Lu, C., Echols, H., Flanagan, J., Hayer, M. K., & Hartl, F. U. (1992) *Nature 356*, 683-689.

Lau, K. F., & Dill, K. A. (1989) *Macromolecules 22*, 3986-3997.

Lau, K. F., & Dill, K. A. (1990) *Proc. Natl. Acad. Sci. U.S.A. 87*, 638-642.

Lee, B., & Richards, F. M. (1971) *J. Mol. Biol. 55*, 379-400.

Lehrman, S. R., Tuls, J. L., Havel, H. A., Haskell, R. J., Putnam, S. D., & Tomich, C.-S. C. (1991) *Biochemistry 30*, 5777-5784.

León, D. A., Dostmann, W. R. G., & Taylor, S. S. (1991) *Biochemistry 30*, 3035-3040.

Li, C. H., & Evans, H. M. (1944) *Science*, 183-184.

Li, C. H., Dixon, J. S., Gordon, D., & Knorr, J. (1972) *Int. J. Peptide Protein Res. 4*, 151-153.

Li, C. H., Chung, D., Lahm, H.-W., & Stein, S. (1986) *Arch. Biochem. Biophys. 245*, 287-291.

Li, C. H., Bewley, T. A., Chung, D., & Oosthuizen, M. M. J. (1987) *Int. J. Peptide Protein Res. 29*, 62-67.

Lim, W. A., & Sauer, R. T. (1989) *Nature 339*, 31-36.

Lim, W. A., Farruggio, D. C., & Sauer, R. T. (1992) *Biochemistry 31*, 4324-4333.

Lu, J., & Dahlquist, F. W. (1992) *Biochemistry 31*, 4749-4756.

Lumry, R., Biltonen, R., & Brandts, J. F. (1966) *Biopolymers 4*, 917-944.

Lyu, P. C., Gans, P. J., & Kallenbach, N. R. (1992) *J. Mol. Biol. 223*, 343-350.

MacKenzie, N. E., Plaisted, S. M., & Brems, D. N. (1989) *Biochim. Biophys. Acta 994*, 166-171.

Mao, B. (1990) *Biopolymers 30*, 645-647.

Markley, J. L. (1975) *Acc. Chem. Res. 8*, 70-80.

Marston, F. A. O., Lowe, P. A., Doel, M. T., Schoemaker, J. M., White, S., & Angal, S. (1984) *Bio/Technology 2*, 800-804.

Matouschek, A., Kellis, J. T., Jr., Serrano, L., & Fersht, A. R., (1989) *Nature 340*, 122-126.

Matthews, B. W., Nicholson, H., & Becktel, W. J. (1987) *Proc. Natl. Acad. Sci. U.S.A. 84*, 6663-6667.

Matsumara, M., Becktel, W. J., & Matthews, B. W. (1988)*Nature 333*, 406.

Matsumara, M., & Matthews, B. W. (1989) *Science 243*, 792-794.

Maxfield, F. R., & Scheraga, H. A. (1975) *Macromolecules 8*, 491-493.

McNutt, M., Mullins, L., Raushel, F. M., & Pace, C. N. (1990) *Biochemistry 29*, 7572-7576.

Middelberg, A. P. J., Bogle, I. D. L, & Snoswell, M.A. (1990) *Biotechnol. Prog. 6*, 255-261.

Miranker, A., Radford, S. E., Karplus, M., & Dobson, C. M. (1991) *Nature 349*,633-636.

Mirsky, A. E., & Pauling, L. (1936) *Proc. Natl. Acad. Sci. U.S.A. 22*, 439.

Mitchinson, C., & Wells, J. A. (1989) *Biochemistry 28*, 4807-4815.

Montelione, G. T., & Scheraga, H. A. (1989) *Acc. Chem. Res. 22*, 70-76.

Muller, N. (1990) *Acc. Chem. Res. 23*, 23.

Mulkerrin, M. G., McDowell, R., Jones, A. J. S., & Bewley, T. A. (1992) *Biophys. J. 61*, A2401.

Mulqueen, P. M., & Kronman, M. J. (1982) *Arch. Biochem. Biophys. 215*, 28-39.

Nemethy, G., & Scheraga, H. A. (1962) *J. Chem. Phys. 36*, 3401.

Niall, H. D. (1971) *Nature New Biol. 230*, 90-91.

Nicoli, D. F., & Benedek, G. B. (1976) *Biopolymers 15*, 2421-2437.

Nicoll, C. S., Mayer, G. L., & Russell, S. M. (1986) *Endocrine Rev. 7*, 169-203.

Nozaki, Y., & Tanford, C. (1963) *J. Biol. Chem. 238*, 4074.

Nozaki, Y., & Tanford, C. (1970) *J. Biol. Chem. 245*, 1648.

Nozaki, Y., & Tanford, C. (1971) *J. Biol. Chem. 246*, 2211.

Ohgushi, M., & Wada, A. (1983) *FEBS Lett. 164*, 21-24.

Ohlendorf, D. H., Finzel, B. C., Weber, P.C., & Salemme, F. R. (1987) in *Protein Engineering* (Oxender, D. L., & Fox, C. F., Eds.) pp 165-173, Alan R. Liss, Inc., New York.

Pace, C. N. (1975) *Crit. Rev. Biochem. 3*, 1-43.

Pace, C. N. (1986) *Methods Enzymol. 131*, 266-280.

Pace, C. N., Grimsley, G. R., Thomson, J. A., & Barnett, B. J. (1988) *J. Biol. Chem. 263*, 11820-11825.

Pace, C. N., Shirley, B. A., & Thomson, J. A. (1989) in *Protein Structure: A practical approach* (Creighton, T. E., Ed.) pp 311-330, IRL Press, Oxford.

Pace, C. N., Laurents, D. V., & Thomson, J. A. (1990) *Biochemistry 29*, 2564-2572.

Pace, C. N., Laurents, D. V., & Erickson, R. E. (1992) *Biochemistry 31*, 2728-2734.

Page, G. S., Smith, S., & Goodman, H. M. (1981) *Nucleic Acids Res. 9*,2087-2104.

Perry, L. J., & Wetzel, R. (1984) *Science 226*, 555-557.

Privalov, P. L. (1979) *Adv. Protein Chem. 33*, 167.

Privalov, P. L., & Gill, S. J. (1988) *Adv. Protein Chem. 39*,191-234.

Ptitsyn, O. (1987) *J. Protein Chem. 6*, 273-293.

Puett, D. (1972) *Biochemistry 11*, 1980-1990.

Ragone, R., Colonna, G., Balestrieri, C., Servillo, L., & Irace, G. (1984) *Biochemistry 23*, 1871-1875.

Rashin, A., & Honig, B. (1984) *J. Mol. Biol. 173*, 515-521.

Richards, F. M. (1974) *J. Mol. Biol. 82*, 1-14.

Richards, F. M. (1977) *Annu. Rev. Biophys. Bioeng. 6*, 151-176.

Richardson, J. S., & Richardson, D. C. (1989) in *Prediction of Protein Structure and The Principles of Protein Conformation* (Fasman, G. D., Ed.) pp. 1-98, Plenum Press, New York.

Robson, B., & Pain, R. H. (1973) in *Conformation of Biological Molecules Polymers, 5th Jerusalem Symp.* (Bergmann, E. D., & Pullman, B., eds.), pp.161-172, Academic Press, New York.

Roder, H., Elöve, G. A., & Englander, S. W. (1988) *Nature 335*,700-704.

Roongta, V., Powers, R., Jones, C., Beakage, M. J., Shields, J. E., & Gorenstein, D. G. (1989) *Biochemistry 28*, 1048-1054.

Rose, G. D., Geselowitz, A. R., Lesser, G. J., Lee, R. H., & Zehfus, M. H. (1985) *Science 229*, 834-838.

Rowlinson, S. W., Barnard, R., Snoswell, M., Bastiras, S., Robins, A. R., Wells, J. R. E., & Waters, M. J. (1989) *Proc. Endo. Soc. (Australia)*, 32.

Rowlinson, S. W., Barnard, R., Bastiras, S., Robins, A. J., Senn, C., Wells, J. R. E., & Waters, M. (1992) *Protein Engineering*, (submitted).

Saito, Y., & Wada, A. (1983) *Biopolymers 22*, 2105-2122.

Salacinski, P. R. P., McLean, C., Sykes, J. E. C., Clement-Jones, V. V., & Lowry, P. J. (1981) *Anal. Biochem. 117*, 136-146.

Sancho, J., Neira, J. L., & Fersht, A. R. (1992) *J. Mol. Biol. 224*, 749-758.

Sandberg, W. S., & Terwilliger, T. C. (1991) *Proc. Natl. Acad. Sci. U.S.A. 88*, 1706-1710

Santoro, M. M., & Bolen, D. W. (1988) *Biochemistry 27*, 8063-8068.

Santoro, M. M., & Bolen, D. W. (1992) *Biochemistry 31*, 4901-4907.

Savitzky, A., & Golay, M. J. E. (1964) *Anal. Chem. 8*, 1627-1639.

Scatchard, G. (1949) *Ann. N. Y. Acad. Sci. 51*, 660-672.

Schein, C. H. (1989) *Bio/Technology 7*, 1141-1149.

Scheiner, S., Redfern, P., & Hillenbrand, E. A. (1986) *Int. J. Quant. Chem. 29*, 817.

Schellman, J. A. (1978) *Biopolymers 17*, 1305-1322.

Schmid, F. X. (1989) in *Protein Structure: A Practical Approach* (Creighton, T. E., Ed.), pp. 251-285, IRL Press, Oxford.

Schmid, F. X., Grafl, R., Wrba, A., & Beintema, J. J. (1986) *Proc. Natl. Acad. Sci. U.S.A. 83*, 872-876.

Secchi, C., Biondi, P. A., Negri, A., Borroni, R., & Ronchi, S. (1986) *Int. J. Peptide Protein Res. 28*, 298-306.

Seeburg, P. H., Sias, S., Adelman, J., de Boer, H. A., Hayflick, J., Jhurani, P., Goeddel, D. V., & Heyneker, H. L. (1983) *DNA 2*, 37-45.

Seely, J. E., & Hollis, J. K. (1986) *Fed. Proc., Fed. Am. Soc. Exp. Biol. 45*, 1544.

Segawa, S., & Sugihara, M. (1984a) *Biopolymers 23*, 2473-2488.

Segawa, S., & Sugihara, M. (1984b) *Biopolymers 23*, 2489-2498.

Serrano, L., Kellis, J. T., Jr., Cann, P., Matouschek, A., & Fersht, A. R. (1992a) *J. Mol. Biol. 224*, 783-804.

Serrano, L., Matouschek, A., & Fersht, A. R. (1992b) *J. Mol. Biol. 224*, 847-859.

Serrano, L., Matouschek, A., & Fersht, A. R. (1992c) *J. Mol. Biol. 224*, 805-818.

Sharp, K. A., Nicholls, A., Friedman, R., & Honig, B. (1991) *Biochemistry 30*, 9686-9697

Shirley, B. A., Stanssens, P., Hahn, U., & Pace, C. N. (1992) *Biochemistry 31*, 725-732.

Shoemaker, K. R., Fairman, R., Kim, P. S., York, E. J., Stewart, J. M., & Baldwin, R. L. (1987) *Cold Spring Harbour Symp. Quant. Biol. LII*, 391-398.

Shortle, D. (1989) *J. Biol. Chem. 264*, 5315-5318.

Shortle, D., & Meeker, A. K. (1986) *Proteins: Struct., Funct., Genet. 1*, 81-89.

Shortle, D., & Meeker, A. K. (1989) *Biochemistry 28*, 936-944.

Shortle, D., Stites, W. E., & Meeker, A. K. (1990) *Biochemistry 29*, 8033-8041.

Shortle, D., Chan, H. S., & Dill, K. A. (1992) *Protein Sci. 1*, 201-215.

Sneddon, S. F., & Tobias, D. J. (1992) *Biochemistry 31*, 2842-2846.

Souza, L. M., Boone, T. C., Murdock, D., Langley, K., Wypych, J., Fenton, D., Johnson, S., Lai, P. H., & Everett, R. (1984) *J. Exp. Zool. 232*, 465-473.

Sternberg, M. J. E., Hayes, R. F. F., Russell, A. J., Thomas, P. G., & Fersht, A. R. (1987) *Nature 330*, 86-88.

Storrs, S. B., & Przybycien, T. M. (1991) in *Protein Folding*, (Georgiou, G., & De Bernardez-Clark, E., eds.) pp. 197-205, ACS Symposium Series Vol. 470, Washington, DC.

Strambini, G., & Gonnelli, M. (1986) *Biochemistry 25*, 2471-2476.

Strickland, E. H. (1974) *C.R.C. Crit. Rev. Biochem. 2*, 113-175.

Strickland, E. H., Kay, E., & Shannon, L. M. (1970) *J. Biol. Chem. 245*, 1233.

Strickland, E. H., Billups, C., & Kay, E. (1972) *Biochemistry 11*, 3657-3662.

Sugimoto, S., Yamaguchi, K., & Yokoo, Y. (1991) *J. Chromatogr. 547*, 131-144.

Tanford, C. (1961) in *Physical Chemistry of Macromolecules*, Chapter 7, Wiley, New York.

Tanford, C. (1962) *J. Phys. Chem. 84*, 4240.

Tanford, C. (1964) *J. Am. Chem. Soc. 86*, 2050-2059.

Tanford, C. (1968) *Adv. Protein Chem. 23*, 121.

Tanford, C. (1970) *Adv. Protein Chem. 24*, 1.

Teale, F. W. J. (1960) *Biochem. J. 76*, 381-388.

Thornton, J. M. (1981) *J. Mol. Biol. 151*, 261-287.

Tsushima, T., & Friesen, H. G. (1973) *J. Clin. Endocrinol. Metab. 37*, 334-337.

Villafranca, J. E., Howell, E. E., Oatley, S. J., Xuong, N., & Kraut, J. (1987) *Biochemistry 26*, 2182-2189.

Vize, P. D., & Wells, J. R. E. (1987) *FEBS Lett. 213*, 155-158.

Vu, T. K. (1988) Honours Thesis, University of Adelaide, South Australia.

Wada, A. (1976) *Adv. Biophys. 9*, 1-63.

Watahiki, M., Yamamoto, M., Yamakawa, M., Tanaka, M., & Nakashima, K. (1989) *J. Biol. Chem. 264*, 312-316.

Weber, P. C., & Salemme, F. R. (1980) *Nature 287*, 82-84.

Weiner, S. J., Kollman, P. A., Case, D. A., Singh, U. C., Ghio, C., Alagona, G., Profeta, S., & Weiner, P. (1984) *J. Am. Chem. Soc. 106*, 765-784.

Wetlaufer, D. B. (1962) *Adv. Protein Chem. 17*, 303-390.

Wetlaufer, D. B. (1973) *Proc. Natl. Acad. Sci. U.S.A. 70*, 697-701.

Wetzel, R., Perry, L. J., Baase, W. A., & Becktel, W. J. (1988) *Proc. Natl. Acad. Sci. U.S.A. 85*, 401-405.

Wilkinson, D. L., & Harrison, R. G. (1991) *Bio/Technology 9*, 443-448.

Wolfenden, R., Andersson, L., Cullis, P. M., & Southgate, C.C. (1981) *Biochemistry 20*, 849-855.

Wong, K.-P., & Tanford, C. (1973) *J. Biol. Chem. 248*,8518-8523.

Wright, P. E., Dyson, H. J., & Lerner, R. A. (1988a) *Biochemistry 27*, 7167-7175.

Wright, P. E., Lerner, R. A., & Dyson, H. J. (1989) in *Advances in Protein Design International Workshop 1988* (Blöcker, H., et al., Eds.,) pp. 13-19 , VCH.

Xie, D., Bhakuni, V., & Freire, E. (1991) *Biochemistry 30*, 10673-10678.

Yang, J. T., Wu, C. S. C., & Martinez, H. M. (1986) *Methods Enzymol. 130*, 208-269.

Yutani, K., Ogasahara, K., Tsujita, T., & Sugino, Y. (1987) *Proc. Natl. Acad. Sci. U.S.A. 84*, 4441-4444.

Zakin, M. M., Poskus, E., Langton, A. A., Ferrara, P., Santome, J. A., Dellacha, J. M., & Paladini, A. C. (1976) *Int. J. Peptide Protein Res. 8*, 435-444.

Additional Comments

(1) p45. In order to verify that a minimum of two hours was a sufficient length of time for equilibration of all samples used in equilibrium denaturation experiments, A_{290}/A_{278} was followed as a function of time near the midpoint concentration of GuHCl (i.e., at 3M GuHCl, where relaxation would be expected to be slowest). 500µl of a 0.45 mg/ml solution of wild-type pGH in 25mM sodium borate pH 9.1 was mixed with 500µl of 25mM sodium borate pH 9.1 containing 6M GuHCl and placed into the thermostatted cuvette compartment (25°C). The figure below shows that the sample reached its final A_{290}/A_{278} value within 2 minutes of mixing (the dotted line depicts the value obtained after two hours).

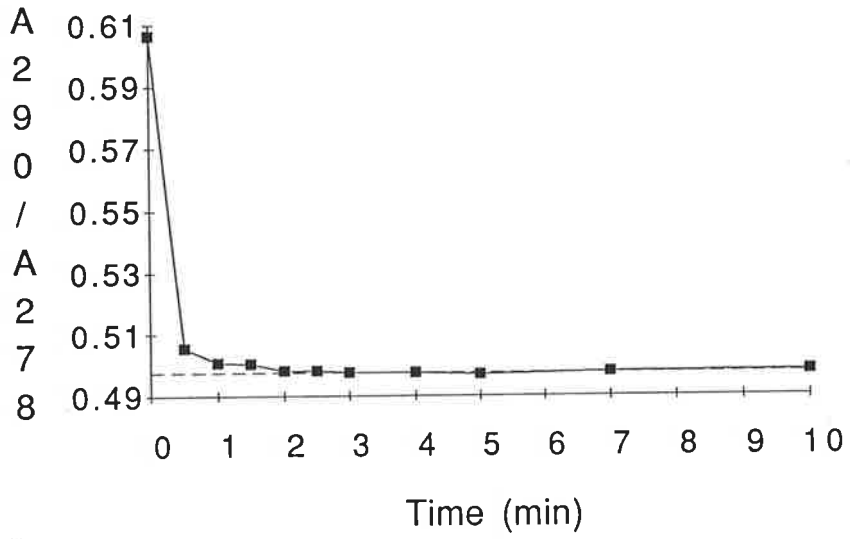

(2) p53. It is stated that prolonged exposure of pGH to urea at elevated pHs increases the possibility of deamidation of asparagines and glutamines. Actually the problem is not deamidation but carbamylation. Urea breaks down to ammonium cyanate which then reacts with unprotonated lysine sidechains resulting in the loss of one positive charge on the protein (Means, G.E., & Feeney, R.E. (1971) in *Chemical Modification of Proteins*, Holden-Day, Inc., San Francisco, CA, pp. 84-89).

p54. Due to its synthesis within the reducing environment of the *E. coli* cell, inclusion body protein contains a substantial amount of free -SH groups. These free -SH groups are necessary to promote disulphide bond shuffling of incorrectly formed disulphides, under the alkaline conditions used in the dissolution/refolding/oxidation conditions employed.